

Pontifícia Universidade Católica  
do Rio de Janeiro



**Rosana Candida Macedo**

**Development of spectrofluorimetric and liquid chromatographic methods for citrus essential oils analysis.**

**Tese de Doutorado**

Thesis presented to the Programa de Pós-graduação em Química of PUC-Rio in partial fulfillment of the requirements for the degree of Doutor em Química.

Advisor: Prof. Ricardo Queiroz Aucélio

Co-Advisor: Prof<sup>a</sup>. Alessandra Licursi Maia Cerqueira da Cunha

Rio de Janeiro  
March 2024

Pontifícia Universidade Católica  
do Rio de Janeiro



**Rosana Candida Macedo**

**Development of spectrofluorimetric and liquid chromatographic methods for citrus essential oils analysis.**

Thesis presented to the Programa de Pós-graduação em Química of PUC-Rio in partial fulfilment of the requirements for the degree of Doutor em Química. Approved by the undersigned Examination Committee.

**Prof. Dr. Ricardo Queiroz Aucélio**

Advisor  
PUC-Rio

**Prof<sup>a</sup>. Dr. Alessandra Licursi Maia Cerqueira da Cunha**

Co-advisor  
IFRJ

**Prof<sup>a</sup>. Dr. Alejandra Rodriguez-Haralambides**

Universidad de la Republica

**Prof<sup>a</sup>. Dr. Ana Maria Percebom**

PUC-Rio

**Dr. Mônica Cardoso Santos**

UFRJ

**Prof<sup>a</sup>. Dr. Raquel Andrade Donagemma**

UFF

Rio de Janeiro, March 20<sup>th</sup>, 2024

All rights reserved.

## Rosana Candida Macedo

Professor in Instituto Federal do Rio de Janeiro (IFRJ). Master's degree in Analytical Chemistry concluded at the Universidade Federal do Rio de Janeiro (UFRJ), in 2011. Licenciated in Chemistry at UFRJ in 2008. She has experience in the field of Analytical Chemistry.

### Bibliographic data

Macedo, Rosana Candida

Development of spectrofluorimetric and liquid chromatographic methods for citrus essential oils analysis / Rosana Candida Macedo; advisor: Ricardo Queiroz Aucélio; co-advisor: Alessandra Licursi Maia Cerqueira da Cunha – 2024.

181 f.: il. Color. ; 30 cm

Tese (doutorado) – Pontifícia Universidade Católica do Rio de Janeiro, Departamento de Química, 2024.

Inclui bibliografia

1. Química – Teses. 2. Óleos essenciais cítricos. 3. Microemulsão sem surfactante. 4. Espectroscopia de fluorescência. 5. Cromatografia líquida de alta eficiência. I. Aucélio, Ricardo Queiroz. II. Da Cunha, Alessandra Licursi Maia Cerqueira. III. Pontifícia Universidade Católica do Rio de Janeiro. Departamento de Química. IV. Título.

CDD: 540

This thesis is dedicated to my daughter, Ana Clara,  
whose laughs, and smiles brightened even the most  
challenging days of writing and research. I love you!

## Acknowledgment

To God for providing me with the strength, guidance, and protection. I also extend my heartfelt thanks to Our Lady Aparecida for her constant presence and blessings.

To my daughter, Ana Clara, for choosing me as her mother. She was my greatest motivation.

To my parents, Eliane and Jorge, and my sister, Rita, for all the love and unconditional support.

To Prof. Ricardo Aucelio, for his competence, patience, and dedication. He inspired me to strive for excellence in my academic pursuits.

To Prof. Alessandra Licursi, for your friendship and teachings. Thanks for introducing me to this research group.

To the master's student and friend Beatriz Bastos, for the conversations and shared company. I also extend my thanks to the members of LEEA and LQCBio research group.

To Marlin Pedrozo-Peñañiel for the friendship and the assistance with the DLS measurements.

To Prof. Carlos Massone for the insights in R-Studio programming. I also extend my thanks to the other professors in the Chemistry Department for their lessons.

To IFRJ and PUC-Rio for the physical structure that made the experiments possible.

To FAPERJ for funding the projects that financed the experiments.

And to all who contributed in any way to the execution of this work.

This study was financed in part by the Coordenação de Aperfeiçoamento de Pessoal de Nível Superior – Brasil (CAPES) – Finance Code 001.

## Abstract

Macedo, Rosana Candida; Aucélio, Ricardo Queiroz (advisor); Da Cunha, Alessandra Licursi Maia Cerqueira (Co-advisor). **Development of spectrofluorimetric and liquid chromatographic methods for citrus essential oils analysis.** Rio de Janeiro, 2024. 181p. Tese de Doutorado - Departamento de Química, Pontifícia Universidade Católica do Rio de Janeiro.

The main goal of this work was the development of spectrofluorimetric and reversed-phase high-performance liquid chromatography (RP-HPLC) methods for citrus essential oils (CEO) analysis. For this purpose, surfactant-free microemulsions (SFMEs) were used as an approach for sample treatment.

First, the SFME formation region was studied at different water:EO weight proportions (1:4, 1:2, 1:1, 2:1, 4:1 w/w) in the presence of propan-1-ol and octan-1-ol (10:3 w/w). Conductometric titrations indicated micellar aggregates containing EO (oil-in-water microemulsion) for the 4:1 proportion (droplets of hydrodynamic radius of  $95.7 \pm 5.3$  nm). In such conditions, fluorescence increased allowing the use of 3D fluorescence spectroscopy to obtain spectroscopic fingerprint pattern that was used aiming discriminant analysis, considering nine EO Brazilian brands, along with unfold principal component analysis (UPCA). A cumulative variance of 96.7% was obtained for the first three principal components and score plots showed distinct location for each group. Preliminary study showed the capability of these systems in evaluating storage conditions, and adulteration. The impact of storage conditions was made over 21 days exposed to light with results showing large

spectral differences compared to a sample stored in amber flask at 22°C. Adulteration of EOs by canola and mineral oil fortification was detected at different levels (1, 5, 10 and 20%, w/w) and, in addition to the spectral differences, a change in microemulsion stability was observed.

In a second stage of the study, these systems were replicated for different CEOs, including sweet and sour orange, tangerine, lemon, and grapefruit. Studies were employed to assess optimal conditions for system formation, aiming to encompass all evaluated CEOs without compromising measurement reproducibility. The new SFME condition adopted was 15  $\mu$ L of the oily phase containing EO and octan-1-ol (1:2 v/v), 19 mL of water, and propan-1-ol up to the 25 mL final volume. In addition to low sample consumption, a significant increase in fluorescence was achieved, despite the lower proportion of the oily phase. Excitation-emission matrix data were utilized for clustering analysis. UPCA was successfully applied, with cumulative variance of 99.5% for the first three principal components. Eigenvectors decomposition revealed a significant influence of the 336/436 nm excitation/emission wavelengths. Complementary analyses by HPLC confirm the relationship between fluorophores and the non-volatile fraction, characteristic of CEOs. The combination of low sample consumption and high-water content makes the application of these systems advantageous for CEO differentiation. Transparency and low viscosity are also considered positive aspects.

In a third and final stage, the effect of the sampling medium on the analysis of polymethoxyflavones (PMFs) in sweet orange EO by RP-HPLC was evaluated, utilizing the knowledge acquired in previous stages regarding the formation of SFME systems. This study was focused on analyzing PMFs present in the non-volatile fraction of sweet orange EO, which includes tetra-*O*-methyl-scutellarein,

sinensetin, tangeretin, nobiletin, and heptamethoxyflavone. Two methods utilizing isocratic elution with different mobile phases, (A) water/methanol and (B) water/acetonitrile, were employed using absorciometric and fluorimetric detection. The sampling medium significantly influenced chromatographic elution, potentially affecting peak width and retention time, especially for tangeretin, where a 300% and 103% increase in peak intensity was obtained for mobile phases A and B, respectively, when mixtures with octan-1-ol were used. Due to co-elution between nobiletin and tetra-*O*-methyl scutelarein observed with mobile phase A, the method was validated using mobile phase B (acetonitrile and water 50:50%, v/v). Fluorescence detection provided lower LOD and LOQ values for sinensetin (1 and 3  $\mu\text{g mL}^{-1}$ ) and nobiletin (13 and 44  $\mu\text{g mL}^{-1}$ ) than reported in the literature. The method was applied to commercial sweet orange EOs samples, yielding consistent results for all PMFs.

## **Keywords**

Citrus essential oils; Surfactant-free microemulsion; High performance liquid chromatography; Fluorimetric detection.

## Resumo

Macedo, Rosana Candida; Aucélio, Ricardo Queiroz; Da Cunha, Alessandra Licursi Maia Cerqueira. **Desenvolvimento de métodos espectrofluorimétricos e cromatográficos a líquido para análise de óleos essenciais cítricos.** Rio de Janeiro, 2024. 181p. Tese de Doutorado, Departamento de Química, Pontifícia Universidade Católica do Rio de Janeiro.

O principal objetivo deste trabalho foi o desenvolvimento de métodos espectrofluorimétricos e de cromatografia líquida de alta eficiência em fase reversa (RP-HPLC, *reversed-phase liquid chromatography*) para análise de óleos essenciais cítricos (OEC). Para este fim, microemulsões livres de surfactante (SFMEs, *surfactante-free microemulsions*) foram utilizadas como uma abordagem para o tratamento das amostras.

Primeiramente, a região de formação das SFMEs foi avaliada para diferentes proporções água:OE (1:4, 1:2, 1:1, 2:1, 4:1, m/m) na presença de propano-1-ol e octan-1-ol (10:3 m/m). Titulações condutométricas indicaram agregados micelares contendo OE (microemulsão do tipo óleo-em-água) para a proporção 4:1 (com partículas dispersas de raio hidrodinâmico de  $95,7 \pm 5,3$  nm). Nessas condições, a fluorescência aumentou, permitindo o uso da espectroscopia de fluorescência 3D para obtenção de padrões de impressão digital que foram utilizados para análise discriminante de nove marcas brasileiras, juntamente com análise de componentes principais com desdobramento dos dados (UPCA, *unfold principal components analysis*). Uma variância cumulativa de 96,7% foi obtida para os três primeiros componentes principais e os gráficos de pontuação mostraram uma localização

distinta para cada grupo. Um estudo preliminar também mostrou a capacidade desses sistemas em avaliar condições de armazenamento e adulteração. O impacto das condições de armazenamento foi realizado ao longo de 21 dias expostos à luz, com resultados mostrando grandes diferenças espectrais em comparação com uma amostra armazenada em frasco âmbar a 22°C. A adulteração de OEs por fortificação com óleo de canola e óleo mineral foi detectada em diferentes níveis (1, 5, 10 e 20%, m/m) e, além das diferenças espectrais, observou-se uma mudança na estabilidade da microemulsão.

Em uma segunda etapa do estudo, esses sistemas foram replicados para diferentes OEC, incluindo laranja doce e azeda, tangerina, limão e grapefruit. Estudos foram empregados para avaliar condições ótimas para a formação do sistema, visando abranger todos os OECs avaliados sem comprometer a reprodutibilidade da medição. A nova condição SFME adotada foi de 15 µL da fase oleosa contendo OE e octan-1-ol (1:2 v/v), 19 mL de água e propan-1-ol até o volume final de 25 mL. Além do baixo consumo de amostra, obteve-se um aumento significativo na fluorescência, apesar da menor proporção da fase oleosa. Os dados da matriz de excitação-emissão foram utilizados para análise de agrupamento. O UPCA foi aplicado com sucesso, com uma variância cumulativa de 99,5% para os três primeiros componentes principais. A decomposição dos autovetores revelou uma influência significativa dos comprimentos de onda de excitação/emissão de 336/436 nm. Análises complementares por HPLC confirmaram a relação entre fluoróforos e a fração não volátil, característica dos OECs. A combinação de baixo consumo de amostra e alto teor de água torna a aplicação desses sistemas vantajosa para a diferenciação de OECs. A transparência e a baixa viscosidade também são consideradas aspectos positivos.

Em uma terceira e última etapa, o efeito do meio de amostragem na análise de polimetoxiflavonas (PMFs) no OE de laranja doce por RP-HPLC foi avaliado, utilizando o conhecimento adquirido nas etapas anteriores em relação à formação de sistemas SFMEs. Este estudo teve como foco a análise de PMFs presentes na fração não volátil do OE de laranja doce, que inclui tetra-*O*-metil-scutelareína, sinensetina, tangeretina, nobiletina e heptametoxiflavona. Dois métodos utilizando eluição isocrática com diferentes fases móveis, (A) água/metanol e (B) água/acetonitrila, foram empregados usando detecção absorciométrica e fluorimétrica. O meio de amostragem influenciou significativamente a eluição cromatográfica, afetando potencialmente a largura dos picos e o tempo de retenção, especialmente para tangeretina, onde um aumento de 300 e 103% na intensidade de pico foi obtido para as fases móveis A e B, quando misturas com octan-1-ol foram utilizadas. Devido à coeluição entre nobiletina e tetra-*O*-metil scutelareína observada com a fase móvel A, o método foi validado utilizando a fase móvel B (acetonitrila/água, 50:50%, v/v). A detecção de fluorescência forneceu valores de limites de detecção e quantificação mais baixos para sinensetina (1 e 3  $\mu\text{g mL}^{-1}$ ) e nobiletina (13 e 44  $\mu\text{g mL}^{-1}$ ) do que os relatados na literatura. O método foi aplicado a amostras comerciais de OE de laranja doce, fornecendo resultados consistentes para todas as PMFs.

## **Palavras-chave**

Óleos essenciais cítricos; Microemulsão sem surfactante; Cromatografia líquida de alta eficiência; Detecção fluorimétrica

## Table of contents

1 Introduction	30
1.1 Contextualization of work	30
1.2 Thesis structure	33
1.3 Objectives	35
1.3.1 General objective	35
1.3.2 Specific objectives	35
2 Theoretical foundations	36
2.1 Citrus essential oils	36
2.1.2 Citrus essential oils authenticity	38
2.2 Surfactant-free microemulsions	40
2.3 Fluorescence spectroscopy	47
2.3.1 3D fluorescence spectroscopy analysis	49
2.4 Unfold principal component analysis	51
2.5 High-performance liquid chromatography	53
3 Material and Methods	56
3.1 Experimental	56
3.1.1 Reagents and chemicals	56
3.1.2 Instruments and apparatuses	58
3.1.3 Software programs	59
3.2 Procedures	60
3.2.1 Sample storage conditions	60
3.2.2 SFME formation regions	61
3.2.3 SFME Structural characterization	62
3.2.4 SFME preparation for 3D fluorescence spectroscopy analysis	63
3.2.5 Spectroscopy analysis and data pre-processing	64
3.2.5.1 Obtention of fingerprint patterns for sweet orange essential	64

3.2.5.2 Discriminant analysis of citrus essential oils	65
3.2.6 Unfold principal component analysis (UPCA)	67
3.2.7 Chromatographic analysis	67
3.2.7.1 Standard solutions preparation	67
3.2.7.2 Sample preparation	68
3.2.7.3 HPLC procedures	69
3.2.7.4 Method validation	70
4 Fingerprinting pattern of orange essential oils in surfactant-free microemulsion by 3D fluorescence spectroscopy	72
4.1 Introduction	72
4.2 Results and discussion	77
4.2.1 SFME systems formation	77
4.2.2 SFME structural characterization	80
4.2.3 3D fluorescence spectroscopy	86
4.2.4 Unfold principal component analysis (UPCA)	89
4.2.5 Other potential applications	99
4.3 Partial conclusion	102
5 Excitation-emission matrix fluorescence spectroscopy in hydro-alcoholic systems to discriminate different citrus essential oils	103
5.1 Introduction	103
5.2 Results and discussion	105
5.2.1 Hydro-alcoholic systems preparation and evaluation	105
5.2.2 3D fluorescence spectroscopy analysis and data pre-processing	112
5.2.3 Chemometrics	115
5.2.4 Chromatographic analysis	120
5.3 Partial conclusion	125

6 Effect of sampling medium on the analysis of polymethoxyflavones in sweet orange essential oil by reversed-phase high-performance liquid chromatography	126
6.1 Introduction	126
6.2 Results and discussion	132
6.2.1 HPLC analysis with absorciometric photodiode array detection (HPLC-DAD)	132
6.2.2 Effect of sampling medium for HPLC introduction	136
6.2.3 Spectrofluorimetric and HPLC analysis with fluorimetric detection (HPLC-FD)	140
6.2.4 Method validation	144
6.3 Partial conclusion	151
7 General conclusion	153
8 References	155
9 Attachment	173
A Published papers in the scope of this thesis	173
B Articles published as co-author	174
C Participation in events	176
10 Supplementary material	177
A R Script used for Ternary Diagram Generation	177
B R Script used for 3D Fluorescence Spectra obtention	180

## List of figures

- Figure 2.1.** Chemical structure of (A) coumarins, (B) psoralens, and (C) polymethoxyflones. 37
- Figure 2.2.** Illustrative scheme of Winsor solutions I, II, III, and IV. The colors in the image are merely indicative to illustrate the phase separation of the system. 40
- Figure 2.3.** Illustrative scheme of (A) O/W microemulsions, and (B) the W/O type. 42
- Figure 2.4.** Illustrative scheme of the titration process with weight monitoring applied to evaluate the formation regions of spontaneous homogeneous dispersions (SFMEs). The colors in the image are purely illustrative for understanding the process and visualizing phase separations. 43
- Figure 2.5.** Illustrative scheme of phase diagram for ternary systems consisting of three phases. In pseudoternary systems, at least one of the vertices consists of a fixed proportion combination of more than one component. 44
- Figure 2.6.** Illustrative scheme of the drop test. The colors in the image are purely illustrative. 45
- Figure 2.7.** Illustrative scheme of the conductivity evaluation profile as a function of the addition of the aqueous phase, considering generic components of a microemulsion system. 46
- Figure 2.8.** Simplified Jablonski diagram. 48
- Figure 2.9.** Scheme of the unfold principal components analysis (UPCA) applied to chemometric treatment of the excitation-emission matrix (EEM) data. 52

**Figure 3.1.** Illustrative scheme of the SFMEs conditions used for discriminant analysis of citrus essential oils. The colors in the image are purely illustrative. 64

**Figure 4.1.** (A) Miscibility test of orange EO in different alcohols (1:5, EO:Alcohol weight proportion), and (B) Visual aspect of systems containing orange EO and water after adding different alcohols (or alcohol mixes) (1:1:5, EO:Water: Alcohol weight proportion). 79

**Figure 4.2.** Pseudo-ternary phase diagram obtained for orange essential oil where each vertex represents 100% (in mass) of a particular component: water, essential oil and alcoholic mixture (propan-1-ol:octan-1-ol at 10:3 w/w). 80

**Figure 4.3.** Variation of the electrical conductivity ( $\mu\text{S}/\text{cm}$ ) with the oil weight fraction for the evaluated systems, based on W:EO weight proportions: (A) 1:4, (B) 1:2, (C) 1:1, (D) 1:2 and (E) 1:4. The highlighted points indicate the studied systems. The components weight proportion used as aqueous (W:propan-1-ol) and oil (EO:octan-1-ol) phase are described in each graph. 83

**Figure 4.4.** Drop test conducted for sweet orange essential oil at a weight proportion of 4:1:12.1, W:EO: Alcohols (w/w). Propan-1-ol:octan-1-ol were used as mixture alcoholic. 84

**Figure 4.5.** Contour surfaces ( $\lambda_{\text{ex}}$  from 250 to 600 nm and  $\lambda_{\text{em}}$  from 300 to 650 nm) obtained from 3D fluorescence spectrometry for orange EO in six different conditions: (A) only EO, and microemulsions in five different combinations, based on W:EO:alcoholic mixture, weight proportions: (B) 1:4:7.5, (C) 1:2:5.5, (D) 1:1:4.8, (E) 2:1:7.3 and (F) 4:1:12.1. The wavelength range used for discriminant analysis is highlighted in (F). Measurements were made using optical filter with 25% of transmittance. Fluorescent intensity

values in arbitrary units (a.u.). Blank subtraction and scattering removing by RStudio software (Package: eemR).

88

**Figure 4.6.** Contour surfaces ( $\lambda_{\text{ex}}$  from 300 to 400 nm and  $\lambda_{\text{em}}$  from 420 to 545.5 nm) for different Brazilian orange EOs in SFME. Each spectrum corresponds to one specific brand codified according to Table 3.1: (A) EO\_01, (B) EO\_02, (C) EO\_03, (D) EO\_04, (E) EO\_05, (F) EO\_06, (G) EO\_07, (H) EO\_08, and (I) EO\_09. Measurements were made using optical filter with 25% of transmittance, except for EO\_05 (where filter with 1% of transmittance was used). Fluorescent intensity values in Raman unit (R.u.). Blank subtraction and scattering removal by RStudio software (Package: eemR).

91

**Figure 4.7.** Screeplot for the first components obtained after chemometric treatment of the data by UPCA, considering 3D fluorescence spectroscopy analysis of nine different Brazilian orange essential oils (sample description in Table 3.1). Results for UPCA including all samples, EO\_01 to EO\_09, as presented in Table 3.1.

93

**Figure 4.8.** Two-, and three-dimensional scores plots for the evaluated Brazilian orange essential oil SFME after UPCA data treatment: (A) PC1  $\times$  PC2 (cumulative variance: 94.4%), (B) PC1  $\times$  PC3 (cumulative variance: 90.5%), (C) PC2  $\times$  PC3 (cumulative variance: 8.8%), and (D) PC1  $\times$  PC2  $\times$  PC3 (cumulative variance: 96.7%). The samples are identified according to the codes as presented in Table 3.1.

94

**Figure 4.9.** Two-dimensional scores plots for the evaluated Brazilian orange essential oil SFME after UPCA data treatment, after excluding the samples codified as EO\_05

and EO\_09 (Table 3.1): (A) PC1 × PC2 (cumulative variance: 89.6%), (B) PC1 × PC3 (cumulative variance: 77.5%), and (C) PC2 × PC3 (cumulative variance: 23.8%). The samples are identified according to the codes as presented in Table 3.1.

97

**Figure 4.10.** Contour surface with the percentage contribution of each excitation and emission wavelengths for the three principal components plotted as contour surfaces.

98

**Figure 4.11.** Contour surfaces obtained from 3D fluorescence spectrometry obtained for storage conditions (A-C), and adulteration with canola (A, D-F) and mineral oil (A,G-I). Before analysis, microemulsions (4:1:12.1 W:EO:Alcoholic mixture, weight ratio) were formed from each sample. Propan-1-ol and octan-1-ol (10:3, w/w) were used as alcoholic mixture (amphiphilic solvent). Excitation recorded between 300 nm and 400 nm and emission from 420 nm to 545,5 nm. Measurements were made using optical filter with 25% of transmittance. Fluorescent intensity values in Raman units (R.u.). Blank subtraction, and Raman normalization by RStudio software (Package: eemR).

101

**Figure 5.1.** Optimization for adjusting the volume of the oily phase (sweet orange EO and octan-1-ol, 1:2 v/v): (A) Fluorescent signal intensity in function of different oily phase volumes (0 to 300  $\mu$ L) and (B) zoom in on volumes between 0 and 15  $\mu$ L to highlight the linear range (in red). (C) Absorbance (300 to 450 nm) and (D) zoom in the 400 to 450 nm range to evaluate inner filter effect for sample systems with emphasis on the response obtained for the system containing 15  $\mu$ L of oily phase (in red). A fixed volume of water (1.0 mL) and propan-1-ol (completing final

volume up to 5 mL) were used to form the homogeneous hydro-alcoholic systems. 107

**Figure 5.2.** (A) Evaluation of the final volume of the hydro-alcoholic systems using a fixed volume (1.0 mL) of water and 15  $\mu$ L oily phase (5  $\mu$ L of sweet orange EO and 10  $\mu$ L of octano-1-ol) using propan-1-ol to adjust the final volume. (B) Fluorescence intensity from diluted systems containing 15  $\mu$ L of oily phase as a function of different water volumes, adjusting final volume to 25 mL using propan-1-ol. 110

**Figure 5.3** Hydro-alcoholic systems using: (A) 15  $\mu$ L of sweet orange EO and octan-1-ol, 1:2 v/v as oily phase and (B) only sweet orange EO (5  $\mu$ L). Final composition of water (19.0 mL) and propan-1-ol (as complement to the 25 mL final volume). 111

**Figure 5.4.** Homogeneous hydro-alcoholic systems for each of the CEOs after four months of monitoring: (A) sweet orange, (B) sour orange, (C) lemon, (D) tangerine, and (E) grapefruit. 15  $\mu$ L of oily phase (EO and octan-1-ol, 1:2 v/v), a fixed volume of water (19.0 mL) and propan-1-ol (up to 25 mL) were used. 112

**Figure 5.5.** EEM contour obtained for CEOs in SFME media with scattering removing and blank subtraction. Intensity fluorescence in arbitrary units (a.u.) after optical filter correction. Dilution factor was not considered. Dashed white line represents the restricts wavelength range selected for chemometrics. 114

**Figure 5.6.** EEM contour obtained for CEOs in SFME media in a restricted wavelength range after scattering removing and blank subtraction. Intensity fluorescence in Raman units (R.u.). Dilution factor was not considered. 115

**Figure 5.7.** Two-three-dimensional scores plots for the citrus essential oils evaluated by 3D fluorescence spectroscopy in SFME media after UPCA treatment: (A) PC1 × PC2 (cumulative variance: 93.3%), (B) PC1 × PC3 (cumulative variance: 79,5%), (C) PC2 × PC3 (cumulative variance: 26,2%).

116

**Figure 5.8.** Contour surface with the relative contribution of each excitation and emission wavelength for the three principal components (PC1, PC2 and PC3) plotted as contour surfaces.

118

**Figure 5.9.** EEM contour for sweet orange EOs in SFME media, considering all replicates (individual samples, 1 to 10) used for UPCA treatment. EEM contour with scattering removing and blank subtraction. Intensity fluorescence in Raman units (R.u.) and with optical filter correction. Dilution factor was not considered.

119

**Figure 5.10** Chromatograms obtained for (A) sweet orange, (B) sour orange, (C) lemon, (D) tangerine, and (E) grapefruit essential oils in hydro-alcoholic system (60 µL of a mixture containing EO and octan-1-ol, 1:2 volume proportion, 2 mL of ultrapure water, and propan-1-ol up to 5 mL). Injection volume of 5.0 µL, and mobile phase consisting of ultrapure water (A) and acetonitrile (B) with a linear gradient (0–7 min, 50% B; 7–13 min, 50–60% B; 13–15 min, 60–80% B; 15–17 min, 80% B; 17–20 min, 80–100% B; 20–25 min, 0% B; 25–27 min, 100–50% B; 27–30 min, 50% B) were used. Chromatograms were acquired using fluorescence detector (336/436 nm). Peaks with the highest intensity were marked (1 to 9).

122

**Figure 5.11.** UV absorption spectra obtained at the same retention times of the highlighted peaks (1 to 9) in the

chromatograms presented in Figure 5.10B-E. UV spectra were normalized for comparison purposes.

123

**Figure 5.12.** (A) Chromatograms of a mixture containing chromen-2-one as internal standard (I.S.) and five polymethoxyflavones: (1) sinensetin, (2) nobiletin, (3) scutellarein, (4) heptamethoxyflavone, and (5) tangeretin, at 100 mg L<sup>-1</sup>. (B) Chromatograms of orange EO and chromen-2-one as I.S. in hydro-alcoholic system (60 µL of a mixture containing EO and octan-1-ol, 1:2 volume proportion, 2 mL of ultrapure water, and propan-1-ol up to 5 mL). Injection volume of 5.0 µL, and mobile phase consisting of ultrapure water (A) and acetonitrile (B) with a linear gradient (0–7 min, 50% B; 7–13 min, 50–60% B; 13–15 min, 60–80% B; 15–17 min, 80% B; 17–20 min, 80–100% B; 20–25 min, 0% B; 25–27 min, 100–50% B; 27–30 min, 50% B) were used. Chromatograms were acquired using fluorescence detector (336/436 nm).

124

**Figure 6.1.** UV absorption spectra obtained during HPLC-DAD analysis for the evaluated polymethoxyflavones (PMFs): tetra-*O*-methyl-scutellarein, **1**; sinensetin, **2**; tangeretin, **3**; nobiletin, **4**; heptamethoxyflavone, **6**. Chromatograms were obtained using acetonitrile/water (50:50% v/v) as mobile phase. Introduced volume of 10 µL (standard solution of PMFs at 100 mg L<sup>-1</sup> in ethanol), flow rate at 1.0 mL min<sup>-1</sup>, and 30°C. Absorbance values were normalized for comparison.

133

**Figure 6.2.** Chromatograms of a mixture containing chromen-2-one as internal standard (I.S.) and five polymethoxyflavones (tetra-*O*-methyl-scutellarein, **1**; sinensetin, **2**; tangeretin, **3**; nobiletin, **4**; heptamethoxyflavone, **6**) at 100 mg L<sup>-1</sup> in ethanol. Chromatograms were obtained by HPLC-DAD at 336 nm

using (A) methanol/water (73:27%, v/v), and (B) acetonitrile/water (50:50%, v/v) as mobile phases. Introduced volume of 10  $\mu\text{L}$ , flow rate at 1.0  $\text{mL min}^{-1}$ , and 30°C.

134

**Figure 6.3:** Chromatograms obtained for sweet orange EO analysis (100  $\mu\text{L}$  EO in 5 mL) with peaks corresponding to the evaluated PMFs highlighted (tetra-*O*-methylscutellarein, **1**; sinensetin, **2**; tangeretin, **3**; nobiletin, **4**; heptamethoxyflavone, **6**). (A) and (B) methanol/water (73:27%, v/v); (C) and (D) acetonitrile/water (50:50%, v/v) were used as mobile phase. Line colors representing solvents used in sampling (sample introduction medium): methanol (black), ethanol (red), acetonitrile (blue), and methanol:octan-1-ol (10:3 w/w) (green). HPLC-DAD at 336 nm.

137

**Figure 6.4.** Chromatograms obtained for sweet orange essential oil analysis (100  $\mu\text{L}$  EO in 5 mL) with the peaks corresponded to the evaluated PMFs (tetra-*O*-methylscutellarein, **1**; sinensetin, **2**; tangeretin, **3**; nobiletin, **4**; heptamethoxyflavone, **6**). (A) Methanol/water (73:27%, v/v), and (B) acetonitrile/water (50:50%, v/v) were used as mobile phase. Line colors represent sample medium: methanol/octan-1-ol 10:1 w/w (magenta), 10:3, w/w (green) and 2:1 w/w (orange) HPLC-DAD at 336 nm.

139

**Figure 6.5.** Fluorescence excitation (black lines) and emission (red lines) spectra for the polymethoxyflavones (at 100  $\text{mg L}^{-1}$  in ethanol): (A) tetra-*O*-methylscutellarein, **1**; (B) sinensetin, **2**; (C) tangeretin, **3**; (D) nobiletin, **4**; and (E) heptamethoxyflavone, **6**.

141

**Figure 6.6.** Chromatograms of a mixture containing five polymethoxyflavones (tetra-*O*-methylscutellarein, **1**; sinensetin, **2**; tangeretin, **3**; nobiletin, **4**;

heptamethoxyflavone, **6**) at 100 mg L<sup>-1</sup> in methanol/octan-1-ol 2:1 w/w. Chromatograms were obtained by HPLC-FD using (A) methanol/water (73:27% v/v) and (B) acetonitrile/water (50:50% v/v) as mobile phase. (C) and (D) correspond to chromatograms (A) and (B), respectively, with a zoom for better observation of peaks for substances with lower intensity. Black lines represent chromatograms obtained at 336/436 nm, and the gray lines correspond to chromatograms obtained at 361/502 nm, 366/430 nm, 377/423 nm, 377/432 nm, and 388/433 nm.

143

**Figure 6.7.** Chromatograms of a mixture containing five polymethoxyflavones (tetra-*O*-methyl-scutellarein, **1**; sinensetin, **2**; tangeretin, **3**; nobiletin, **4**; heptamethoxyflavone, **6**) at 100 mg L<sup>-1</sup>, and chromen-2-one (internal standard, I.S.) at 100 mg L<sup>-1</sup> solubilized in methanol: octan-1-ol 2:1 weight proportion. (a) Mobile phase A by HPLC-DAD, (b) Mobile phase A by HPLC-FD, and (c) overlapped chromatograms (a) and (b). (d) Mobile phase B by HPLC-DAD, (e) Mobile phase B by HPLC-FD, and (f) overlay of chromatograms (d) and (e) with zoom.

145

**Figure 6.8.** Chromatograms obtained for sweet orange essential oil analysis (100 µL of EO in 5 mL) with the peaks corresponded to the evaluated PMFs highlighted (tetra-*O*-methyl-scutellarein, **1**; sinensetin, **2**; tangeretin, **3**; nobiletin, **4**; heptamethoxyflavone, **6**). Chromatograms were obtained after HPLC analysis (mobile phase B) with two detectors: (A) DAD at 336 nm and (B) FLD at 336/436 nm ( $\lambda_{ex}/\lambda_{em}$ ). Methanol: octan-1-ol 2:1 w/w were used as solvent of injection.

150

## List of tables

<b>Table 3.1.</b> Summary with relevant information of the orange EO (originated from Brazil) used in this work. Each code represents a different brand.	57
<b>Table 3.2.</b> Conditions established for SFMEs systems used for fingerprinting analysis of orange essential oils by 3D fluorescence spectroscopy.	63
<b>Table 3.3.</b> Conditions employed in HPLC methods used for the determination of polymethoxyflavones using C18 column (4.6 × 250 mm, 5 µm particle size).	69
<b>Table 4.1.</b> Comparison of methods reported in the literature for the essential oil analysis by excitation-emission matrix (EMM) fluorescence spectroscopy coupled to chemometrics.	75
<b>Table 4.2.</b> Experimental data for the weight proportions of each component, and a summary of physicochemical characterization for the studied systems. In the second column, values within parentheses are the individual weight proportion of propan-1-ol and octan-1-ol in the alcoholic mixture, respectively. Propan-1-ol and octan-1-ol (10:3 w/w) were used as alcoholic mixture.	85
<b>Table 4.3.</b> Experimental data for refractive index, density, and kinematic viscosity (25°C) obtained for the evaluated SFME systems and ultrapure water. Propan-1-ol and octan-1-ol (10:3 w/w) were used as alcoholic mixture.	86
<b>Table 4.4.</b> Maximum fluorescence intensity (in arbitrary units or a.u.) obtained after orange EO analysis by 3D fluorescence spectroscopy, in five different conditions, based on W:EO weight proportions (1:4; 1:2; 1:1; 2:1; 4:1). Propan-1-ol and octan-1-ol (10:3, w/w) was used as	

alcoholic mixture. Excitation wavelengths ( $\lambda_{ex}$ ) from 300 nm and 450 nm and emission wavelengths ( $\lambda_{em}$ ) from 430 nm to 550 nm. 89

**Table 6.1.** Polymethoxyflavones reported for non-volatile fraction of sweet orange essential oils. 127

**Table 6.2.** Methods reported in the literature for the analysis of oxygen heterocyclic compounds in citrus essential oils using reverse-phase high (and ultra-high) performance liquid chromatography (RP-HPLC and RP-UHPLC) without sample pre-treatment, with a highlight for the evaluated polymethoxyflavones (tetra-*O*-methyl-scutellarein, **1**; sinensetin, **2**; tangeretin, **3**; nobiletin, **4**; hexamethoxyflavone, **5**; and heptamethoxyflavone, **6**). 129

**Table 6.3.** Validation parameters for the calibration curves obtained by HPLC analysis (method with mobile phase B, indicated in Table 3.3). In this case, methanol: octan-1-ol was used as solvent injection and chromen-2-one as internal standard (at 100 mg L<sup>-1</sup>). PMFs: tetra-*O*-methyl-scutellarein (**1**), sinensetin (**2**), tangeretin (**3**), nobiletin (**4**), and heptamethoxyflavone (**6**). 148

**Table 6.4.** Comparison of the figures of merit of similar methods reported in the literature for the quantification of polymethoxyflavones (PMFs) in citrus essential oils using reverse-phase high (and ultra-high) performance liquid chromatography (RP-HPLC and RP-UHPLC) without sample pre-treatment. Only the evaluated PMFs were presented: tetra-*O*-methyl-scutellarein (**1**), sinensetin (**2**), tangeretin (**3**), nobiletin (**4**), and heptamethoxyflavone (**6**). Linearity range, LOD, and LOQ are expressed in mg L<sup>-1</sup>. 149

**Table 6.5.** Concentration in mg L<sup>-1</sup> of the evaluated PMFs (tetra-*O*-methyl-scutellarein, **1**; sinensetin, **2**; tangeretin, **3**;

nobiletin, **4**; heptamethoxyflavone, **6**) in the analyzed sweet orange essential oil sample. Method with mobile phase B (Table 3.3) was used for HPLC analysis.

## List of abbreviations

3D	Three-dimensional
a.u.	arbitrary units
ACN	Acetonitrile
ANN	Artificial neural network
API	Atmospheric pressure ionization
BC	Bicontinuous
CAS	Chemical Abstracts Service
CEO	Citrus essential oil
CV	Coefficient of variation
DAD	Diode array detection
DLS	Dynamic Light Scattering
EEM	Excitation-emission matrix
EO	Essential oil
EtOH	Ethanol
FD	Fluorescence detection
FF-TEM	Freeze fracture transmission electron microscopy
FID	Flame ionization detection
GC	Gas chromatography
H <sub>2</sub> O	Water
HPLC	High-performance liquid chromatography
I.S.	Internal standard
IT	Ion trap
LSMS	Liquid chromatograph mass spectrometer
ME	Microemulsion
MeOH	Methanol
MLP	Multilayer perceptron
MS	Mass spectrometry
NMR	Nuclear Magnetic Resonance
NP	Normal phase
O/W	Oil in water

PARAFAC	Five components parallel factor analysis
PC	Principal component
PCA	Principal component analysis
PDA	Photodiode array detector
PFC	Relative Centrifugal Force
PMF	Polymethoxyflavone
PTFE	Polytetrafluoroethylene
R.u.	Raman units
R <sup>2</sup>	Coefficient of determination
RP	Reversed phase
s <sub>b</sub>	Standard deviation
SFME	Surfactant-free microemulsion
SOM	Self-organized map
THF	Tetrahydrofuran
TOF (ToF)	Time-of-flight
UPCA	Unfold principal component analysis
UPLC	Ultra performance liquid chromatography
UV	Ultraviolet
v/v	Volume proportion
W	Water
W/O	Water in oil
w/w	Weight proportion
wt	weight
λ <sub>em</sub>	Emission wavelength
λ <sub>ex</sub>	Excitation wavelength

*"Success is not the key to happiness. Happiness is the key to success. If you love what you are doing, you will be successful."*

Albert Schweitzer

# 1

## Introduction

### 1.1

#### Contextualization of work

Citrus essential oils (CEOs) from various species, particularly sweet orange (*Citrus sinensis*), stand out as one of the most commercialized EOs, with Brazil well positioned in the global ranking of production. Their high aggregated value and complexity, in terms of composition, justify the importance of investing in complementary analytical methods for routine analysis, traceability, and quality control. Furthermore, these products find wide-ranging applications in industries such as cosmetics, food, and aromatherapy, highlighting the need to ensure authenticity and quality amidst challenges such as adulteration and variations in composition.

Gas chromatography coupled to mass spectrometry (GC-MS) is the most used technique for EO analysis. Sensory analysis, and physicochemical properties (specific gravity, refractive index, optical rotation, and solubility) are also employed in more simplistic evaluations. On the other hand, some adulteration mechanisms are not easily detectable, such as the addition of lower quality EOs, dilution with vegetable or synthetic oils, or even the presence of residual solvents. In this sense, the importance of investing in complementary analytical methods for routine analysis, traceability, and quality control is crucial.

Obtained by cold pressing the peels of citrus fruits, CEOs contain a characteristic non-volatile fraction comprising a variety of coumarin derivatives,

including psoralens, coumarins, and polymethoxyflavones, which are known for their aromatic and bioactive properties. This fraction also serves as a significant marker of adulteration due to its relatively simple composition compared to other CEOs components. The presence and concentration of these compounds can vary among different citrus species and may provide valuable insights into the authenticity and quality of the EO. As these compounds can be potential fluorophores, fluorescence spectroscopy emerges as a promising alternative for a complementary evaluation.

Fingerprint analysis by 3D fluorescence spectroscopy can serve as a valuable alternative for obtaining fingerprint patterns, which are crucial tools for sample traceability and authentication. This technique enables the comprehensive analysis of complex samples, providing detailed information about the composition, and offering high resolution and sensitivity. The main advantage of excitation/emission matrix (EEM) fluorescence spectroscopy is its selectivity, simplicity, and cost-effectiveness. While applications in vegetable oils have been reported, there is a notable scarcity of studies focusing on EOs for this purpose.

When it comes to EO analysis, various challenges arise due to the properties of these products. The high viscosity and the color of EOs samples can significantly compromise the spectrum acquisition and lead to other analytical implications, such as difficulty in cleaning materials and the risk of cross-contamination. Additionally, the presence of chromophores, which are compounds that absorb light at specific wavelengths, further complicates the analysis process. Chromophores can interfere with fluorescence signals, resulting in reduced signal intensity.

Within this context, the use of surfactant-free microemulsions (SFMEs) can be an interesting approach. SFMEs are macroscopically homogeneous and thermodynamically stable systems, comprising two immiscible phases (oily and aqueous) stabilized by the addition of short-chain alcohols. In these systems, alcohols act as an amphiphilic solvent, reducing the incompatibility between the aqueous and oily phases through the formation of weak micelle-like aggregates. SFMEs can be classified based on their structure: water in oil (W/O), where micelles with the aqueous phase are dispersed in the oily phase; oil in water (O/W), where the inverse situation occurs; and bicontinuous (BC), where both oil and water form continuous phases.

Considering fluorescence spectroscopy analysis, the micelle-like aggregates formed by W/O and O/W SFME systems can increase the fluorescence signal intensity by decreasing non-radiative decay of fluorophores in excited state. Additionally, the high dilution contributes to reducing the internal filter effect, minimizing the need for spectral correction. The minimal sample requirement and tolerance to high water content also reduce the risk of cross contamination.

Another analytical technique with great potential for analyzing the non-volatile fraction of CEOs is high-performance liquid chromatography (HPLC). However, sample preparation requirements, long analysis times, and the use of mobile phases with complex compositions are limiting factors for the broader application of this technique. Considering reverse-phase liquid chromatography analysis (RP-HPLC), some studies suggest direct sample injection after dilution in short-chain alcohols. However, the accumulation of terpenes in the hydrophobic stationary phase is a significant concern that can lead to decreased column performance over time, affecting the accuracy and reproducibility of results.

In RP-HPLC analysis, it is important to consider the possibility of SFME formation upon mixing the sample with the mobile phase, typically composed of water and organic solvent. Therefore, a meticulous evaluation of optimal solvent combinations can significantly enhance sample solubility. This optimization can result in substantial improvements in the elution process on the stationary phase, thereby prolonging the useful life of the chromatographic column. At present, there are no studies in literature focusing on this evaluation.

## 1.2

### **Thesis structure**

This thesis is structured into seven chapters. Chapter 1 begins with a brief contextualization followed by the presentation of the objectives of the study. In Chapter 2, pertinent information is provided for understanding and interpreting the thesis, starting with a brief initial description of CEOs with relevant information for the study. A concise review of the theoretical foundations of the SFME and of the analytical techniques employed (fluorescence spectroscopy and liquid chromatography) is also presented.

Chapter 3 contains detailed information about the materials, instruments, and software programs used. It also presents the detailed protocols of each method employed, including the formation and characterization of the SFME. Additionally, it outlines the methods for analyzing CEOs by high-performance liquid chromatography and fluorescence spectroscopy. Details about the chemometric treatment used for discriminant analysis are also provided.

In the subsequent chapters (4, 5, and 6), the results of the conducted research are presented. These chapters provide a brief introduction, a comprehensive description of the results, and a partial conclusion for each respective study.

Chapter 4 refers to the initial study involving the first SFME systems, including their potential application to obtain fingerprint patterns for sweet EO, focusing on traceability, storage conditions evaluation, and non-volatile oil adulteration. This study was recently published in a scientific journal.

Chapter 5 introduces new SFME systems. An optimization process was carried out to establish a new condition with lower sample content and higher water volume. Discriminant analysis was also conducted; however, unlike the previous study, these new conditions were replicated for different CEOs. An investigation into the fluorophores responsible for the observed fluorescence was also conducted, associating them with compounds present in the non-volatile fraction. This study was recently submitted for publication.

Chapter 6 presents the results of the latest study, involving an assessment of the effect of sampling medium on the analysis of polymethoxyflavones in sweet orange EO by RP-HPLC. The studies presented in the previous chapters concluded that the presence of octan-1-ol as a diluent in EO facilitates the formation of MEs in hydroalcoholic medium (SFME). In this chapter, it was possible to demonstrate that the use of octan-1-ol as an injection solvent can significantly contribute to the chromatographic elution process. As a result, a new method was proposed and validated. This study has already been completed and it is in submission phase to a scientific journal.

In Chapter 7, the thesis concludes with a summary and concise discussion of findings. References and supplementary materials are provided in the subsequent sections.

## **1.3**

### **Objectives**

#### **1.3.1**

##### **General objective**

The proposal of this thesis was the development of spectrofluorimetric and reversed-phase high-performance liquid chromatography methods for citrus essential oils analysis.

#### **1.3.2**

##### **Specific objectives**

- Adjust conditions for SFME formation from sweet orange EO samples and assess the effect of this systems on the spectral profile using 3D fluorescence spectroscopy aiming fingerprint analysis.
- Expand the conditions for SFME formation to obtain new systems with low sample consumption and high-water content and replicate for other CEO varieties and evaluate their effect on the spectral profile using 3D fluorescence spectroscopy.
- Evaluate the effect of the sampling medium on the polymethoxyflavones analysis in sweet orange EO by HPLC applying the knowledge acquired regarding the formation of SFME systems. Compare the use of fluorescence detectors (HPLC-DF) with the diode-array absorbance detection system (HPLC-DAD).

## 2

### Theoretical foundations

#### 2.1

##### Citrus essential oils

Citrus essential oils (CEOs), extracted from species of the *Rutaceae* family, are derived from *Citrus*, the genus known for its most popular fruit crops, which include oranges, grapefruits, mandarins, tangerines, lemons, and limes, all important for the human diet [1]. In citrus fruit peels, the EOs are commonly localized in specific glands or sacs. These glands contain the aromatic compounds responsible for imparting the fruit with its characteristic scent and flavor. CEOs are typically obtained by cold-pressing citrus waste peels, which are a by-product of the juice industry. During the cold pressing extraction method, these oils are released from the glands and collected for various uses [2].

Although the composition of EOs depends on several factors such as the part of the plant from which they were obtained, the cultivation method, the extraction procedure, and exposure factors, plant genetics is often the most determining factor. EOs from the same botanical family may have similar components [3]. A common characteristic among CEOs is the presence of limonene as a primary component (around 90% of the overall composition). Short-chain alcohols, aldehydes, esters, acids, monoterpenes, sesquiterpenes, and their corresponding terpenoids are also present in its composition. Their highly hydrophobic nature contributes to the low water solubility, a typical characteristic of CEOs [1,4].

For cold-pressed CEOs, another relevant characteristic is the presence of a non-volatile fraction, mainly composed of oxygen heterocyclic compounds (10 – 20%). This portion also includes long-chain hydrocarbons, fatty acids, sterols, and carotenoids [1,4,5]. In sweet orange EO, this fraction has the lowest content (around 1% of the total composition). However, for CEOs from other species, this value can reach up to 15% [6]. Psoralens, coumarins, and polymethoxyflavones (Figure 2.1) comprise the group of oxygen heterocyclic compounds characteristic of the CEO non-volatile fraction [5]. Polymethoxyflavones (PMFs) are recognized for their various beneficial biological activities [7]. However, psoralens are known for their photo-activity and potential to cause adverse skin reactions when exposed to UV [8].

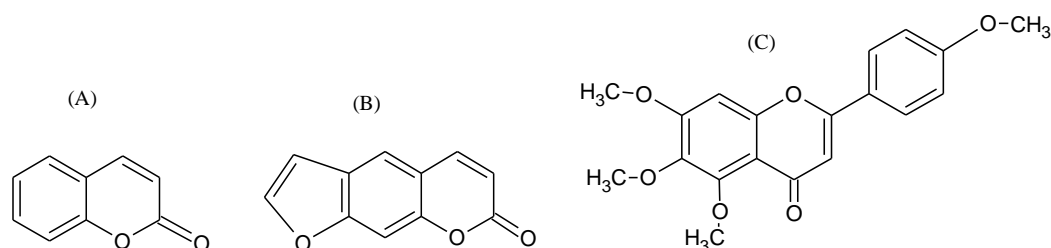


**Figure 2.1.** Chemical structure of (A) coumarins, (B) psoralens, and (C) polymethoxyflones.

The CEOs, especially orange (*Citrus sinensis* (L.) Osbeck and others), and Sicilian lemon (*Citrus limon* (L.) Osbeck), are among the most produced and commercially EOs in the world. In this market, Brazil holds a prominent position, ranking among the top five global producers. The growing demand for natural products and the increasing interest in alternative therapies, such as aromatherapy, make this market promising. However, the low extraction yields may pose a

challenge, potentially hindering production from adequately meeting the growing market demand [9,10]. All these issues underscore the need for efficient quality control of these products. Only in this way can they reach the consumer meeting the highest standards of quality and safety. Moreover, stringent control throughout the production chain is essential to ensure the authenticity, purity, and efficacy of EOs, providing consumers with the confidence needed to fully enjoy their therapeutic and aromatic benefits.

### **2.1.2**

#### **Citrus essential oils authenticity**

Due to their high complexity in terms of composition, with up to 400 components [11], ensuring the authenticity of EOs remains an important analytical challenge. For EOs in general, several aspects are relevant, such as traceability, storage conditions, and identifying adulteration. The EO production by their respective originating plants can vary drastically due to factors such as physiological variations, environmental conditions, and geographic variations [12]. In many cases, the EO origin can determine its final selling value. In this context, investing in techniques capable of tracing samples according to their origin is extremely relevant. Additionally, it is crucial to ensure that proper storage conditions are maintained. Factors such as high temperatures, exposure to light, and oxygen availability should be considered. Improper storage conditions could result in alterations such as changes in color, increased viscosity, or the development of unpleasant odors due to shifts in composition and the presence of oxidized compounds. Oxidized terpenoids also might trigger allergic skin reactions [13,14].

Considering the high aggregated value of these products, the relentless pursuit of profit, and high demand, cases of EO adulteration are to be expected. The most common adulteration processes include the addition of non-volatile oils such as vegetable or mineral oils, dilution in solvents like ethanol, and the addition of natural or synthetic compounds, such as the addition of citral to lemon EO (*Citrus lemon* L.). For CEOs, another common adulteration method is blending higher-value CEOs with sweet orange EO, which, due to its larger-scale production, has more affordable prices, and a similar qualitative composition [15,16].

For EOs analysis, the most widely used analytical technique is gas chromatography with flame ionization detection (GC-FID) or coupled with mass spectrometry (GC-MS) [17]. Due to high injector temperatures or catalytically active surfaces like columns or liners, structural changes in thermally unstable compounds may occur during GC analyses [18]. Additionally, some adulteration mechanisms may go unnoticed through conventional GC analysis. Adulteration of high-value CEOs through the addition of less valuable CEOs, such as sweet orange oil, is an example [19]. For CEOs, another viable approach is the use of the non-volatile fraction as an adulteration marker. Because it is less complex in terms of composition (Figure 2.1), this fraction can be considered important for tracing the authenticity of citrus oils [4]. Due to implications such as the high risk of cross-contamination due to dealing with oily matrices and the high complexity in terms of composition, there are not many methodologies available in the literature for this approach. Consequently, investing in complementary analytical methodologies aimed at studying these compounds may represent an interesting alternative.

## 2.2

### Surfactant-free microemulsions

Microemulsions (MEs) are generally defined as transparent, fluid, optically isotropic, and thermodynamically stable solutions of at least two immiscible liquids (usually water and oil) and an amphiphilic compound (which may or may not be associated with a co-surfactant) [20]. These systems were reported for the first time by Hoar and Schulman in 1943 [21]. Additionally, in 1948, Winsor and Hahn categorized mixtures of water, oil, and an amphiphilic compound into four phase equilibrium systems, termed Winsor I, II, III, and IV (Figure 2.2) [22]. In this study, the researchers concluded that conversion between Winsor systems is achievable by adjusting the mixture composition. This finding was relevant as it unveiled the potential for manipulation to create systems with specific characteristics. Few years later, in 1959, the term ‘microemulsion’ was coined by Shulman, Stoeckenius, and Price [23].

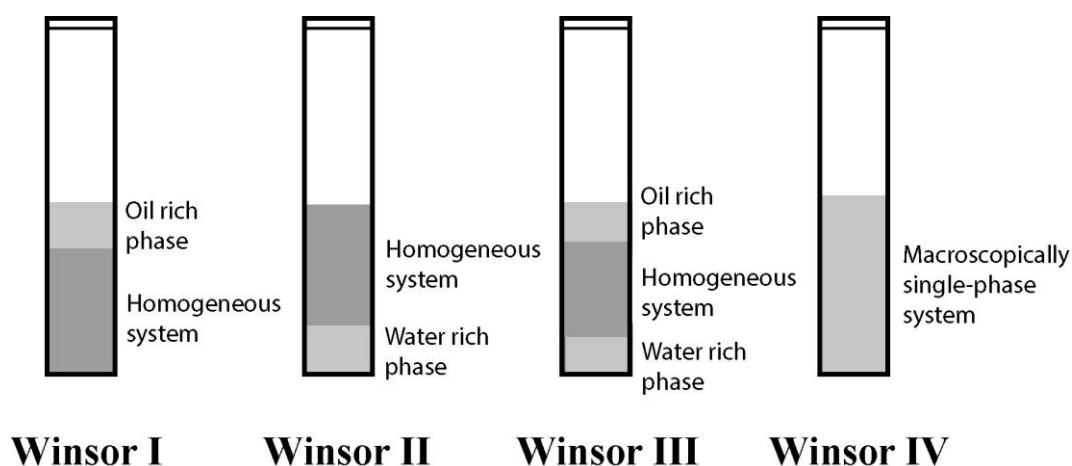


**Figure 2.2.** Illustrative scheme of Winsor systems I, II, III, and IV. The colors in the image are merely indicative to illustrate the phase separation of the system.

Comparing the MEs systems with emulsions, the main differences are the translucent appearance, thermodynamic stability, and spontaneous formation [24]. The ME formation process is spontaneous because it is energetically favorable. To better understand, consider Equation 2.1, which is used to describe the energy involved in the emulsification process.

$$\Delta G_f = \Delta H_f - T \cdot \Delta S_f \quad (\text{Eq. 2.1})$$

$\Delta G_f$  is free energy of emulsion formation,  $T$  is the temperature,  $\Delta S_f$  is the entropy, and  $\Delta H_f$  is the enthalpy of emulsion formation (consider  $\Delta H_f = \gamma \cdot \Delta A$ , where  $\gamma$  is the surface tension and  $\Delta A$  the surface area).

In MEs, surfactants organize into micellar aggregates that significantly reduce the interfacial tension of the system. As a result, the term  $\Delta H_f (= \gamma \cdot \Delta A)$  becomes sufficiently small in this case. Additionally, micelle formation causes an increase in the disorder of the system ( $\Delta S_f$ ), driven by the hydrophobic effect. Consequently, the free energy ( $\Delta G_f$ ) of the process becomes negative, indicating a spontaneous formation process [25] Depending on the proportion between the polar and nonpolar phases, MEs can be classified as oil-in-water (O/W) and water-in-oil (W/O) (Figure 2.3). Bicontinuous (BC) systems are also a possibility, when oil and water are both continuous phases [26].

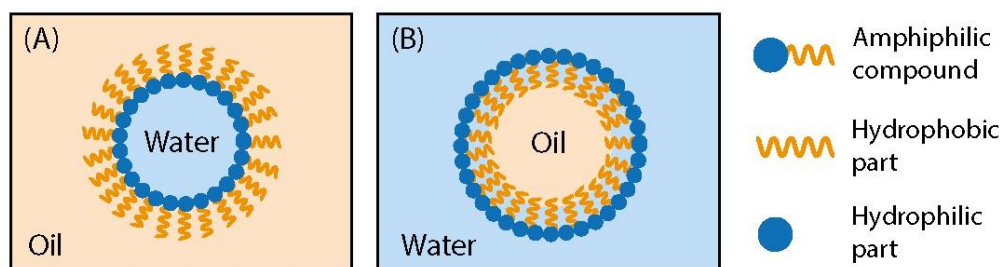


**Figure 2.3.** Illustrative scheme of (A) O/W microemulsions, and (B) the W/O type.

In the first studies, only surfactants were used to promote the stabilization of the oil and water phases. However, in 1977, one study conducted by Smith, Donelan & Barden, reported the formation of W/O MEs in systems containing hexane, water, and isopropanol. Additionally, the researchers assessed the ME system formation capability for various short-chain alcohols. They concluded, that branched-chain alcohols required larger volumes compared to straight-chain alcohols with the same number of carbons [27]. In the following years, several other studies reported similar systems, including O/W and BC systems. Currently, these systems are known as surfactant-free microemulsions (SFME).

Weight titration (Figure 2.4), along with ternary phase diagrams (Figure 2.5), are extensively utilized to evaluate and illustrate the formation region of SFMEs. When the presence of a co-surfactant is required, the amphiphilic mixture is considered as a single component, and the system is then termed as pseudoternary. During the titration process, it is common to observe the aspect of the system regarding the number of phases. In titrations involving biphasic mixtures with the sequential addition of the chosen alcohol, it is common to obtain a monophasic solution, but slightly turbid just before the formation of systems in SFME. This phenomenon is known as the 'Ouzo effect', in reference to the Greek drink 'Ouzo' [28]. Thus, during the ternary diagram confection, it is also possible to

identify the pre-Ouzo region, corresponding to combinations close to the Ouzo effect. This phenomenon has been observed in SFME systems, including combinations containing octan-1-ol, ethanol, and water [29,30].

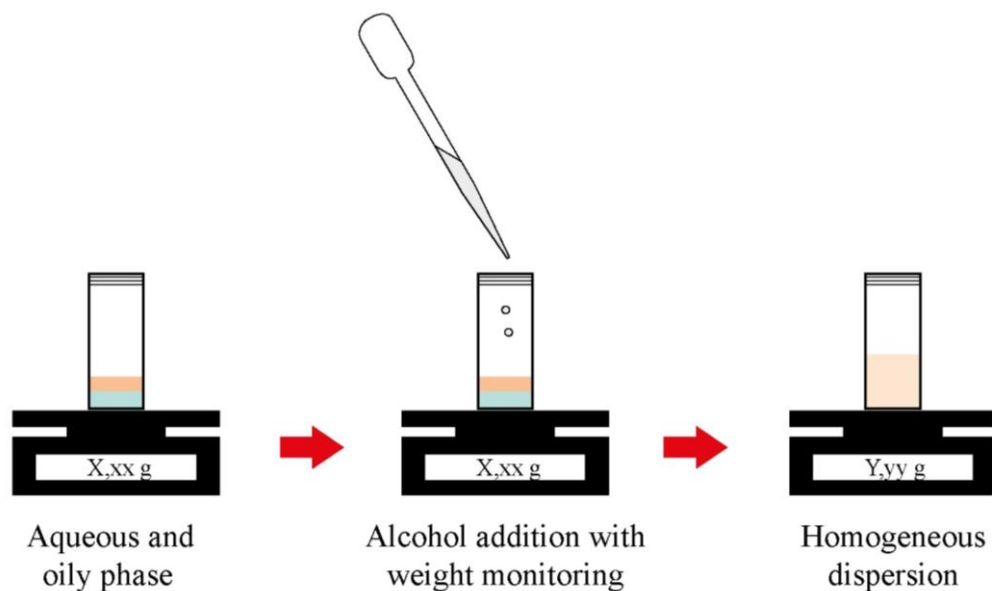


**Figure 2.4.** Illustrative scheme of the titration process with weight monitoring applied to evaluate the formation regions of spontaneous homogeneous dispersions (SFMEs). The colors in the image are purely illustrative for understanding the process and visualizing phase separations.

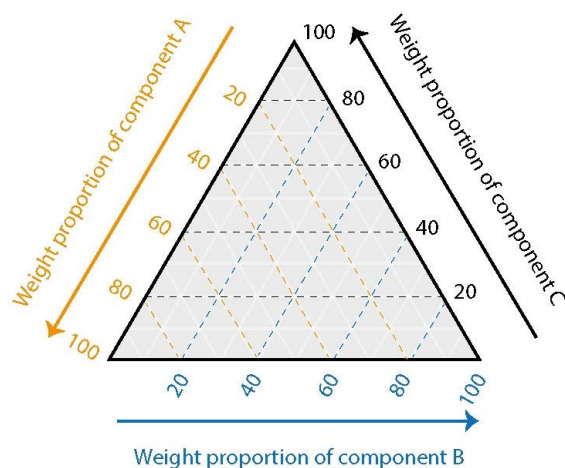


**Figure 2.5.** Illustrative scheme of phase diagram for ternary systems consisting of three phases. In pseudoternary systems, at least one of the vertices consists of a fixed proportion combination of more than one component.

For investigating the SFME structures, dynamic light scattering (DLS) and conductivity measurements are the most commonly used. Through DLS measurements, it's possible to estimate the hydrodynamic radius of dispersed particles, and conductometric titrations are an important tool for evaluating the SFME structure (W/O, O/W, or BC). Conductometric titration is a technique used to measure the electrical conductivity ( $\kappa$ ) of a solution as a function of ion concentration. In the case of MEs,  $\kappa$  values can provide valuable information about their structure. During titration of ME components, whether using the aqueous or oily phase as a titrant, significant variations in electrical conductivity occur. These changes in electrical conductivity are directly linked to the formation and transition between different ME structures (W/O, BC, and O/W) [31].

Clausse et al. [32,33] demonstrated that, for titration processes where the aqueous phase is used as titrant, initially the electrical conductivity abruptly increases until  $\kappa$  reaches a critical value. The pronounced linear rise in  $\kappa$  values can

be associated with the formation of W/O MEs. When a reduction in  $\kappa$  values is observed, the condition can then be associated with the formation of O/W systems. The intermediate stage, where conductivity increases slowly and nonlinearly, represents the condition for the formation of bicontinuous systems. An illustrative scheme of the conductivity evaluation profile as a function of the aqueous phase addition for MEs systems is presented in Figure 2.6. For SFME systems, similar profiles have been reported; however, some studies have reported the use of the oil phase as more efficient for this evaluation [34–36].

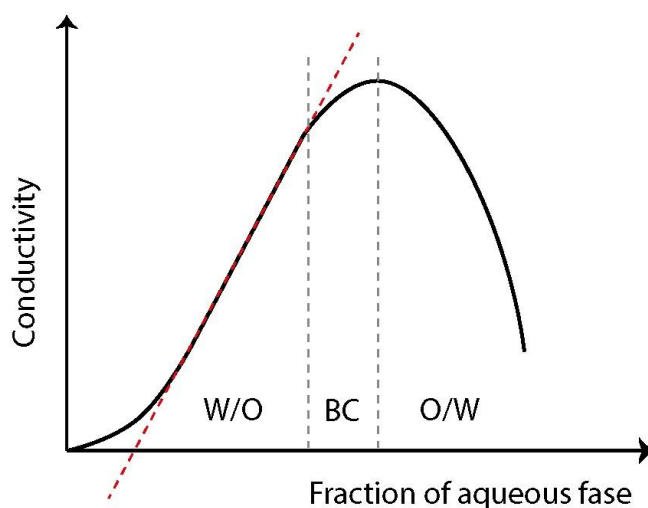


**Figure 2.6.** Illustrative scheme of the conductivity evaluation profile as a function of the aqueous phase addition, considering generic components of a microemulsion system.

Images obtained from freeze fracture transmission electron microscopy (FF-TEM) are also applicable; however, due to its high cost and the requirement for specific infrastructure, it often requires collaboration or partnerships for implementation [37]. A simple bench test, often known as a 'drop test' or 'dilution test' (Figure 2.7), is an alternative commonly used as a complementary evaluation

for characterizing MEs to identify the structure (W/O, O/W, or BC). In this test, a ME drop is carefully added to a dispersing medium. The aqueous and oily phases are used separately as the dispersing medium. It is expected that W/O MEs systems disperse rapidly when the drop is deposited onto the oily phase. Conversely, the opposite is expected for O/W MEs. Despite its simple execution, this technique provides valuable preliminary information about the structure of MEs (or SFME, in this case).

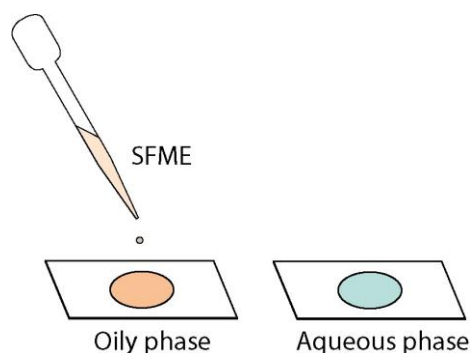


**Figure 2.7.** Illustrative scheme of the drop test. The colors in the image are purely illustrative.

In addition to those mentioned previously, techniques such as cyclic voltammetry, and NMR (Nuclear Magnetic Resonance), among others, although less common, have also been reported as alternatives for characterizing SFMEs. The choice of the appropriate technique depends on the intrinsic nature of the sample and needs to be carefully evaluated [37].

## 2.3

### Fluorescence spectroscopy

Molecular fluorescence is the radiation emitted by a molecule after a radiative transition from the excited state to the ground state with the same multiplicity in a singlet-to-singlet transition ( $S_n \rightarrow S_0$ ), where  $S_n$  is generally the first excited energy state, with  $n = 1$ , and  $S_0$  indicates the ground singlet state. As shown in the partial Jablonski diagram presented in Figure 2.8, during the fluorescence emission process, the excited molecule from  $S_0 \rightarrow S_n$  quickly descends to its lowest vibrational sublevel through non-radiative processes, after, the molecule loses the remaining energy in the form of UV-visible radiation, returning to its ground state  $S_0$  emitting fluorescence. Involving a transition between states of the same multiplicity, fluorescence is quantum mechanically favorable and occurs with short lifetimes ( $10^{-9}$  to  $10^{-7}$  s). At the electronic level  $S_n$ , the excited molecule can lose excess energy through various pathways. A more common form is energy loss through non-radiative transitions such as relaxation by molecular vibration or energy transfer after collisions. Other processes, such as the change in multiplicity from the  $S_1$  state to the  $T_n$  state (intersystem crossing), may also occur, but to maintain the focus of this text, they will not be discussed [38–40].

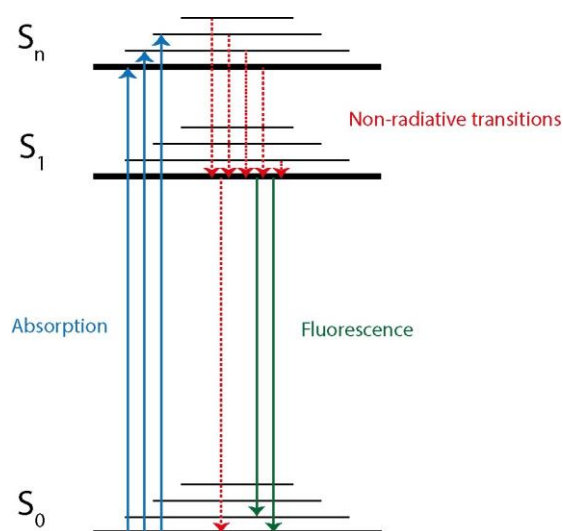


**Figure 2.8.** Simplified Jablonski diagram.

Fluorescence spectroscopy is a highly sensitive and selective technique with limits of detection that can reach the range of  $\text{ng mL}^{-1}$ . As both wavelengths (excitation and emission) depend on the molecular structure, small structural differences can result in significant changes in these values [41]. It is not possible to predict fluorescence solely based on chemical structure, but certain requirements such as structural rigidity and the presence of conjugated  $\pi$  electrons can be considered relevant. Factors that contribute to the non-radiative decay pathways of fluorophores can reduce the fluorescence intensity. Additionally, factors such as temperature, pH, solvent, and the presence of quenchers can affect the intensity of emitted fluorescence [40]. Micellar medium can also contribute to an increase in emitted fluorescence, as the formation of microenvironments can reduce the vibrational freedom of fluorophores signal [42].

### 2.3.1

#### 3D fluorescence spectroscopy analysis

In conventional fluorescence scanning, the emission spectrum is obtained by scanning the wavelength of maximum emission ( $\lambda_{em}$ ) while the sample is excited at a fixed maximum excitation wavelength ( $\lambda_{ex}$ ). When emission spectra are collected sequentially for a particular range of  $\lambda_{ex}$ , a total luminescence scanning is obtained. These spectra, when combined, provide contour surfaces, which are three-dimensional (3D) graphical representations of variations in the intensities of spectral bands. This approach can be particularly intriguing for obtaining a fingerprint signature for a specific system, especially in multicomponent samples. Each component present in the sample contributes uniquely to the resulting spectrum, generating characteristic patterns that can be used for product authentication, quality control, and traceability [43].

This technique, also known as 3D fluorescence spectroscopy, excitation-emission fluorescence spectroscopy, or fluorescence fingerprinting, has been widely applied in dissolved organic matter and petroleum characterizations [41,44–46]. The fingerprint pattern obtention by 3D fluorescence spectroscopy offers significant advantages, including simplicity in execution and low cost. In most cases, the contour surfaces are obtained without the need for sample preparation, making it a non-destructive process. As disadvantages, the long analysis times (which can reach 30 minutes or more depending on the parameters used) may lead to sample degradation, and the need for careful evaluation and mathematical treatment of the spectra to avoid misinterpretation must be considered.

Three types of scattering can affect the signals of a 3D spectrum: Mie, Rayleigh, and Raman. Mie scatter occurs when particulate matter is present in the sample. In these cases, filtration with suitable filters can be an interesting alternative. Considering Rayleigh and Raman scatter, both occur when the molecule is excited by a photon with insufficient energy to fully excite it, leading it to a state of low stability virtual energy. In Rayleigh scatter, the return to the initial state occurs at the same frequency as the excitation (elastic scattering). It is a more probable process, with higher intensity, but without analytical value. Therefore, it is common in 3D spectrofluorimetry analyses to treat the obtained spectra by scattering removal. In Raman scatter, the return to the initial state occurs at a frequency different from the incident radiation (inelastic scattering). Unlike Rayleigh scatter, its intensity is not as high, and for the most common cases, the only molecule with a concentration high enough to produce visible Raman scattering is water. When 3D spectrofluorimetry is used for discriminant analysis (usually with the aid of chemometric treatments), a large number of replicates is required, often resulting in the need to perform the analyses on different days. In these cases, Raman scatter can be very useful for spectral correction. The measured signal for ultrapure water can then be used to normalize the spectra and minimize instrumental effects. When Raman normalization is performed, the unit of the fluorescence intensities must be reported as Raman units (R.u.) rather than arbitrary units (a.u.) [43,47].

The inner filter effect, also known as the self-absorption effect, occurs when any component of the sample absorbs energy at the same excitation and/or emission wavelength as another component. It can affect the fluorescent response non-linearly, which may compromise analyses focusing on quantification. Performing

a dilution to an acceptable absorbance level can be convenient, provided it does not compromise the system's response in terms of emitted fluorescence. Mathematical treatments using absorption measurements can also be convenient for systems where dilution is not possible [48]. Although initially the treatment of spectra may seem labor-intensive, there are already numerous software solutions available, equipped with programming codes, significantly aiding this process. These software platforms automate spectra treatment, offering a wide array of applications [49,50].

## **2.4**

### **Unfold principal component analysis**

Principal Component Analysis (PCA) is one of the most important methods for chemometric data treatment. It is a statistical tool used for dimensionality reduction and data exploration. Its goal is to transform a set of possibly correlated variables into a set of linearly uncorrelated variables called principal components (PCs). These PCs are ordered in terms of the variance they capture, with the first PC capturing the maximum variance and subsequent PCs capturing decreasing amounts of variance. PCA achieves this transformation by rotating the original data axes in such a way that the greatest variance lies on the first axis (PC1), the second greatest variance on the second axis (PC2), and so forth. This reduction in dimensionality facilitates the visualization and interpretation of complex datasets, enabling the identification of underlying patterns, trends, and relationships within the data [51].

PCA is a technique designed to handle linear data organized in a two-dimensional matrix. However, when dealing with complex data, such as those from

an EEM obtained after 3D spectrofluorimetric analyses, direct application of PCA may be inadequate due to its 3D structure. To overcome this limitation, it is necessary to unfold the EEM into a two-dimensional matrix before applying PCA. This approach is commonly referred to as Unfold Principal Component Analysis (UPCA). For UPCA treatment, the EEM (corresponding to 3D spectrum data after pre-treatment) are unfolded and rearranged into a two-dimensional matrix ( $X$ ) containing  $n$  rows (samples) and  $k$  columns (variables). The PCA decomposition of  $X$  takes the form of Equation 2.2 [52].

$$X = TP^T \quad (\text{Eq. 2.2})$$

Where,  $T$  is the scores matrix where rows correspond to the  $n$  samples and columns are equivalent to representative principal components PCs ( $N$ );  $P^T$  is the loading matrix, where the rows correspond to  $N$  and the columns are equivalent to the  $k$  variables. A scheme of UPCA treatment is present in Figure 2.9.

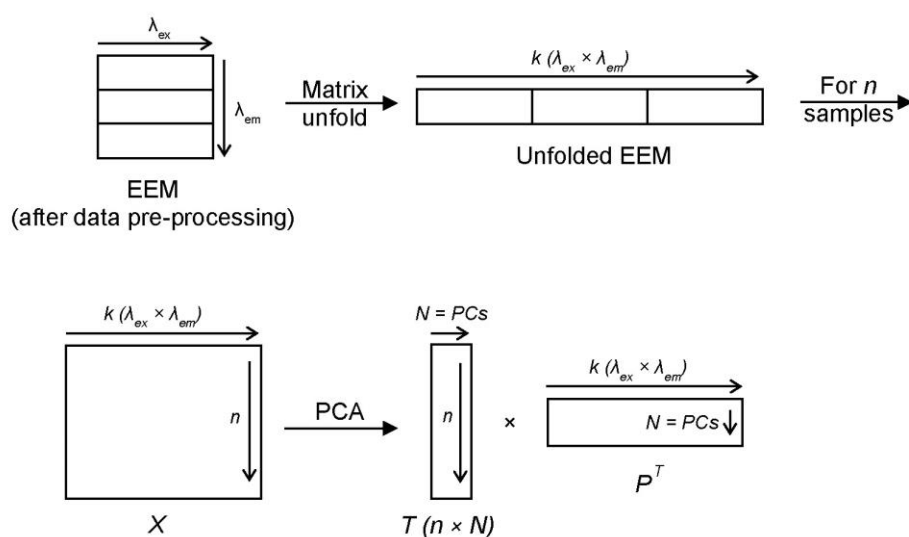


**Figure 2.9.** Scheme of the unfold principal components analysis (UPCA) applied to chemometric treatment of the excitation-emission matrix (EEM) data.

UPCA is a powerful technique that extends the capabilities of PCA to handle multidimensional data. By unfolding the EEM matrix into a two-dimensional representation, UPCA allows for more effective application of PCA. When applying UPCA, researchers can explore complex relationships among spectral variables, identify significant trends, and distinguish between different sample classes based on their spectral profiles. This approach is particularly useful in fields such as chemometrics and spectroscopic data analysis, where interpretation of multidimensional data is essential for gaining meaningful insights into the chemical systems under study.

## 2.5

### **High-performance liquid chromatography**

High-performance Liquid Chromatography (HPLC) is a widely used analytical technique for separating, identifying, and quantifying components in a complex sample. Its theoretical principles involve the separation of compounds based on their different interactions with a stationary phase (chromatographic column) and a mobile phase (partition between these phases). Among the different stationary phases, two main types are generally used: normal phase and reverse phase (NP-HPLC and RP-HPLC, respectively). Reverse phase chromatography (characterized by less polar stationary phases) is more commonly used due to its versatility and applicability to a wider range of analytes. However, RP chromatography may not be suitable for analyzing highly nonpolar compounds, as they will be retained in the stationary phase, or samples containing high concentrations of organic solvents, such as oily samples [53].

The elution order of components depends on the interaction of the analyte with the medium, including the sample solvent, the mobile phase, and the stationary phase. For RP-HPLC methods, the most common mobile phases include methanol, tetrahydrofuran (THF), and acetonitrile (ACN). The choice of solvent influences the strength of interactions between analytes and the stationary phase, thereby affecting the speed and efficiency of separation. However, when choosing THF as a mobile phase, it's important to consider its potential reactivity with water, which can lead to the formation of peroxides and adversely affect the column and analytes [54].

The composition, flow rate, and elution mode of the mobile phase (isocratic or gradient) can affect the separation process, but the solvent in which the sample is diluted (solvent sampling) can also affect the separation. The solvent's polarity can influence the interactions between analytes and the stationary phase, impacting their retention times and resolution. Additionally, the viscosity and volatility of the solvent can affect the efficiency of the chromatographic process. Therefore, it is crucial to choose a diluent solvent that is compatible with the chromatographic system and does not adversely affect the separation or detection of analytes. Often overlooked, this should be one of the points to be optimized in the HPLC method development process [55].

Considering the detection systems, different options can be employed. Absorptiometric and fluorometric detection are the most commonly used due to their versatility, sensitivity, and wide applicability to various types of analytes. One of the main advantages of fluorescence detectors compared to absorbance detectors is the potential for improved sensitivity, which can reach up to three orders of

magnitude, and selectivity, as two wavelengths need to be selected (excitation and emission).

### 3

## Material and Methods

### 3.1

#### Experimental

##### 3.1.1

#### Reagents and chemicals

Commercial grapefruit (*Citrus paradise*), lemon (*Citrus limonum*), sour orange (*Citrus aurantium*), sweet orange (*Citrus sinensis*), and tangerine (*Citrus reticulata*) EOs, from the same Brazilian brand, were sourced locally in Rio de Janeiro. Eight other Brazilian orange EOs (*Citrus aurantium* and *Citrus sinensis*, Brazil), from different manufacturers, were also used for discriminant analysis. To facilitate the discussion of results, the orange EOs were codified from EO-01 to EO-09. A summary with relevant information of these samples (EO-01 to EO-09) is presented in Table 3.1. Commercial canola and mineral oil (respectively, refined and pure oils obtained in a local market, Rio de Janeiro, Brazil) were used as adulterant. Chemicals selected to prepare MEs were ultrapure water (from the Milli-Q gradient A10 ultra-purifier – Millipore, USA), octan-1-ol (Neon, Brazil) and propan-1-ol (Vetec, Brazil). For chromatographic analyses, HPLC grade solvents, including methanol (Merck, Germany), ethanol (Dinâmica, Brazil), propan-1-ol (Vetec, Brazil), octan-1-ol (Sigma-Aldrich, USA), and acetonitrile (Merck, Germany) were used. The 2H-chromen-2-one was purchased from Ambeed, while heptamethoxyflavone, nobiletin, and sinensetin were purchased from TargetMol, USA. Scutellarein and tangeretin were purchased from TCI, USA.

**Table 3.1.** Summary with relevant information of the orange EO (originated from Brazil) used in this work. Each code represents a different brand.

Code	Specie*	Variety**	Cultivation	Extraction process	Relative commercial value <sup>b</sup>
EO_01	<i>Citrus aurantium</i>	<i>dulcis</i>	conventional	cold pressing	2×
EO_02	<i>Citrus aurantium</i>	<i>dulcis</i>	conventional	cold pressing	2×
EO_03	<i>Citrus aurantium</i>	<i>dulcis</i>	conventional	cold pressing	2×
EO_04	<i>Citrus aurantium</i>	<i>dulcis</i>	conventional	cold pressing	2×
EO_05	<i>Citrus aurantium</i>	<i>dulcis</i>	conventional	cold pressing	1×
EO_06	<i>Citrus sinensis</i>	<i>dulcis</i>	conventional	cold pressing	2×
EO_07	<i>Citrus sinensis</i>	<i>dulcis</i>	conventional	cold pressing	2×
EO_08	<i>Citrus sinensis</i>	<i>dulcis</i>	organic	cold pressing	7×
EO_09 <sup>b</sup>	<i>Citrus sinensis</i>	<i>pera</i>	conventional	cold pressing	2×

\* According to the product label. The names '*Citrus aurantium*' and '*Citrus sinensis*' are used to describe the same species associated with sweet orange. <sup>b</sup>Relative value based on the lowest cost sample. \*\* Orange essential oil derived from a different variety than the others (Valencia orange).

### 3.1.2

#### Instruments and apparatuses

Fluorescence measurements were made on a PerkinElmer (USA) LS 55 luminescence spectrometer equipped with a red-sensitive R928 photomultiplier detector (Hamamatsu, Japan). Neutral density filters with transmittance nominal values of 1%, 25%, 50%, and 90% (Newport, USA) were used to attenuate the fluorescence when saturation of the detector occurred. Absorbance measurements were made on a Varian Cary 100 spectrophotometer (Australia). In order to obtain the hydrodynamic radius of droplets, dynamic light scattering (DLS) experiments were performed using a SZ-100 Nanopartica, Horiba (Japan), equipped with a 10 mW laser at 532 nm. Refractive index measurements were carried out on an Abbe refractometer (RMI/RMT, Bel Photonics, Italy). A Gay-Lussac pycnometer and Cannon-Fenske viscometer were used to determine density and kinematic viscosity at 25°C, respectively. A low-frequency electrical conductivity meter (SevenCompact S230, Mettler Toledo, Switzerland), equipped with an inLab 741-ISM electrode (Mettler Toledo, Switzerland), was used for electrical conductivity measurements. In order to evaluate the ME formation regions, titrations were monitored using a portable scale (SuFeng, 0.01 g accuracy) and system homogenization was performed using a Vortex mixer (NA3600, Norte Científica, Brazil). Centrifuge BE 4000 Brushless (Bio-Eng, Brazil) was used to study the stability of the systems. High-performance liquid chromatography (HPLC) analyses were performed on Agilent 1200 series HPLC (Agilent Technologies, Japan) equipped with degasser, binary pump, autosampler, column oven, and absorbometric diode-array and fluorescence detectors (DAD and FD, respectively). The separation was conducted employing an Agilent Eclipse XDB C18 column (4.6

× 250 mm, 5 µm particle size). An ultrasonic bath Q9.5/40 model (Ultronique, Brazil) was used for degassing solvents employed as mobile phases. Borosilicate glass microfiber membrane (0.2 µm, Whatman, UK) was used to filter the mobile phase solvents. PTFE syringe filters (0.45 µm, Macherey-Nagel, Germany) were used to filter samples before HPLC analyses. The Shimadzu AUW220D semi-micro analytical weighing balance, with a sensitivity of ± 0.1 mg (Shimadzu Corp., Japan), was employed for preparing standard stock solutions. All used equipment is located at PUC-Rio except for the low-frequency electrical conductivity meter that belongs to IFRJ (Realengo *campus*).

### 3.1.3

#### Software programs

The FL WinLab software (PerkinElmer, USA), Cary WinUV (Varian, Australia), and ChemStation (Agilent, Japan) software were used to control the instruments (luminescence and absorbance spectrophotometers and liquid chromatography system respectively) and collect data. OpenLab LC ChemStation software (Agilent Technologies, Japan) was used for data acquisition and treatment. Origin software (OriginPro version 2022b, OriginLab Corporation, USA) was applied for the treatment of conductivity data, for assembling figures (except for the pseudoternary diagram). The open source RStudio software (RStudio Inc. version 4.1.3, RStudio Team, USA) was used for pseudo-ternary phase diagrams creation (Package: ggtern, see supplementary material A [56,57]), EEM pre-processing, which includes blank removal, Raman normalization and Rayleigh scattering removal (Packages: dplyr, tidyr, eemR and stardom, see supplementary material B [49,50,58–60]) and chemometric treatment of the unfolded data by PCA

(Packages: ggplot2, factoextra, pca3D and scatterplot3d). For chemometric treatment, Origin software was used in conjunction for a more comprehensive analysis, including EEM data unfolding and PCA refolding.

## **3.2**

### **Procedures**

#### **3.2.1**

##### **Sample storage conditions**

In order to maintain the integrity of the samples, all EOs used in this study, with the exception of the samples used for the evaluation of storage conditions and adulteration by addition of vegetable oils, were stored in their original bottles, protected from light, and refrigerated ( $-20^{\circ}\text{C}$ ) until analysis. To evaluate the effect caused by improper storage, two portions of 1 mL of orange EO were stored, under different conditions, for 21 days. One portion was stored in a sealed amber flask, protected from light at temperatures between  $(22 \pm 1)^{\circ}\text{C}$ . The second portion was also stored in a sealed flask, but under sunlight with no temperature control (within  $25\text{-}35^{\circ}\text{C}$  range, according to the weather forecast). With the purpose of evaluating the method ability to detect adulteration due to a non-volatile oil addition, canola and mineral oil were used as adulterant at four different levels: 1, 5, 10 and 20% (in weight). The brand codified as EO\_01 (Table 3.1) was the sample used during these experiments.

### 3.2.2

#### **SFME formation regions**

The formation regions of the SFMEs systems were evaluated for the sweet orange EOs by preparing binary mixtures with water (W) in five different W:EO proportions (1:4, 1:2, 1:1, 2:1, 4:1, w/w) and subsequent titration with an alcoholic mixture of propan-1-ol:octan-1-ol, 10:3 w/w. The starting weight of citrus EO was adapted according to the capacity of the glass flasks employed (3 mL), varying of 0.1 g (for MEs with smaller proportions of EO) to 0.4 g (for MEs with higher proportions of EO).

The weight was determined after each addition of the alcoholic mixture, using a portable balance. The procedure was stopped after the spontaneous formation of a single-phase and homogeneous system. The systems were mixed by a Vortex for 10 s. The phase boundary points were obtained visually observing the systems to check for optical transparency (or turbidity due to instability that leads to phase separation). Each experiment was conducted in triplicate, at room-temperature. Results were organized in spreadsheets, from which pseudo-ternary phase diagrams were constructed for better organization and evaluation of SFME systems formation regions [37].

For each tested system, after homogeneity is achieved by the addition of the alcoholic mixture, the thermodynamic stability was evaluated at two different temperatures (4°C, 25°C). The systems were monitored for phase separation, flocculation, or precipitation for two weeks (daily observations). After the first two weeks, they were monitored once a week for six months. Stability tests were also

conducted by subjecting the systems to centrifugation (1080 RFC for 20 min) with any change in their homogeneity observed by visual inspection after centrifugation.

### 3.2.3

#### **SFME Structural characterization**

All evaluated orange EO MEs were characterized, regarding the organization of the systems, by using conductivity measurements at 25°C. For this experiment, octan-1-ol was considered as part of the oil phase. As will be explained further in Chapter 4 (subsection 4.2.2), a mixture containing EO and octan-1-ol was added to a mixture of propan-1-ol and water. The components proportions used for each fraction (oily and aqueous) were equivalent to each evaluated system. These combinations were established after the SFME systems formation as previously described (subsection 3.2.2). A drop test was also made by carefully adding a drop of each ME in the aqueous phase (in this case ultrapure water) and oil phase (in this case the orange EO) separately, then observing the dispersion capacity of the added drop. In this test, it is expected that O/W MEs disperses promptly in aqueous phase, while W/O systems are more compatible, easily dispersing, in the oil phase.

Extreme conditions for W:EO:Alcoholic mixtures (at 1:4:7.5 and 4:1:12.1, w/w/w) were also evaluated in terms of the hydrodynamic radius of dispersed objects. A volume of 2.5 mL of each sample was placed in a polystyrene cuvette (four optically clear sides and path length of 10 mm). Measurements were made 1 h after manual homogenization (60 s) in ten replicates, at 25 °C and at an angle of 90°. Previously, the MEs were filtered using 0.45 µm PTFE syringe filter (Sigma-Aldrich, USA) to remove dust particles. Refractive index, density and kinematic viscosity were measured at 25°C.

### 3.2.4 SFME preparation for 3D fluorescence spectroscopy analysis

For the first study (Chapter 4), the five boundary conditions established from the evaluated W:EO weight proportions (4:1, 2:1, 1:1, 1:2, and 1:4) were used. A summary of these conditions is provided in Table 3.2.

**Table 3.2.** Conditions established for SFMEs systems used for fingerprinting analysis of orange essential oils by 3D fluorescence spectroscopy.

<b>Weight proportion</b>		
<b>Water</b>	<b>Essential oil</b>	<b>Alcoholic mixture (propan-1-ol:octan-1-ol, 10:3 w/w)</b>
1	4	7.5
1	2	5.5
1	1	4.5
2	1	7.3
4	1	12.1

In the second study (Chapter 5), new SFME systems were optimized and replicated for other citrus EOs (sweet and sour orange, tangerine, lemon, and grapefruit). As will be explained further, these new systems take into consideration that octan-1-ol acts as a diluent in the oily phase rather than as an amphiphilic solvent as originally thought in the initial experiments. In this case, 19 mL of ultrapure water and 15  $\mu$ L of the oily phase, consisting of EO diluted in octan-1-ol (1:2, v/v), were added to a 25 mL volumetric flask (Figure 3.1). The final volume was adjusted with propan-1-ol, followed by manual agitation. These systems were also monitored (in triplicate) for three months (at 4 and 25°C), and thermodynamic stability was evaluated by subjecting the systems to centrifugation (1080 RFC, 20 min).

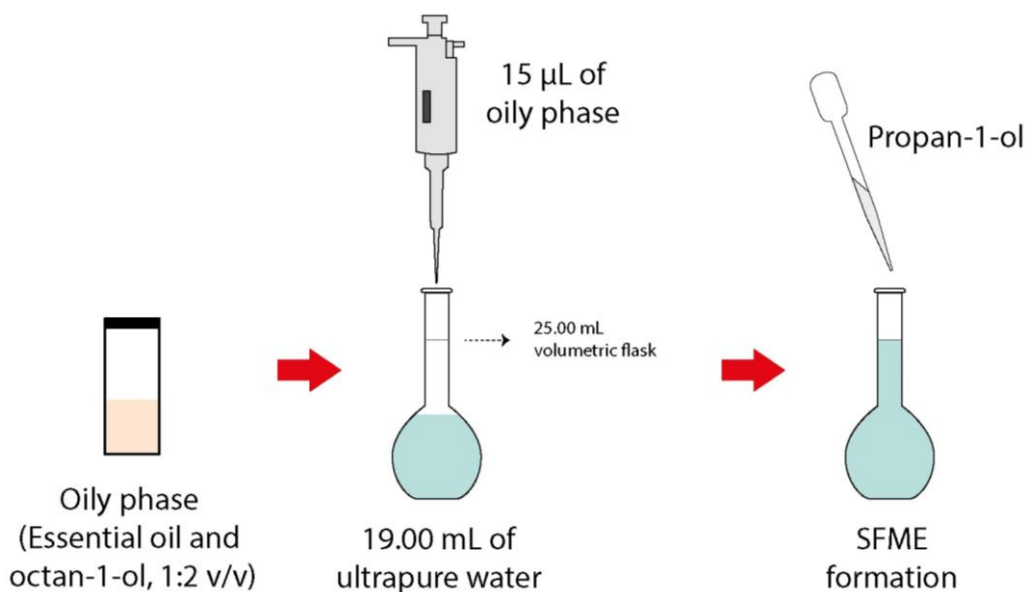


**Figure 3.1.** Illustrative scheme of the SFMEs conditions used for discriminant analysis of *Citrus* essential oils. The colors in the image are purely illustrative.

### 3.2.5

#### Spectroscopy analysis and data pre-processing

##### 3.2.5.1

##### Obtention of fingerprint patterns for sweet orange essential

In the first study (Chapter 4), fingerprint patterns were evaluated for pure orange EO, and in SFME systems (at five different weight proportions of water and EO as described in Table 3.2) to choose the best condition for discriminant analysis. Preliminary studies, using sweet orange EO, were performed using a larger excitation ( $\lambda_{\text{ex}}$  from 250 to 600 nm with steps of 5 nm) and emission ( $\lambda_{\text{em}}$  from 300 to 650 nm with steps of 0.5 nm) wavelengths. Emission and excitation spectral band widths were set at 10 nm, and a scan rate of 1500 nm min<sup>-1</sup> was chosen for the emission monochromator with measured values in arbitrary units (a.u.). When required, neutral density filters (Newport, USA) with nominal values of 25% of

transmittance were used to attenuate measured fluorescence when saturation of the detector occurred. Initial experiments were made by selecting a restrict wavelength range to be used for discriminant analysis, where  $\lambda_{\text{ex}}$  were recorded between 300 and 400 nm (steps of 10 nm), and with  $\lambda_{\text{em}}$  between 420 and 545.5 nm (steps of 0.5 nm). Experiments were performed using a 3 mL quartz cuvette.

Before chemometric treatment, Raman normalization was applied to adjust measurements and to minimize instrumental effects. Then, fluorescence signal, obtained in arbitrary units (a.u.) was converted for Raman units (R.u.) [47]. In this case, measurements using ultrapure water were performed daily (in triplicate), using a large excitation (250 to 600 nm, each 10 nm) and emission (300 to 650 nm, each 0.5 nm) wavelength range, as needed for blank subtraction and Raman normalization. Analysis was also carried out with propan-1-ol and octan-1-ol as well to ensure that neither of them displayed fluorescence within the wavelength range used in the study.

### 3.2.5.2

#### Discriminant analysis of citrus essential oils

In the second study (Chapter 5), for the optimization experiments, the fluorescent signal intensities were acquired at 336/436 nm (excitation and emission wavelengths,  $\lambda_{\text{ex}}/\lambda_{\text{em}}$ ). With this purpose, emission fluorescence spectra (360 to 500 nm) were obtained with excitation fixed at 336 nm with 10 nm spectral bandpass (excitation and emission) and 1500 nm min<sup>-1</sup> scan rate. The same parameters were used in the last study (Chapter 6) for spectrofluorimetric analyses employed to determine the optimal excitation and emission wavelengths ( $\lambda_{\text{ex}}/\lambda_{\text{em}}$ ) for the evaluated PMFs (tetra-*O*-methyl-scutellarein, sinensetin, tangeretin, nobiletin, and

heptamethoxyflavone) in ethanol (standard solutions at 100 mg L<sup>-1</sup>). To evaluate the presence of the inner filter effect [48], absorbance spectra (300 to 600 nm) were acquired with scan rate of 300 nm min<sup>-1</sup> and data interval of 0.5 nm.

For discriminant analysis, SFMEs systems (Figure 3.1) were reproduced for each evaluated citrus EO and analyzed by 3D fluorescence spectroscopy using 3 mL quartz cuvette. Excitation spectra were recorded between 200 nm and 650 nm ( $\lambda_{ex}$ ) with increasing steps of 10 nm, whereas the emission wavelengths were recorded from 280 nm to 700 nm ( $\lambda_{em}$ ) with increasing steps of 0.5 nm. Emission and excitation spectral bandpasses were set at 10 nm, and scan rate of 1000 nm min<sup>-1</sup> was selected for the emission monochromator. The raw data were obtained in arbitrary units (a.u.). For sweet orange EO, a 50% transmittance (nominal value) neutral density filter (Newport, USA) was used. For the other CEOs (grapefruit, lemon, sour orange, and tangerine) a 1% transmittance (nominal value) neutral density filter (Newport, USA) was required. Data pre-treatments were carried out using blank subtraction and scattering removal.

For chemometric treatment, 10 replicates of each sample were used. In order to reduce total analysis time, excitation spectra were recorded between 200 nm and 400 nm with increasing steps of 10 nm, and emission wavelengths ranged from 340 nm to 550 nm with increasing steps of 0.5 nm. Data pre-treatments were carried out using Raman unit (R.u.) conversion (25), blank subtraction and scattering removal. For this, measurements were made, using ultrapure water in a 3 mL quartz cuvette, at 200-650 nm with increasing steps of 10 nm (excitation) and 280-700 nm with increasing steps of 0.5 nm (emission).

### 3.2.6

#### Unfold principal component analysis (UPCA)

In order to demonstrate clustering of samples based on spectral similarities/differences, 3D fluorescence analysis was associated with UPCA using excitation-emission matrices (EEM) pre-processed with blank subtraction, Rayleigh scattering removal, and Raman normalization. All EEM data, after pre-processing, were unfolded, and rearranged into a two-dimensional matrix, and a principal component analysis (PCA) was performed with variables centered and scaled for better accuracy. Results were evaluated using the principal components (PCs) and cumulative variance to estimate the method accuracy.

### 3.2.7

#### Chromatographic analysis

##### 3.2.7.1

#### Standard solutions preparation

Standard stock solutions were prepared for five PMFs (tetra-*O*-methylscutellarein, sinensetin, tangeretin, nobiletin, and heptamethoxyflavone) at 1.0 mg mL<sup>-1</sup> in ethanol. These solutions were used to prepare individual standards, at 0.1 mg mL<sup>-1</sup> (100 mg L<sup>-1</sup>), used for monitoring the optimal excitation and emission wavelengths ( $\lambda_{\text{ex}}/\lambda_{\text{em}}$ ) by spectrofluorimetry. A mixture with PMFs, at 100 mg L<sup>-1</sup>, was also prepared from the stock solution, and used during the assessment of solvents for sampling in HPLC analyses.

Once the optimal conditions were determined, a new stock solution containing the same PMFs, at 100 mg L<sup>-1</sup>, was prepared using a mixture of methanol

and octan-1-ol (at 2:1, w/w proportion). From this solution, samples with different concentrations, ranging from 0.01 to 100 mg L<sup>-1</sup>, were obtained for analytical curve construction. This wide working range was necessary due to the difference in responses obtained using two detectors (absorption in a DAD and fluorescence). Before the final volume adjustment, 50 µL of internal standard (I.S.) solution (chromen-2-one at 10 mg mL<sup>-1</sup>) were added to each sample and standards at a final concentration of 0.1 mg mL<sup>-1</sup> (100 mg L<sup>-1</sup>).

### 3.2.7.2

#### Sample preparation

Sweet orange EO (100 µL) was transferred to a 5.0 mL volumetric flask. To evaluate the influence of the medium used for sampling, the final volume was adjusted using acetonitrile, methanol, and ethanol and a mixture of methanol:octan-1-ol at 10:3 (w/w); 10:1 (w/w) and 2:1 (w/w).

After selecting the best solvent for sampling (methanol:octan-1-ol, 2:1, w/w), new samples of sweet orange EO (100 µL) were prepared in six authentic replicates by adding the I.S. (50 µL of chromen-2-one at 10.0 mg mL<sup>-1</sup> for 5.0 mL final volume) for the monitoring and quantification of five evaluated PMFs (tetra-*O*-methyl-scutellarein, sinensetin, tangeretin, nobiletin, and heptamethoxyflavone). Before HPLC analysis, samples were filtered using PTFE syringe filters (0.45 µm).

### 3.2.7.3

#### HPLC procedures

Chromatographic analyses were carried out under isocratic elution at 1.0 mL min<sup>-1</sup> flow rate and column oven temperature set to 30°C. The response was evaluated using two different mobile phases: methanol/water at 73:27% v/v (Method A) and acetonitrile/water at 50:50% v/v (Method B). For the analysis of sweet orange EO samples, a cleaning procedure (4 min) with 100% organic solvent (methanol or acetonitrile, depending on the mobile phase used) followed by a re-equilibration time with the respective mobile phase (2 min) was applied between each sample introduction. Given the high complexity of the sample compositions, this cleaning process ensured the fidelity of results. Chromatograms were recorded at 330 and 336 nm using absorciometric detection and at 336/436 nm for the fluorescence detection. The volume of sample introduced was 10.0 µL. All monitored PMFs exhibited retention times below 12 min for both mobile phases. A summary of the conditions for each method is provided in Table 3.3.

**Table 3.3.** Conditions employed in HPLC methods used for the determination of polymethoxyflavones using C18 column (4.6 × 250 mm, 5 µm particle size).

Parameters	Condition chosen	
	Method A	Method B
Injection volume	10.0 µL	
Flow rate	1.0 mL min <sup>-1</sup>	
Mobile phase	methanol/H <sub>2</sub> O (73:27%, v/v)	acetonitrile/H <sub>2</sub> O (50:50%, v/v)
Column temperature	30°C	
Detectors*	DAD (336 nm) and FD (336/436 nm)	

\* DAD: diode array detector (absorciometric detector); FD: fluorescence detector.

In the second study (Chapter 5), HPLC analysis was used as a complementary technique to corroborate the hypothesis that the response obtained after spectrofluorimetric analysis originated from compounds present in the non-volatile fraction of citrus EOs. In this case, to adapt the analytical conditions for all samples, some parameters were adjusted, such as injection volume (5.0  $\mu\text{L}$ ) and mobile phase. Ultrapure water (A) and acetonitrile (B) were used as the mobile phase with a linear gradient (0–7 min, 50% B; 7–13 min, 50–60% B; 13–15 min, 60–80% B; 15–17 min, 80% B; 17–20 min, 80–100% B; 20–25 min, 0% B; 25–27 min, 100–50% B; 27–30 min, 50% B). Chromatograms were acquired using diode array photometric absorption (210–400 nm, at 330 nm) and fluorescence (336/436 nm) detectors. A specific condition was also established for the SFME systems: 60  $\mu\text{L}$  of a mixture containing EO and octan-1-ol (1:2, volume proportion), 2 mL of ultrapure water, and propan-1-ol up to 5 mL.

#### 3.2.7.4

##### Method validation

Analyses were carried out in triplicate using a mixture containing five PMFs (tetra-*O*-methyl-scutellarein, sinensetin, tangeretin, nobiletin, and heptamethoxyflavone) in the range 0.01 to 100  $\text{mg L}^{-1}$  at nine different concentrations (0.01, 0.05, 0.10, 1.00, 5.00, 10.00, 25.00, 50.00, and 100  $\text{mg L}^{-1}$ ). All samples were fortified with chromen-2-one (I.S.) at final concentration of 100  $\text{mg L}^{-1}$ . The linearity range was evaluated for each analyte separately by determining the coefficient of determination ( $R^2$ ) extracted from the linear regression (simple least-square method) of the analytical curves.

The lowest detectable concentration of each analyte was measured in ten replicates. From these signal measurements, the standard deviations ( $s_b$ ) were used to calculate the signals corresponding to the limit of detection (LOD) and limit of quantification (LOQ), according to the Equations 3.1 and 3.2. Ten analyte LOD and LOQ values were calculated from the respective analytical curves.

$$LOD = 3s_b \quad (\text{Eq. 3.1})$$

$$LOQ = 10s_b \quad (\text{Eq. 3.2})$$

Inter-day precision was calculated from experiments performed in two consecutive days at the same concentration level ( $5 \text{ mg L}^{-1}$  in 10 replicates). The paired t-test at a 95% level of significance was performed to compare the mean absorbance of the samples.

## 4

### **Fingerprinting pattern of orange essential oils in surfactant-free microemulsion by 3D fluorescence spectroscopy**

Paper published as “*Fingerprinting pattern of orange essential oils in surfactant-free microemulsion by 3D fluorescence spectroscopy*”. R.C. Macedo, M.J. Pedrozo-Peñafiel, A.L.M.C. da Cunha, R.Q. Aucelio, *Food Chemistry Advances*, 3 (2023) 100482.

DOI: 10.1016/j.focha.2023.100482 (see attachment I).

#### 4.1

##### **Introduction**

Essential oils (EOs) are complex mixtures of secondary metabolism products of plants, playing an important role in the plants defense against microorganisms, often presenting antibacterial, antifungal, antiviral and insecticidal activities [61,62]. About 10% of the 3000 established EOs have commercial value [63] being the orange EO considered the most popular [10,64], presenting many biological activities, and wide range of applications [65,66]. The great demand, coupled with the high market value, makes investment in quality control of EOs crucial to guarantee traceability, authenticity, and shelf life under proper storage conditions [4,16].

Gas chromatography in combination with mass spectrometry (GC-MS) is the most commonly used technique to monitor EOs authenticity. Physical characteristics (specific gravity, refractive index, optical rotation, and solubility) are also used as reference for quality control [16,17]. But, despite the large number

of publications on the matter, it is essential to develop complementary methods with better cost-benefit in terms of implementation of screening of samples and routine assays with high analytical frequency. In this context, spectroscopic techniques can also be useful for traceability, authentication, and monitoring of EOs, for instance using absorption of infrared [67–77] and Raman spectroscopies [67,69,75,76,78–84]. Fluorimetric analysis is another alternative, but less frequently used (Table 4.1). Feudjio et al. (2014) [85] detected the characteristic fluorophores in 14 Tunisian EOs, also finding that oils of the same species have similar luminescent profiles. The same group [86] used fluorescence spectroscopy to discriminate pure EOs from their respective adulterated samples, showing the potential of the technique in discriminating pure samples from counterfeit. Finally, Al Riza et al. (2019) [87] used fluorescence spectroscopy to obtain fingerprinting of Indonesian patchouli EO samples from different geographical origins. In all of these works, it was necessary to use chemometrics, for instance, unfold principal component analysis (UPCA) and parallel factor analysis (PARAFAC) [85], artificial neural networks (ANNs) [86] and the standard principal component analysis (PCA) [87] in order to extract the information required for proper discrimination due to similarities between the spectra obtained for samples.

Typically, EOs are complex mixtures comprising of up to 400 chemicals in their composition, which vary depending upon factors such as plant origin, environment, the way they were produced and storage condition [11]. However, for orange EO, about 90% of total weight is constituted by limonene [88] making discriminant analysis even more difficult, since the differentiation relies on the proportion of minority constituents. Thus, the detection capability of small variations, in terms of composition, is crucial to achieve success in such type of

analysis, not to mention the advantage of using lower amounts of samples for analysis (very important issue as EOs have a high market value). One way to increase the sensitivity is to carry out fluorescence analysis in organized media, through the proper choice of microemulsion (ME) systems that provide low fluorescence background.

**Table 4.1.** Comparison of methods reported in the literature for the essential oil analysis by excitation-emission matrix (EMM) fluorescence spectroscopy coupled to chemometrics.

Ref.	Essential oil	Study objective	Sample preparation	Excitation / Emission range (nm)	Data pre-processing	Chemometric treatment(s)*
[85]	Thyme ( <i>Thymus vulgaris</i> ) Mint ( <i>Mentha piperita</i> ) Myrthe ( <i>Myrtus communis</i> ) Neroli ( <i>Citrus aurantium L.</i> ) Orange ( <i>Citrus sinensis</i> ) Rosemary ( <i>Rosmarinus officinalis L.</i> ) Schinus ( <i>Schinus terebinthifolius</i> ) Wormwood ( <i>Artemisia absinthium L.</i> ) Lavander ( <i>Lavandula angustifolia</i> ) Ginger ( <i>Zingiber officinalis</i> )	Fingerprinting pattern, and fluorophores identification.	n.a.	320-600/ 340-700	Correction of instrumental biases, and Rayleigh scattering removal.	UPCA PARAFAC
[86]	Neroli ( <i>Citrus aurantium</i> ) Peppermint ( <i>Mentha piperita</i> ) Black pepper ( <i>Piper nigrum</i> ) Petit grain ( <i>Citrus aurantium</i> ) Ginger ( <i>Zingiber officinalis</i> )	Detection of adulteration.	n.a.	280-600/ 300-700	Correction of the fluctuation of the excitation compartment's transmittance, and Rayleigh scattering removal.	ANNs
[87]	Patchouli ( <i>Pogostemon cablin</i> )	Authentication of the geographical origin (8 different regions).	n.a.	280-680/ 300-700	Raman unit conversion	UPCA
Present work	Sweet Orange ( <i>Citrus aurantium</i> or <i>Citrus sinensis v. dulcis and pera</i> )	Fingerprinting pattern, and traceability, storage conditions, and adulteration, evaluation.	SFME (low sample consumption)	300-400/ 420-545,5	Blank subtraction, Rayleigh scattering removal, and Raman unit conversion.	UPCA

\* ANN – Artificial neural network; MLP - Multilayer perceptron; PARAFAC - Five components parallel factor analysis; SFME – Surfactant-free microemulsion; SOM – Self-organized map; UPCA - Unfold principal component analysis.

MEs are dispersions formed by two immiscible liquids, usually oil and water, stabilized in the presence of a surfactant, associated or not with a co-surfactant. The amphiphilic character of the surfactant (that conjugate more polar and a less polar groups within its structure) allow it to be adsorbed at the interface of two immiscible components (due to affinity with hydrophilic groups, located in the aqueous phase, and with hydrophobic groups, present in the oil phase), thus reducing incompatibility as organization is established [89]. MEs are characterized by being fluid, thermodynamically stable and optically isotropic, due to the small size (down to the nanometer) of the formed droplets [90]. When alcohols are used as amphiphilic solvents, to promote the thermodynamic stabilization between oily and aqueous phases, these systems are called surfactant-free microemulsions (SFME) [25]. Alcohols, such as ethanol and isopropanol, for instance, have good solubility in the nonpolar and polar phases, being able to promote interaction between them (miscibility that enables optical transparency) [37].

The structure of SFMEs can be classified as water in oil (W/O), when droplets of aqueous phase are dispersed in the oil phase; oil in water (O/W), when the inverse situation occurs; but it is also possible to find bicontinuous (BC) MEs, when oil and water are both continuous phases [37]. Considering W/O and O/W ME systems, the formation of small droplets (on a nanometric scale) creates a microenvironment capable of restricting the vibrational degree of freedom of the luminophores present in the dispersed phase. These circumstances can result in a reduction in non-radiative processes and, consequently, an amplification of the fluorescence intensity signal [42]. Based on these considerations, for this work, it is expected that the formation of O/W ME systems will enhance the fluorescence

of the luminophores present in the orange essential oil (dispersed phase, in this case), making these systems more interesting for fingerprint pattern acquisition.

The aim of this work was to evaluate the effect caused by SFME systems in orange EO analysis by 3D fluorescence spectroscopy. By providing better sensitivities in fluorescence response, it is expected to differentiate samples with small variations in terms of composition, allowing discriminant analysis, according to the fingerprinting pattern with a focus on traceability, through of Brazilian EOs samples from nine different brands. In order to evaluate the discriminant capability, UPCA was applied, where the excitation-emission matrices (EEM), obtained from 3D fluorescence, were rearranged into a two-dimensional matrix prior to performing chemometrics.

## **4.2**

### **Results and discussion**

#### **4.2.1**

##### **SFME systems formation**

Preliminary studies were carried out to select conditions to achieve clear and stable MEs, based on visual inspection of the system over time. Initially, the miscibility of orange EO in different alcohols (methanol, ethanol, isopropanol, or propan-1-ol) was evaluated. Then, to a mixture containing EO and water (in a 1:1 w/w proportion) was added these different alcohols attempting to reach a homogeneous and stable system. Combinations with octan-1-ol were also studied and the mixture of propan-1-ol and octan-1-ol (at 10:3, w/w proportion) was chosen to proceed the next steps as it provided satisfactory stabilization of the mixture

containing oil and water, with homogeneity, clarity in appearance, and longer stability (during at least seven days of period of observation). Octan-1-ol is in fact present in orange EO composition [91–93] and the presence of this alcohol may have contributed to a better EO mixing with water. Images showing the results obtained for preliminary studies are presented in Figure 4.1.

In continuity, five mixtures with different proportions of water and EO (W:EO at 1:4, 1:2, 1:1, 2:1, 4:1, w/w) were titrated with the chosen alcoholic mixture (propan-1-ol:octan-1-ol at 10:3, w/w) in order to profile the ME formation region (Figure 4.2). The resultant phase diagram is represented by an equilateral triangle, where each vertex represents 100% (in weight) of one particular component. But, in this case, one vertex represents the chosen alcoholic mixture instead of only one component and, therefore, these diagrams were referred as pseudo-ternary phase diagrams. The behavior of these five chosen W:EO proportions were evaluated during the titration, with the alcoholic mixture, until a homogeneous system was formed. Experimental data showing the mass proportion of components, after addition of the alcoholic mixture, that produced the changing from a cloudy to an optically clear system (with no visual separation of phases), are indicated as dark points in Figure 4.2. Prior to the 3D fluorescence spectroscopic analysis, these obtained optically clear systems were evaluated to assess their stability over time and they were also characterized by conductivity and dynamic light scattering (DLS) measurements.

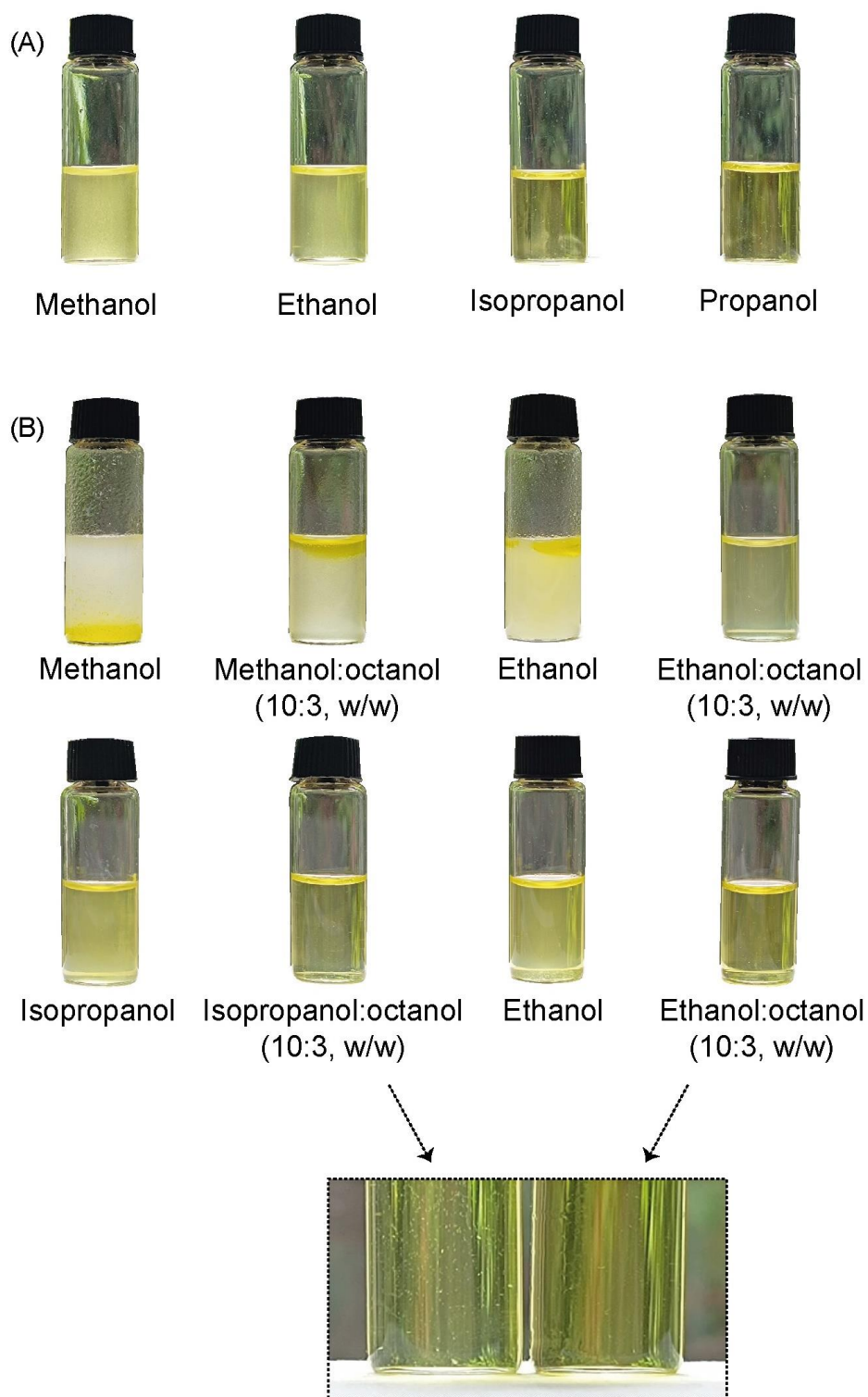


**Figure 4.1.** (A) Miscibility test of orange EO in different alcohols (1:5, EO:Alcohol weight proportion), and (B) Visual aspect of systems containing orange EO and water after adding different alcohols (or alcohol mixes) (1:1:5, EO:Water: Alcohol weight proportion).

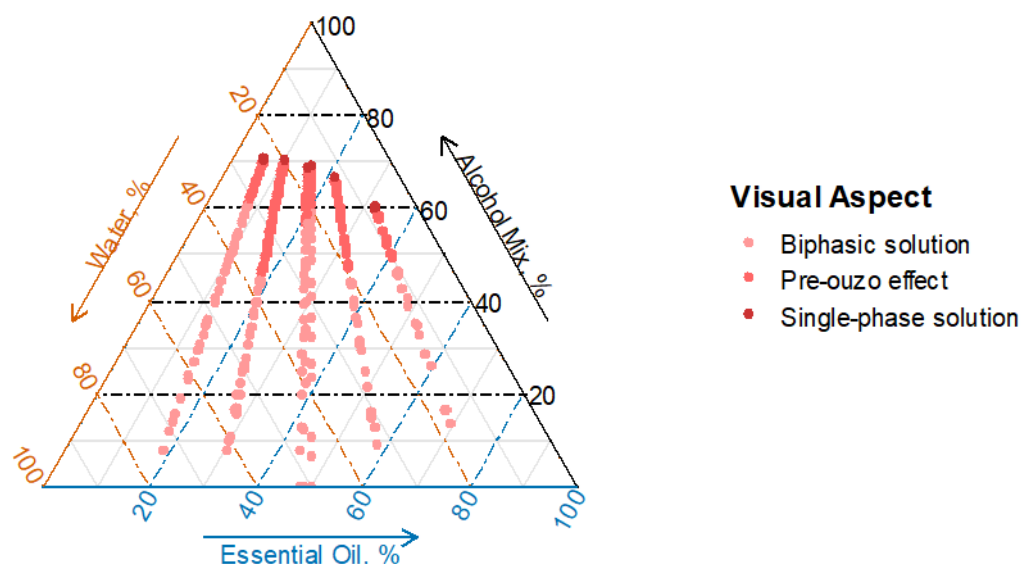


**Figure 4.2.** Pseudo-ternary phase diagram obtained for orange essential oil where each vertex represents 100% (in mass) of a particular component: water, essential oil and alcoholic mixture (propan-1-ol:octan-1-ol at 10:3 w/w).

All of the optically clear systems remained stable (optically clear), at either 4°C or room-temperature (about 25°C), for more than six months, not presenting phase separation, flocculation, precipitation, nor any other visual alteration. In addition, after centrifugation, there were no noticeable changes, demonstrating stability of these formulations against physical disturbance. These results indicate thermodynamic stability of system at all tested conditions, characteristic of MEs [37].

#### 4.2.2

##### SFME structural characterization

Characterizing ME structure as W/O, O/W or BC allows a better assessment on how the organization of dispersed structures affects the fluorescence measured

from samples (EO components in this case) in terms of both intensity and spectral position. In order to evaluate these systems, conductometric titrations were made by increasing the oil content, as reported in the literature for similar systems [34–36]. During this process, as the oil phase is added, the initial increasing in conductivity indicates the formation of O/W MEs. When the conductivity starts to decrease, it was indicative that BC is being formed and, when a linear conductivity decreasing occurs, it is consequence of the formation of W/O system [46]. However, for the chosen conditions in this study, during the titration with EO, it was observed the conductivity values oscillating between the titration points, making it difficult to visualize the phase inversion, especially the change from BC to W/O, which is characterized by a linear decrease in electrical conductivity.

Bošković et al. (2015) [94] reported that ternary systems, formed by water, ethanol, and octan-1-ol tend to form weak micelle aggregates, like a SFME. Therefore, for the systems involved in the present work, both octan-1-ol and EO was treated altogether as the oil phase with conductivity depending not only on the EO fraction, but also when mixed with octan-1-ol. Based on these considerations, the conductometric titrations were repeated with the increasing of both EO and octan-1-ol respecting the proportion of each specific system. During the conductometric titrations, as the oil phase, composed by both EO and octan-1-ol, was added, the initial increasing in conductivity indicated the formation of O/W MEs. When the conductivity started to decrease, it was indicative that BC is being formed and, when a linear conductivity decreasing occurred, it is consequence of the formation of W/O system [34].

According to results (for orange EO), W/O ME occurred for the system with W:EO:Alcohols at 1:4:7.5 weight proportion (Figure 4.3A). The intermediate

conditions (2:1, 1:1, and 1:2, W:EO weight proportions) probably are BC type of MEs, since no linear decay was observed (Figure 4.3B-D). In addition, O/W ME occurred in systems with W:EO:Alcohols at 4:1:12.1 weight proportion (Figure 4.3E). A comparison of the W/O and O/W MEs will be very important for the evaluation of the influence of system organization over the fluorescence measured from EO fluorophore components.

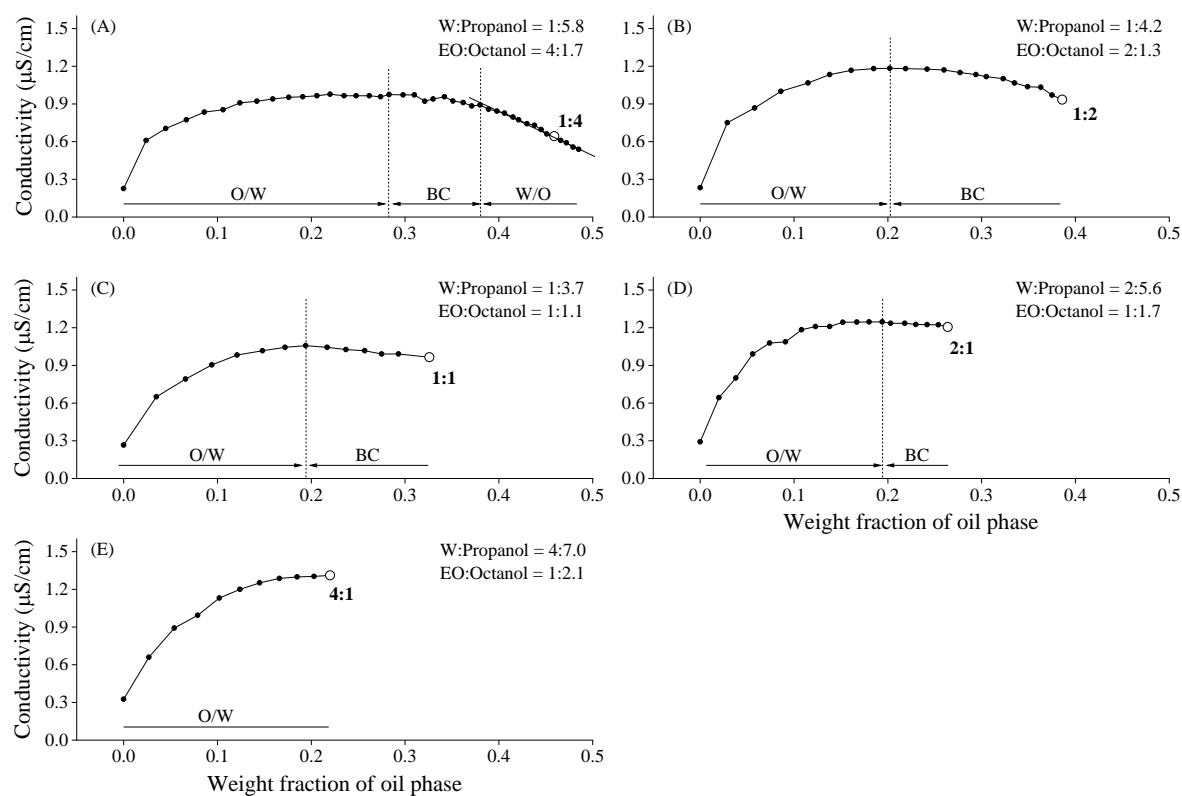


**Figure 4.3.** Variation of the electrical conductivity ( $\mu\text{S/cm}$ ) with the oil weight fraction for the evaluated systems, based on W:EO weight proportions: (A) 1:4, (B) 1:2, (C) 1:1, (D) 1:2 and (E) 1:4. The highlighted points indicate the studied systems. The components weight proportion used as aqueous (W:propan-1-ol) and oil (EO:octan-1-ol) phase are described in each graph.

In addition, the systems were also evaluated using the drop test and the results agreed with what was determined from electrical conductivity measurements. A drop of the system with W:EO:Alcohols at 1:4:7.5 (weight proportion) was promptly solubilized in the oily phase (containing orange EO) as expected for W/O MEs. In contrast, a drop of the system consisting of W:EO:Alcohols at 4:1:12.1 (weight proportion) was readily solubilized in aqueous phase as expected for an O/W ME (Figure 4.4). Drops of the systems for intermediate conditions (1:2, 1:1, and 2:1, W:EO w/w) presented solubility in both phases (aqueous and oily).

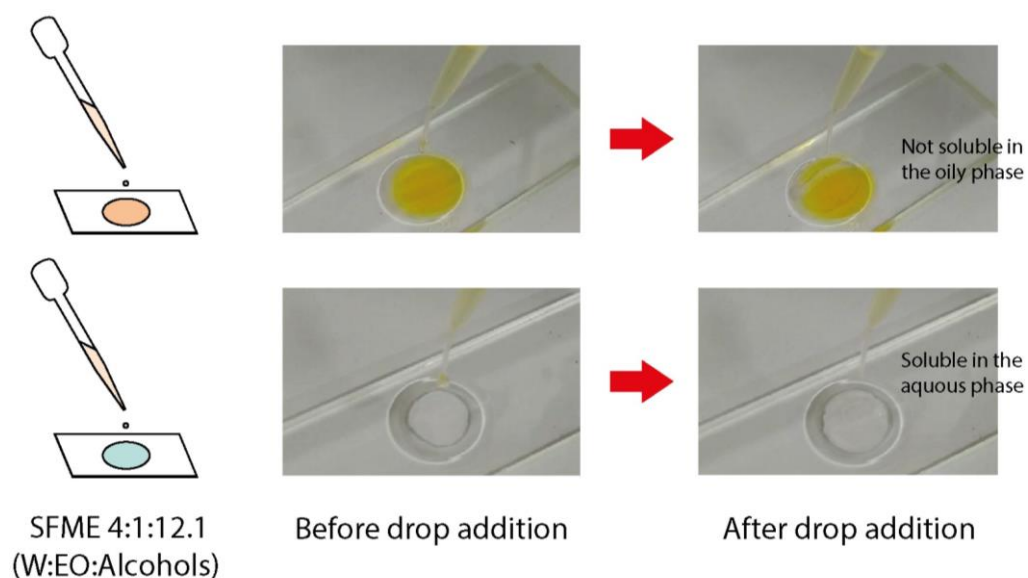


**Figure 4.4.** Drop test conducted for sweet orange essential oil at a weight proportion of 4:1:12.1, W:EO: Alcohols (w/w). Propan-1-ol:octan-1-ol were used as mixture alcoholic.

After evaluation of the structure, the systems classified as W/O and O/W were also studied by dynamic light scattering (DLS) to obtain information about size of microdroplets through their hydrodynamic radius. ME formed using a W:EO at 1:4 w/w proportion presented average hydrodynamic diameter of  $173 \pm 4$  nm ( $n = 10$ ) while for the W:EO at 4:1 w/w proportion, the average hydrodynamic radius was  $96 \pm 5$  nm ( $n = 10$ ). These results confirmed the presence of disperse droplets and a degree of organization of these heterogeneous but optically clear systems. A summary of the results is presented in Table 4.2. Refractive index, density and kinematic viscosity were also measured for each system. Results are presented in Table 4.3.

**Table 4.2.** Experimental data for the weight proportions of each component, and a summary of physicochemical characterization for the studied systems. In the second column, values within parentheses are the individual weight proportion of propan-1-ol and octan-1-ol in the alcoholic mixture, respectively. Propan-1-ol and octan-1-ol (10:3 w/w) were used as alcoholic mixture.

W:EO*	Alcoholic mixture, n=3	EO (% wt)	Structure**	Particle size** (nm) <sup>b</sup> , n=10
1:4	7.5 ± 0,2 (5.8:1.7)	34.8	W/O	173.3 ± 3.8
1:2	5.5 ± 0,1 (4.2:1.3)	23.5	BC	n.a.
1:1	4.8 ± 0,8 (3.7:1.1)	14.7	BC	n.a.
2:1	7.3 ± 0,1 (5.6:1.7)	9.7	BC	n.a.
4:1	12.1 ± 0,1 (9,3:2.8)	5.8	O/W	95.7 ± 5.3

\* Orange essential oil codified as EO\_01. \*\* Determined by conductivity and drop test. <sup>b</sup> DLS Measurements were used for hydrodynamic radius determination (particle size, nm).

**Table 4.3.** Experimental data for refractive index, density, and kinematic viscosity (25°C) obtained for the evaluated SFME systems and ultrapure water. Propan-1-ol and octan-1-ol (10:3 w/w) were used as alcoholic mixture.

<b>W:EO*:Alcoholic mixture (Weight proportion)</b>	<b>Refractive index</b>	<b>Density (g mL<sup>-1</sup>)</b>	<b>kinematic viscosity (g cm<sup>-1</sup> s<sup>-1</sup>)</b>
1:4:7.5	1.4132	0.83092	3.40 x 10 <sup>-3</sup>
1:2:5.5	1.4078	0.83368	3.75 x 10 <sup>-3</sup>
1:1:4.5	1.4003	0.83618	4.18 x 10 <sup>-3</sup>
2:1:7.3	1.3939	0.83816	4.41 x 10 <sup>-3</sup>
4:1:12.1	1.3895	0.85118	4.75 x 10 <sup>-3</sup>
Ultrapure water	1.3328	0.99701	8.91 x 10 <sup>-4</sup>

\* Orange essential oil codified as EO\_01.

### 4.2.3

#### 3D fluorescence spectroscopy

Preliminary studies exploring a larger excitation (from 250 nm to 600 nm) and emission (from 300 nm to 650 nm) wavelength ranges were performed. Excitation-emission spectra obtained for orange EO systems (at different proportion of components) are presented in Figure 4.5A-F. Based upon fluorescence intensity values (Table 4.4), corrected in function of the percent value of orange EO in each system, it was possible to conclude that there was an improvement in detection of spectral features for systems containing lower oil fraction in their composition. The systems with water and EO at 1:4 (probably, a W/O SFME), 1:2, 1:1 and 2:1 weight proportions presented similar spectral profiles. In contrast, for the system at W:EO 4:1, it was found a significant spectral profile difference, confirming phase inversion towards a O/W system. Due to their optical transparency, lower sample content (5.8% in weight) and a more complex spectral feature, consequence of the presence of three regions with relevant fluorescence intensity values, this condition (W:EO at 4:1 w/w) turned out to be the most attractive for fingerprinting analysis.

The analysis of orange EOs in SFME systems allowed for a reduction in sample consumption, which is advantageous considering the high market value of these products. SFMEs systems also eliminated sample turbidity, making conventional fluorescence measurements viable. For the analysis of highly complex oily matrices, such as EOs, methods developed with this approach often recommend front-face spectrofluorimetry. Additionally, taking into account the practical aspects of the analysis, the chosen condition favored cuvette cleaning, which is a relevant concern for direct analysis of oily samples.

A restricted wavelength range (from 300 to 400 nm for excitation and from 420 to 545.5 nm for emission) was also selected for this study, as highlighted in Figure 4.5F, which eliminated the region of Rayleigh scattering, allowed a significant reduction in data collection time also simplifying datasets used for chemometric treatment.

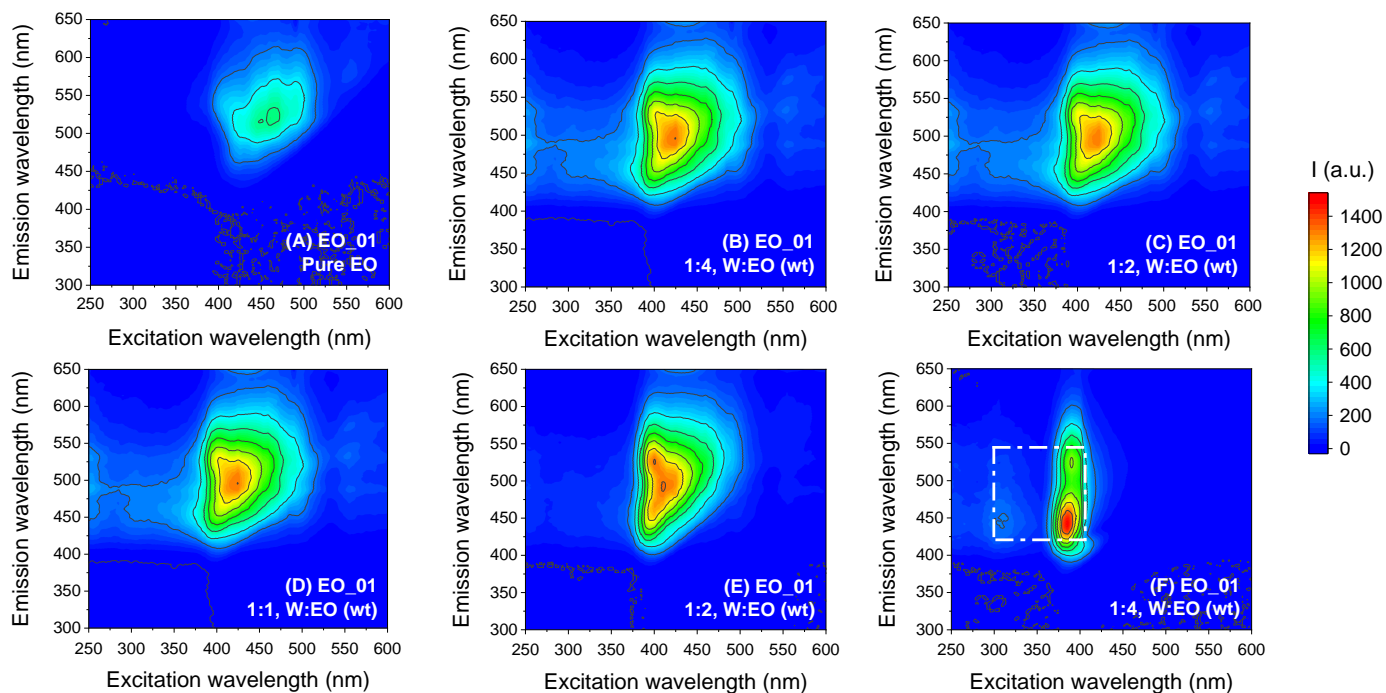


**Figure 4.5.** Contour surfaces ( $\lambda_{ex}$  from 250 to 600 nm and  $\lambda_{em}$  from 300 to 650 nm) obtained from 3D fluorescence spectrometry for orange EO in six different conditions: (A) only EO, and microemulsions in five different combinations, based on W:EO:alcoholic mixture, weight proportions: (B) 1:4:7.5, (C) 1:2:5.5, (D) 1:1:4.8, (E) 2:1:7.3 and (F) 4:1:12.1. The wavelength range used for discriminant analysis is highlighted in (F). Measurements were made using optical filter with 25% of transmittance. Fluorescent intensity values in arbitrary units (a.u.). Blank subtraction and scattering removing by RStudio software (Package: eemR).

**Table 4.4.** Maximum fluorescence intensity (in arbitrary units or a.u.) obtained after orange EO analysis by 3D fluorescence spectroscopy, in five different conditions, based on W:EO weight proportions (1:4; 1:2; 1:1; 2:1; 4:1). Propan-1-ol and octan-1-ol (10:3, w/w) was used as alcoholic mixture. Excitation wavelengths ( $\lambda_{ex}$ ) from 300 nm and 450 nm and emission wavelengths ( $\lambda_{em}$ ) from 430 nm to 550 nm.

<b>W:EO:alcoholic mixture (w/w)</b>	<b>EO (% wt)</b>	<b><math>\lambda_{ex}/\lambda_{em}</math></b>	<b>Measured fluorescence/a.u. (corrected value considering 100% EO)</b>
1:4:7.5	34.8	308/445	415 (1192)
		420/477	1109* (3187)
1:2:5.5	23.5	322/440	581 (2472)
		408/463	1092* (4647)
1:1:4.8	14.7	322/439	732 (4980)
		404/451	1104* (7510)
2:1:7.3	9.7	328/436	842 (8680)
		394/448	1341* (13825)
4:1:12.1	5.8	306/438	730 (10282)
		386/448	1117* (15732)
		390/529	955 (13451)

\* Corrected due to the use of reflectance optical density filters (90 and 50% of transmittance).

#### 4.2.4

##### Unfold principal component analysis (UPCA)

For discriminant analysis by UPCA, after defining the restrict excitation and emission wavelength ranges ( $\lambda_{ex}$  from 300 to 400 nm, and  $\lambda_{em}$  from 420 to 545.5 nm), the experiment was reproduced for nine different Brazilian orange EOs, prepared as SFMEs in the chosen condition (W:EO:Alcohol mixture at 4:1:12.1 weight proportion). A summary of characteristics of samples was presented in Table 3.1. The brand codified as EO\_01 was the EO used during initial experiments (evaluation of ME systems), and in the evaluations of storage condition and adulteration. It is worth mentioning that, except for the oil coded as EO\_09, all other

ones are sweet orange EOs. The names *aurantium dulcis* and *sinensis* are nomenclatures commonly used to describe the same species associated with sweet orange EO (European Commission, 2009 [95]). In Table 3.1, they were also classified according to the species provided by the manufacturers.

To better guarantee the reliability of the chemometric treatment, fluorescence intensities were normalized and represented as Raman units (R.u.), instead of using arbitrary units (a.u.) of signal, as presented in Figure 4.6A-I. This precaution was necessary to minimize the effect of instrumental variations. All spectra were also obtained using the same optical filter, with 25% of transmittance, to reduce the influence of filter changing for chemometric treatment, except for the sample EO\_05, where a filter with 1% do transmittance was necessary, because of the values of higher fluorescence intensity obtained.

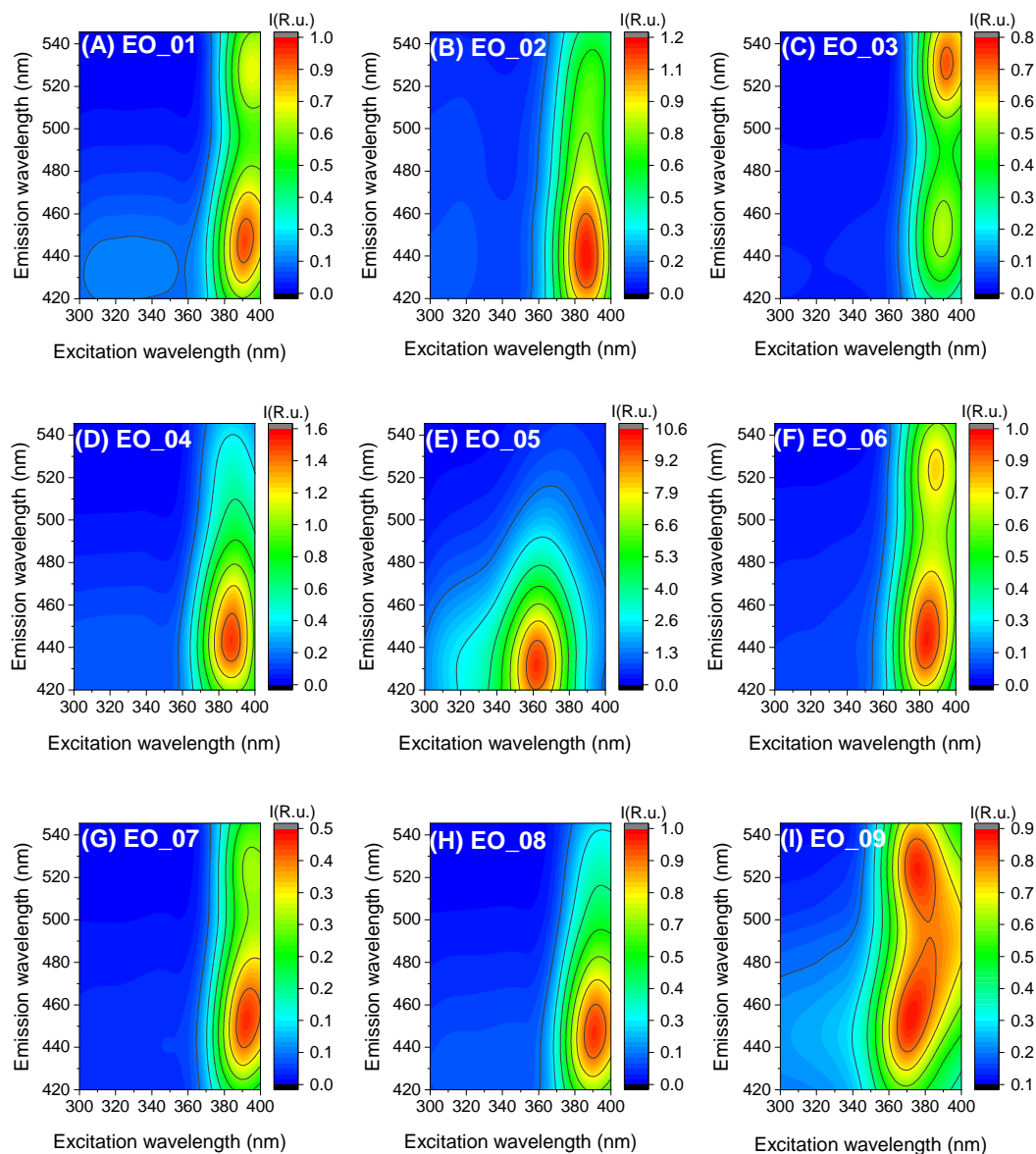


**Figure 4.6.** Contour surfaces ( $\lambda_{\text{ex}}$  from 300 to 400 nm and  $\lambda_{\text{em}}$  from 420 to 545.5 nm) for different Brazilian orange EOs in SFME. Each spectrum corresponds to one specific brand codified according to Table 3.1: (A) EO\_01, (B) EO\_02, (C) EO\_03, (D) EO\_04, (E) EO\_05, (F) EO\_06, (G) EO\_07, (H) EO\_08, and (I) EO\_09. Measurements were made using optical filter with 25% of transmittance, except for EO\_05 (where filter with 1% of transmittance was used). Fluorescent intensity values in Raman unit (R.u.). Blank subtraction and scattering removal by RStudio software (Package: eemR).

After pre-processing (including blank subtraction, and Raman normalization), the EEM ( $11 \times 252$ ), obtained from the 3D spectra of Brazilian EO samples (Table 3.1), were unfolded and grouped into a two-dimensional matrix  $X$ , containing 270 rows, representing the authentic replicates for each orange EO, and 2,772 columns, corresponding to the variables ( $\lambda_{ex}/\lambda_{em}$ ). The matrix  $X$  was used in PCA treatment to obtain the pattern of samples. The variables were centered and scaled before PCA for better accuracy of results. In chemometric treatment by PCA, new artificial variables, called principal components (PCs), were generated through the linear transformation of the original variables. The PCs were sequentially numbered (PC1, PC2, PC3 ...) in function of its importance to explain the variance of the data, being PC1 is the most relevant component [52]. In this case, considering all samples, the first three PCs were capable to explain 96.7% of the data variance with cumulative variances of 88.2, 6.2, and 2.3% for PC1, PC2, and PC3, respectively (see the screeplot for the first ten components in Figure 4.7). The two-, and three-dimensional plot for the first three PCs, presented in Figure 4.8A-D, shows that each group occupies a distinct location in the PC scores plot.

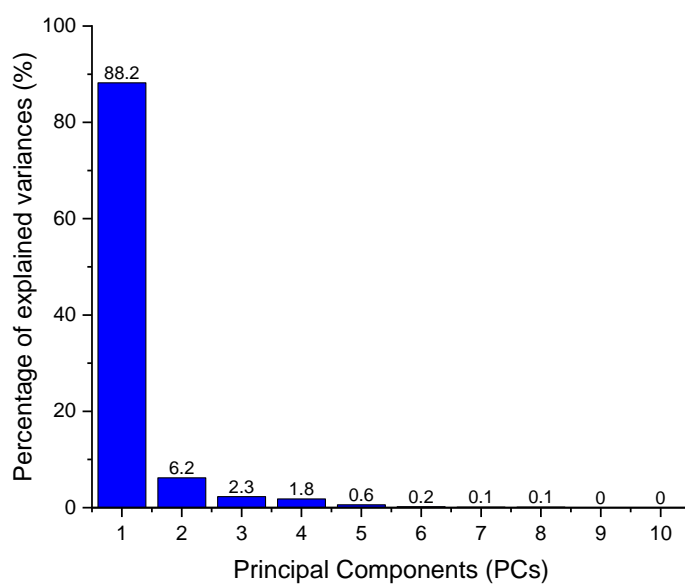


**Figure 4.7.** Screeplot for the first components obtained after chemometric treatment of the data by UPCA, considering 3D fluorescence spectroscopy analysis of nine different Brazilian orange essential oils (sample description in Table 3.1). Results for UPCA including all samples, EO\_01 to EO\_09, as presented in Table 3.1.

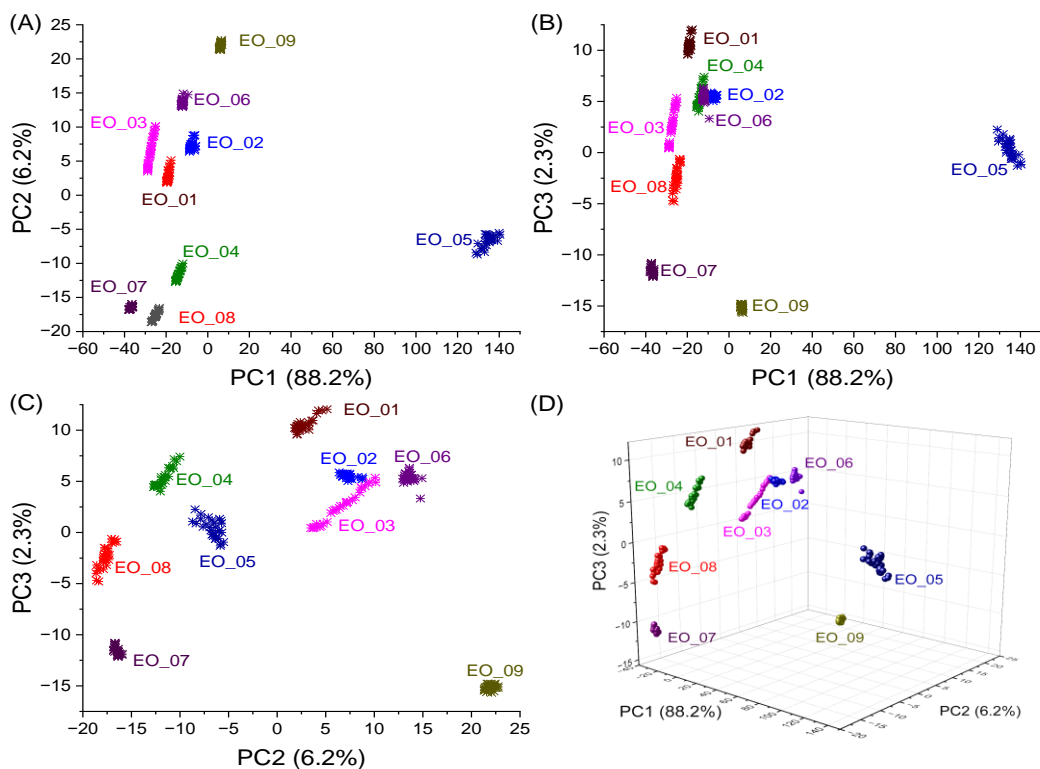


**Figure 4.8.** Two-, and three-dimensional scores plots for the evaluated Brazilian orange essential oil SFME after UPCA data treatment: (A) PC1  $\times$  PC2 (cumulative variance: 94.4%), (B) PC1  $\times$  PC3 (cumulative variance: 90.5%), (C) PC2  $\times$  PC3 (cumulative variance: 8.8%), and (D) PC1  $\times$  PC2  $\times$  PC3 (cumulative variance: 96.7%). The samples are identified according to the codes as presented in Table 3.1.

Orange EOs have limonene as their main component (about 90%), which tends to produce minimal variation in chemical profiles between oils of different origins [11]. When using samples prepared as SFME systems, it was possible to detect even small variations in terms of composition for the evaluated OEs. UPCA results confirm that the spectral differences observed on contour surfaces (Figure 4.6A-I) achieved in SFME systems are enough to promote discriminatory power. Analyzing the plots presented in Figure 4.8A-D, it is possible to observe a that

samples coded as EO\_05 is clearly segregated from the others (especially when considering PC1  $\times$  PC2 and PC1  $\times$  PC3, also in the three-dimensional score plot). The sample coded as EO\_05 is the EO with the lowest commercial value, which points to the possibility of this technique being used for quality control and classification. Sample EO\_09, which also appears significantly segregated from the others (especially in PC2  $\times$  PC3, also in the three-dimensional score plot), is the only one whose oil comes from a different orange variety (Table 3.1), what was to be expected, because different varieties originate oils with particular characteristics. For the other oils, it is also important to point out that score plots using combination of PCs (Figure 4.8A-D) have also some degree of discrimination, although they all come from sweet orange oils. Results confirm that the spectral differences observed on contour surfaces (Figure 4.6A-I) achieved in SFME systems are enough to promote discriminatory power and this technique could be used to evaluate traceability of these products.

To better understanding which regions of the 3D fluorescence spectrum are the most important for the discrimination of sweet orange EOs only (samples with greater similarity in terms of composition), a new chemometric treatment was carried out, but without samples EO\_05 and EO\_09. A summary of the results, through the two-dimensional plot for the first three PCs, can be found in Figure 4.9A-C). Regarding the range adopted for excitation and emission wavelengths, in order to evaluate the importance of the chosen region in PC obtained with the chemometric treatment, the values of the eigenvectors for the first four PCs were refolded and plotted in function of the respective  $\lambda_{\text{ex}}$  and  $\lambda_{\text{em}}$  (Figure 4.10A-C). By doing this, it was possible to evaluate the regions with the greatest influence for each PC individually. This new UPCA treatment made possible to evaluate, through

the eigenvectors, how each region of the fluorescence spectrum performs in terms of discriminating power. Considering the emission-excitation matrix (EEM), the data entered in the wavelength ranges between 360-390 nm (for excitation) and 420-500 nm (for emission) were found to be important for the discrimination of orange oils, which justifies the restricted range adopted for the discriminant analysis. These are also the regions of greatest spectral information as seen in Figure 4.6A-I.

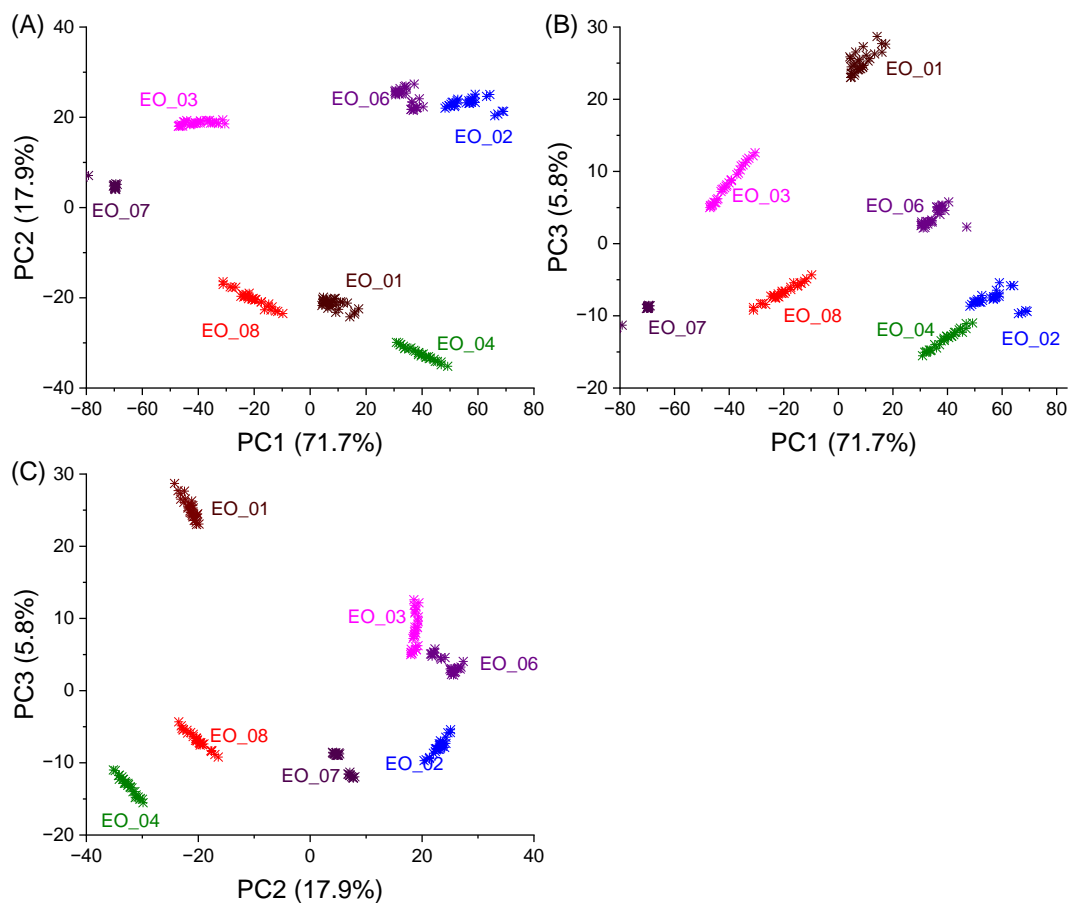


**Figure 4.9.** Two-dimensional scores plots for the evaluated Brazilian orange essential oil SFME after UPCA data treatment, after excluding the samples codified as EO\_05 and EO\_09 (Table 3.1): (A) PC1  $\times$  PC2 (cumulative variance: 89.6%), (B) PC1  $\times$  PC3 (cumulative variance: 77.5%), and (C) PC2  $\times$  PC3 (cumulative variance: 23.8%). The samples are identified according to the codes as presented in Table 3.1.

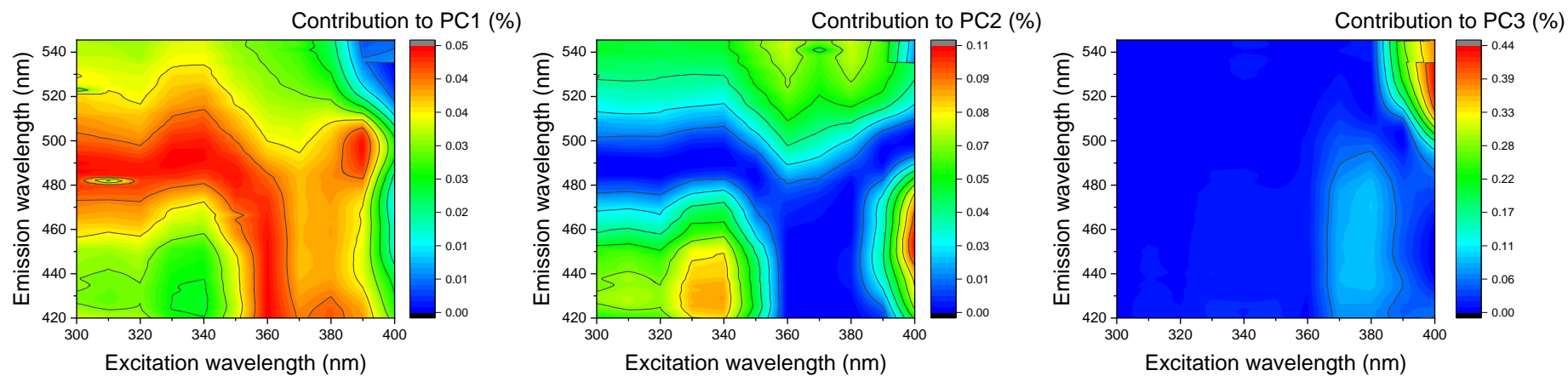


**Figure 4.10.** Contour surface with the percentage contribution of each excitation and emission wavelengths for the three principal components plotted as contour surfaces.

#### 4.2.5

##### Other potential applications

A preliminary study was carried out to evaluate 3D fluorescence spectroscopy of the EOs SFME as a way for identifying inadequate storage and adulteration conditions. Despite being just initial tests, it was possible to identify a great potential in this matter. Temperature and light exposure can affect the integrity of EOs, as their components can be oxidized and polymerized, resulting in a loss of quality and affecting their pharmacological properties, compromising consumer well-being [14]. Therefore, providing tools to enable rapid detection of alterations in EO composition, due to inadequate storage conditions, is important. An aliquot of orange EO was stored in a closed glass vessel for three weeks under exposure to ambient light and without any temperature control. Results showed a significant increase in the measured fluorescence observed at 380/445 nm ( $\lambda_{ex}/\lambda_{em}$ ) when compared with the control sample (stored in the dark and at  $22 \pm 2^\circ\text{C}$ ), demonstrating that the proposed procedure is effective for monitoring alterations in EO composition due to photo-degradation and thermal degradation.

Aiming to detect EO adulteration, samples were fortified with vegetable (canola) and mineral oils in order to detect spectral differences that characterize change in oil composition. There are many ways to adulterate EO samples and, in fact, the addition of non-volatile oils (including vegetable and mineral oils) [16] is one of the known counterfeiting practices. When designing the experiment, canola and mineral oil addition were made at four weight proportions (1, 5, 10, and 20%). However, for the samples fortified at 20% there was no formation of a homogeneous system when using the amount of the alcoholic mixture established to produce the O/W ME in the present work. This result was obtained both for

samples fortified with canola and for those with the addition of mineral oil. For the lower amounts of adulterant (1, 5 and 10%), homogeneous systems were formed, but they did not have the same stability of the ones composed by EO/octan-1-ol as the only oily phase, remaining as a single phase for a maximum of 15 days since ME formation regions are particular to each oil characteristics. As mentioned, the large proportion of limonene, present in orange EOs, causes minimal variation in chemical profiles between oils of different origins [11] However, when the non-volatile oil, as adulterant, was added, the EO profile is affected, changing ME formation region. After fluorescence spectroscopy analysis, it was also observed that when the quantity of the adulterant increases, the overall fluorescence intensity also increased as the high viscosity of non-volatile oils tend to favor excited state radiation energy decay. Emission spectrum also shifts towards blue probably due to the change in the polarity of the oil phase, caused by the addition of non-volatile oils in the EO. Results of this preliminary test are present in Figure 4.11.

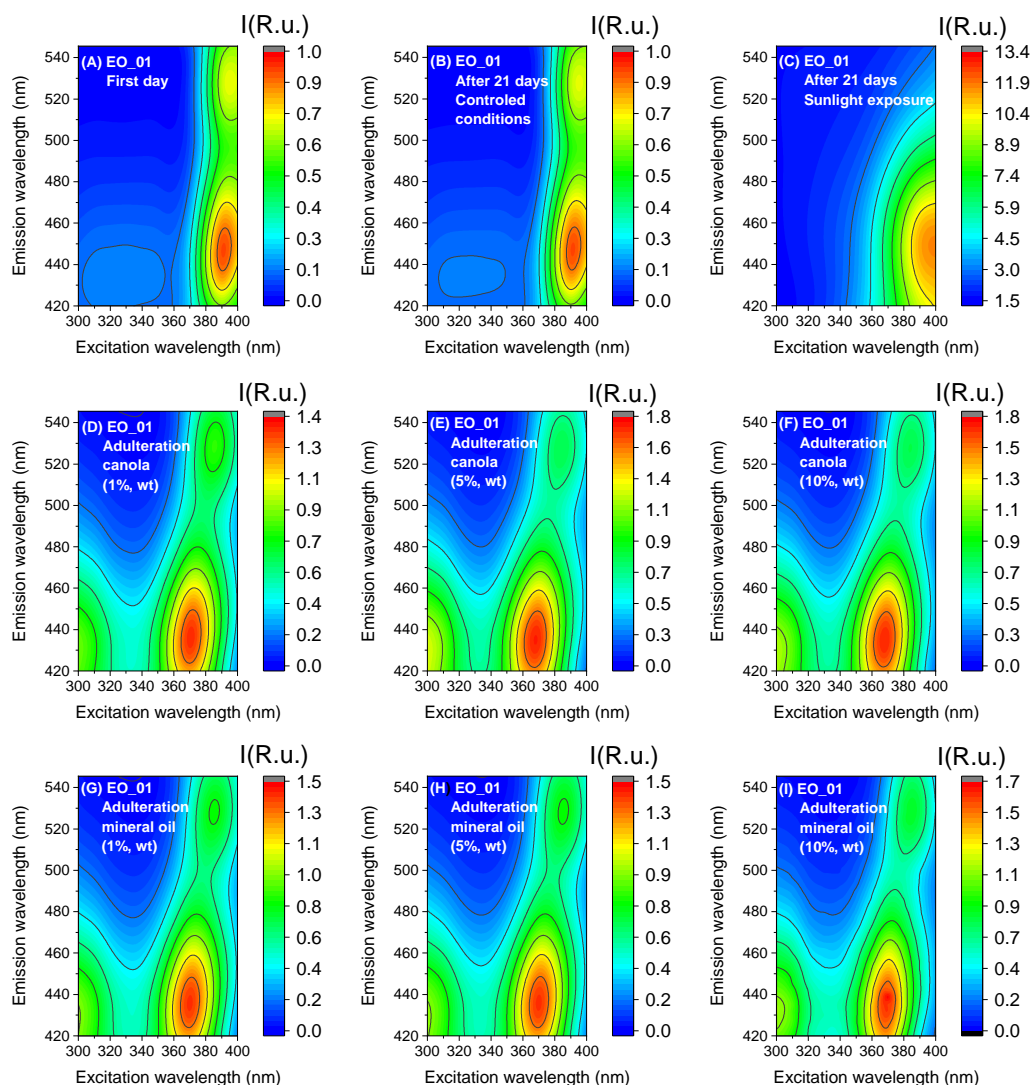


**Figure 4.11.** Contour surfaces obtained from 3D fluorescence spectrometry obtained for storage conditions (A-C), and adulteration with canola (A, D-F) and mineral oil (A,G-I). Before analysis, microemulsions (4:1:12.1 W:EO:Alcoholic mixture, weight ratio) were formed from each sample. Propan-1-ol and octan-1-ol (10:3, w/w) were used as alcoholic mixture (amphiphilic solvent). Excitation recorded between 300 nm and 400 nm and emission from 420 nm to 545,5 nm. Measurements were made using optical filter with 25% of transmittance. Fluorescent intensity values in Raman units (R.u.). Blank subtraction, and Raman normalization by RStudio software (Package: eemR).

### 4.3

#### **Partial conclusion**

The use of SFMEs systems in orange essential oil analysis was evaluated by 3D fluorescence spectroscopy. With low sample consumption and a simple method, it was possible to obtain useful fingerprint patterns for the evaluation of traceability, influence of storage conditions and detection of adulteration. Comparing with pure essential oils, the ME system (characterized as an oil-in-water) with the lower essential oil content (about 6% in weight) was capable to greatly increase fluorescence and spectral details, turning this condition more interesting for obtaining fingerprint patterns by 3D fluorescence spectroscopy. The method allowed, in terms of traceability assessment, discrimination between nine orange essential oils of different Brazilian brands. Spectral differences brought by sample microemulsification, allowed application of the chemometric treatment UPCA to prove group separation with cumulative variances of 88.2 % (PC1), 6.2 % (PC2) and 2.3 % (PC3) and score plots showed distinct location for each group, confirming the spectral differences observed on excitation-emission matrix spectra. Storage conditions, considering the effect of light exposure, and adulteration by addition with canola and mineral oil were promptly identified. The method was found to be efficient in the proposed application in terms of quality control of essential oils. The obtained fingerprint patterns have the potential to act as valuable supplements to conventional techniques, aiding in the identification and monitoring of key parameters crucial for monitoring these products. Integrating our method into existing procedures can strengthen the control and assurance processes, ultimately contributing to a more comprehensive understanding of the essential oil's characteristics.

## 5

### **Excitation-emission matrix fluorescence spectroscopy in hydro-alcoholic systems to discriminate different citrus essential oils**

#### 5.1

##### **Introduction**

Citrus essential oils (CEOs) are one of the most commercialized essential oils (EOs) in the world [10] as they have gained popularity because of their biological activities [65]. Currently, many industrial sectors, such as food and beverages, cosmetics and pharmaceuticals have a great demand for EOs [65,96]. Because of their high economic importance, it is necessary to invest in methods to guarantee authenticity and traceability. In this matter, gas chromatography (GC) and high-performance liquid chromatography (HPLC) are extensively used [17,97]. Sensory analysis, and physicochemical properties are also employed in more simplistic evaluations [16]. Raman [98] and absorption infrared spectroscopies [99] can be also considered. Another alternative, but not fully explored, is using fluorescence spectroscopy, for instance applying excitation-emission matrix (EEM) to obtain fingerprinting patterns.

EEM fluorescence spectroscopy, also called 3D fluorescence spectroscopy, is a method used for complex samples [44], first described by Johnson et al (1977) [100], and widely applied in dissolved organic matter and petroleum characterizations [45,101]. The main advantage of EEM fluorescence spectroscopy is the selectivity, simplicity, and cost-benefit. New applications in food quality control and authenticity analysis, especially for vegetable oils, have been reported

[102,103], but only a few studies have employed EEM fluorescence spectroscopy to EOs [85–87,104]. While possessing great potential, it remains relatively unexplored due to practical implications, such as the relatively large oil amounts required in batch analysis combined with the need for replicates for mathematical treatment. Furthermore, EOs are hydrophobic and present strong odor, requiring meticulous cleaning to prevent cross-contamination, especially when using mini cells [85]. The extended analysis time should also be considered. Besides, some EO are susceptible to photobleaching [86]. Finally, the presence of numerous chromophores in its composition must also be considered (internal filter effect), necessitating spectral corrections [48].

An alternative, recently proposed by Macedo et al. (2023) [104], is the use of hydro-alcoholic systems, also known as surfactant-free microemulsions (SFME) [37,105]. In SFMEs, short-chain alcohols are used to stabilize biphasic mixtures (water and oil), forming optically clear dispersions through formation of weak micelle-like aggregates. Compared to surfactant-based microemulsions (SBME), the SFME employs higher content of water in its composition [106]. Micellar aggregates result in microenvironments that encapsulate fluorophores, imposing movement and vibration restrictions that minimize probability of non-radiative decay processes, consequently enhancing the inherent fluorescence of some of the components in EOs [42]. As reported by Macedo et al. (2023) [104], these systems were able to enhance spectral detailing when applied to the analysis of sweet orange EO [104], being useful for fingerprinting.

In the present work, new systems with smaller sample proportions were evaluated to achieve better analytical performance in EEM spectrofluorimetry for CEOs using these surfactant-free organized systems. The reproduction for different

citrus species, including grapefruit (*Citrus paradise*), lemon (*Citrus limonum*), sour orange (*Citrus aurantium*), sweet orange (*Citrus sinensis*), and tangerine (*Citrus reticulata*), was also obtained for the proposed method for discriminating samples.

## 5.2

### Results and discussion

#### 5.2.1

##### Hydro-alcoholic systems preparation and evaluation

The final condition for the hydro-alcoholic systems was adapted from Macedo et al. (2023) [104] where it was concluded that weak micelle-like aggregates, formed through pseudo-ternary liquid mixtures (utilizing sweet orange EO and octan-1-ol as the oily phase, along with water and propan-1-ol) significantly increased the fluorescent intensity measured from EOs, making these systems useful for obtaining fingerprinting patterns. In contrast, in the present work, preliminary experiments showed that by using lower proportions of the oily phase, a significant increase in fluorescence signal was obtained, specially at 336/436 nm ( $\lambda_{ex}/\lambda_{em}$ ). Based on these considerations and aiming to achieve stable systems with lower sample content, a univariate optimization was performed by monitoring systems with reduced levels of the oily phase (composed of sweet orange essential oil and octan-1-ol, 1:2, v/v). Hydro-alcoholic systems containing different volumes of the oily phase (from 5 to 300  $\mu$ L), water (with volume set at 1 mL), and propan-1-ol (to complete final volume of 5.0 mL) were monitored by fluorescence spectroscopy at 336/436 nm.

Considering the added volumes of the oily phase, results (Figures 5.1A-B) indicated that fluorescence intensity increased up to a volume of 225  $\mu\text{L}$ . The increase in fluorescence, despite the lower proportion of oily phase, can be explained by the formation of weak micelle-like aggregates in SFME systems, which hinders molecular vibration and reduces possibility of collisional quenching of luminophores dispersed in the organized phase, thus improving radiative decay following photon-excitation. Fluorescence decreasing as oil phase volume is decreased is due to the reduction in the concentration of fluorophores stabilized in system aggregates. The increasing in fluorescence is linear as volume is varied from 0 to 15  $\mu\text{L}$  which shows transparency of these systems. In contrast, fluorescence increasing rate is reduced as the amount of the oil phase comprises the content above 15 up to 225  $\mu\text{L}$  until signal saturation and further decreasing of fluorescence at higher contents of oily phase. The reduction in the increasing rate is probably related to different factors. First, as the oily phase in increases the size of the oily droplets dispersed in the system increases, thus affecting transparency and increasing scattering. In addition, internal filter effect increases due to the higher amounts of chromophores in the system (from sample components), absorbing at the excitation and emission wavelengths as can be seen in Figure 5.1C-D. Based on the results, 15  $\mu\text{L}$  of oily phase was chosen for continuity of the study in order to guarantee transparency of the medium.

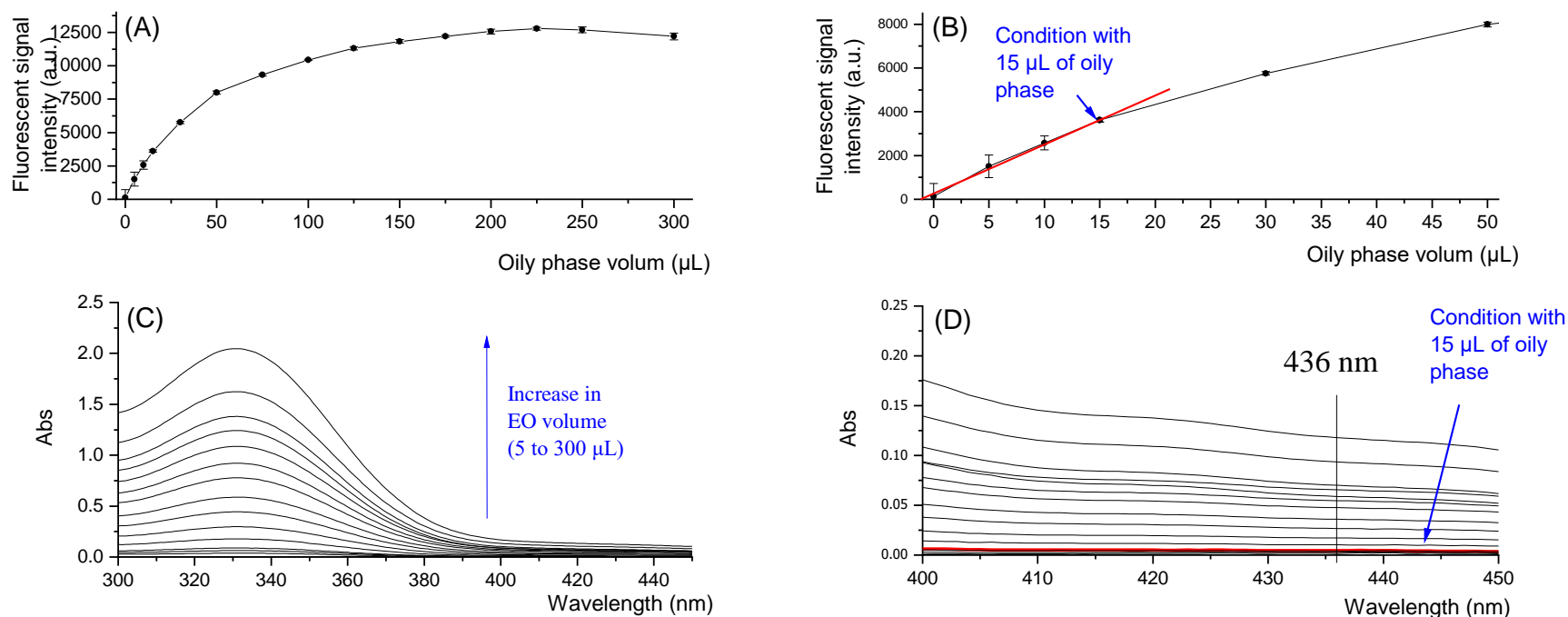


**Figure 5.1.** Optimization for adjusting the volume of the oily phase (sweet orange EO and octan-1-ol, 1:2 v/v): (A) Fluorescent signal intensity in function of different oily phase volumes (0 to 300  $\mu\text{L}$ ) and (B) zoom in on volumes between 0 and 15  $\mu\text{L}$  to highlight the linear range (in red). (C) Absorbance (300 to 450 nm) and (D) zoom in the 400 to 450 nm range to evaluate inner filter effect for sample systems with emphasis on the response obtained for the system containing 15  $\mu\text{L}$  of oily phase (in red). A fixed volume of water (1.0 mL) and propan-1-ol (completing final volume up to 5 mL) were used to form the homogeneous hydro-alcoholic systems.

After establishing ideal oily phase volume for sweet orange EO (5  $\mu\text{L}$  in a 15  $\mu\text{L}$  total oily phase), this system was successfully reproduced for the other CEOs (grapefruit, lemon, sour orange, sweet orange, and tangerine). Subsequent fluorescence spectroscopy analysis revealed that all of these other evaluated varieties exhibited a superior fluorescence response compared to the system comprising sweet orange oil. In fact, for grapefruit EO, the signal was so intense that even the optical density filter of 1% transmittance was not capable to adjust fluorescence under the detector saturation point. However, as observed in Figure 5.1B, higher signal variations (based on replicate study and reflected in the error bars) were obtained for systems with smaller volumes of oil phase. This fact can be attributed to difficulties in reproduce systems when sampling lower volumes of the oily phase due to the viscosity and oily nature of the samples.

In order to find a compromise between oil sample content and the fluorescence intensity characteristic from all of the analysed samples, a further study was made aiming to find a proper dilution factor for the system finding one single preparation condition for all. In this sense, the SFME systems prepared with 15  $\mu\text{L}$  of oil phase and 1 mL of water was further adjusted, with propan-1-ol, to the final volumes: 10, 25 and 50 mL (see Figure 5.2A for sweet orange EO). At 25 mL final volume, the fluorescence from sweet orange EO could still be measured leaving room to observe fluorescence from the other EOs within the range before detector saturation. The complement to this study was made aiming to replace part of the propano-1-ol content by water enabling signal improvement up to the limit of visual transparency of the system. In Figure 5.2B fluorescence measured from orange EO SFME systems containing 5, 10 and 19 mL of water (respectively containing 20, 15 and 6 mL of propan-1-ol as complement) are shown. Above 19

mL of water, system became visually turbid showing that this was the limit for the water content. Finally, a study was made using only sweet orange EO as oil phase (5  $\mu$ L) ignoring the prior dilution with octano-1-ol but using the water and propan-1-ol proportions set in the prior experiments. In agreement with the results obtained by Macedo et al. (2023) [104], the formation of SFMEs did not occur as can be observed in Figure 5.3.

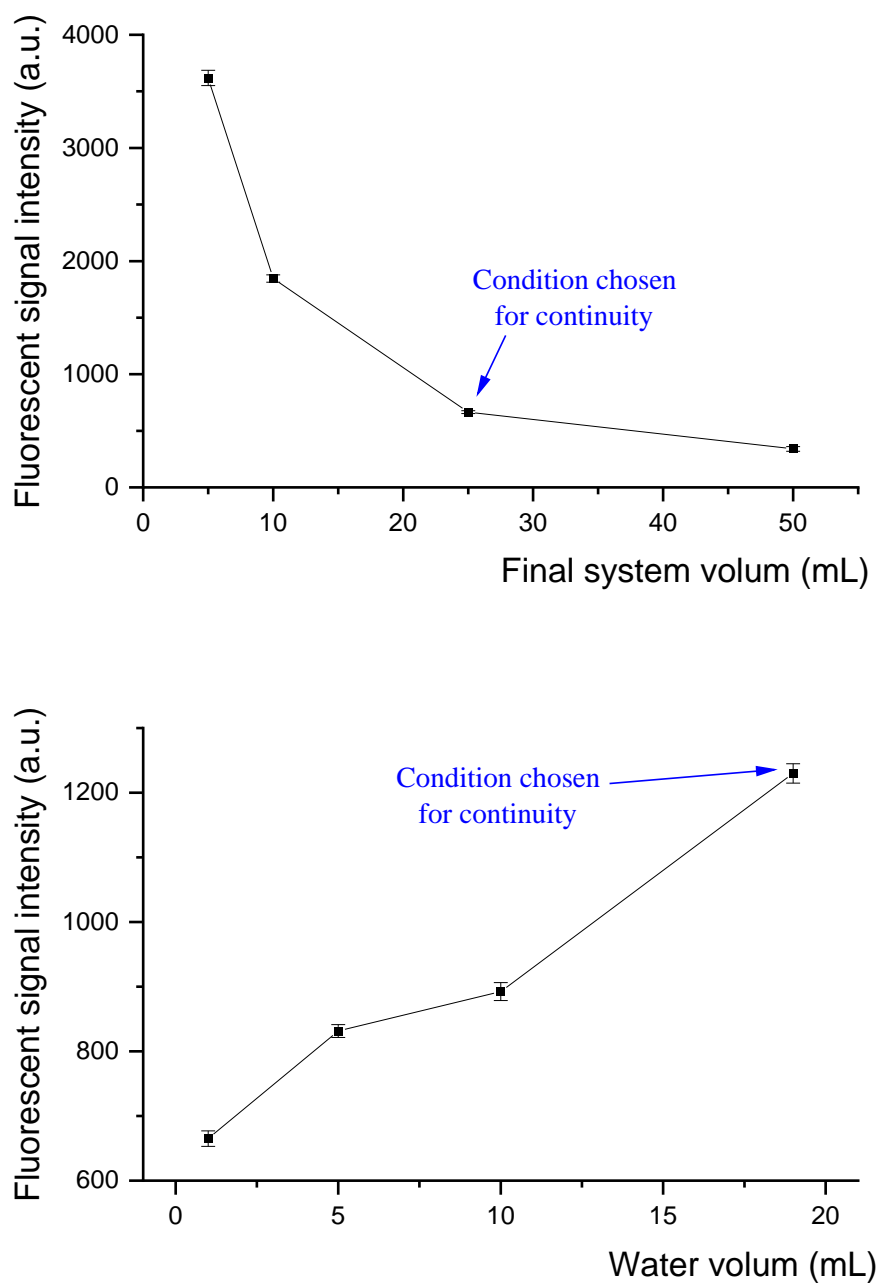


**Figure 5.2.** (A) Evaluation of the final volume of the hydro-alcoholic systems using a fixed volume (1.0 mL) of water and 15  $\mu\text{L}$  oily phase (5  $\mu\text{L}$  of sweet orange EO and 10  $\mu\text{L}$  of octano-1-ol) using propan-1-ol to adjust the final volume. (B) Fluorescence intensity from diluted systems containing 15  $\mu\text{L}$  of oily phase as a function of different water volumes, adjusting final volume to 25 mL using propan-1-ol.

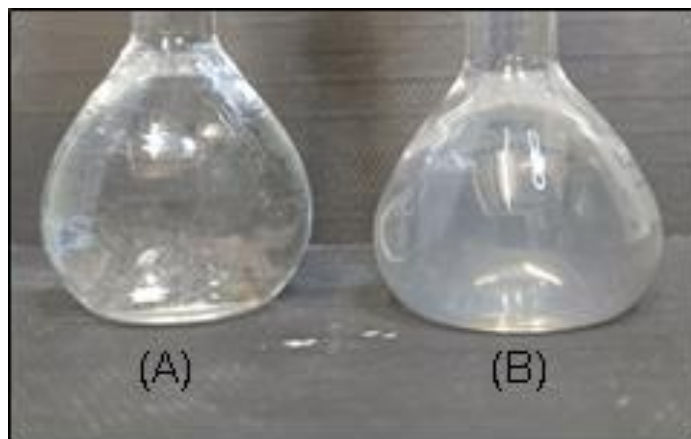


**Figure 5.3** Hydro-alcoholic systems using: (A) 15  $\mu\text{L}$  of sweet orange EO and octan-1-ol, 1:2 v/v as oily phase and (B) only sweet orange EO (5  $\mu\text{L}$ ). Final composition of water (19.0 mL) and propan-1-ol (as complement to the 25 mL final volume).

Taking into consideration the high fluorescences measured from some of CEOs (especially grapefruit), the compromise condition among sample amount, signal intensity from all of CEOs to adjust response under the saturation limit of the detector and reproducibility of results was found to be appropriate, using 15  $\mu\text{L}$  of the oil phase (mixture containing essential oil diluted in octan-1-ol at 1:2, v/v), 19 mL of ultrapure water, and propan-1-ol until volume adjustment to 25 mL. Systems stability was evaluated for all CEOs in such conditions and, as present in Figure 5.4, there was no evidence of visual alteration, such as phase separation and turbidity, during sample monitoring (three months at 4 and 25°C) also after centrifugation test (1080 RFC for 20 min). These results indicated thermodynamic stability, what is characteristic of SFMEs [37].

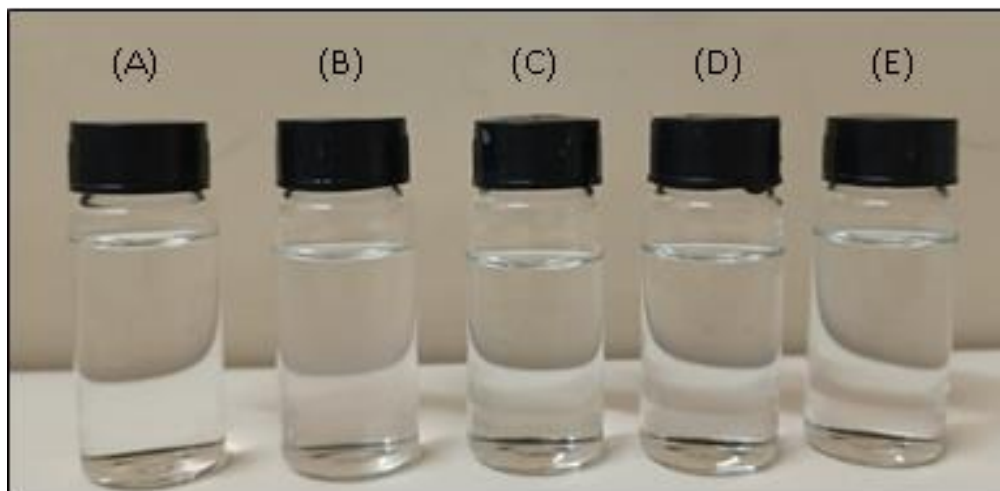


**Figure 5.4.** Homogeneous hydro-alcoholic systems for each of the CEOs after four months of monitoring: (A) sweet orange, (B) sour orange, (C) lemon, (D) tangerine, and (E) grapefruit. 15  $\mu\text{L}$  of oily phase (EO and octan-1-ol, 1:2 v/v), a fixed volume of water (19.0 mL) and propan-1-ol (up to 25 mL) were used.

### 5.2.2

#### 3D fluorescence spectroscopy analysis and data pre-processing

The hydro-alcoholic systems of each CEO were evaluated by 3D fluorescence spectroscopy analysis. Results revealed that all CEOs included in the study exhibited significant fluorescent signal intensity values in the same region as sweet orange EO (at 336/436 nm,  $\lambda_{\text{ex}}/\lambda_{\text{em}}$ ). Additional experiments with non-citrus EOs were also conducted, and none of them exhibited maximum fluorescence emission in the same region, indicating that this could be a characteristic response of compounds present in CEOs. In the light of this, samples were then replicated, and the results of the 3D fluorescence spectroscopy analyses were processed to assess the feasibility of applying these systems for the differentiation of CEOs.

Initially, an extended wavelength (200-650 nm and 280-700 nm for excitation and emission wavelengths, respectively) was used to verify the overall

spectral response and results are presented in Figure 5.5. Then, it was decided to restrict the wavelength ranges (200-400 nm and 340-550 nm for excitation and emission wavelengths, respectively), in order to enhance the region of greater spectral detail, also reducing total analysis time (from 26 min to 5 min) and simplifying the data matrix to be used in the chemometric treatment (from  $46 \times 840$  to  $21 \times 420$ ). Data pre-processing was carried out to minimize the instrumental variation effects and using Raman unit (R.u.) conversion [47], blank subtraction and scattering removal. The fingerprint patterns obtained for each CEO in hydro-alcoholic system after wavelength range adjustment, and data pre-treatment are present in Figure 5.6.

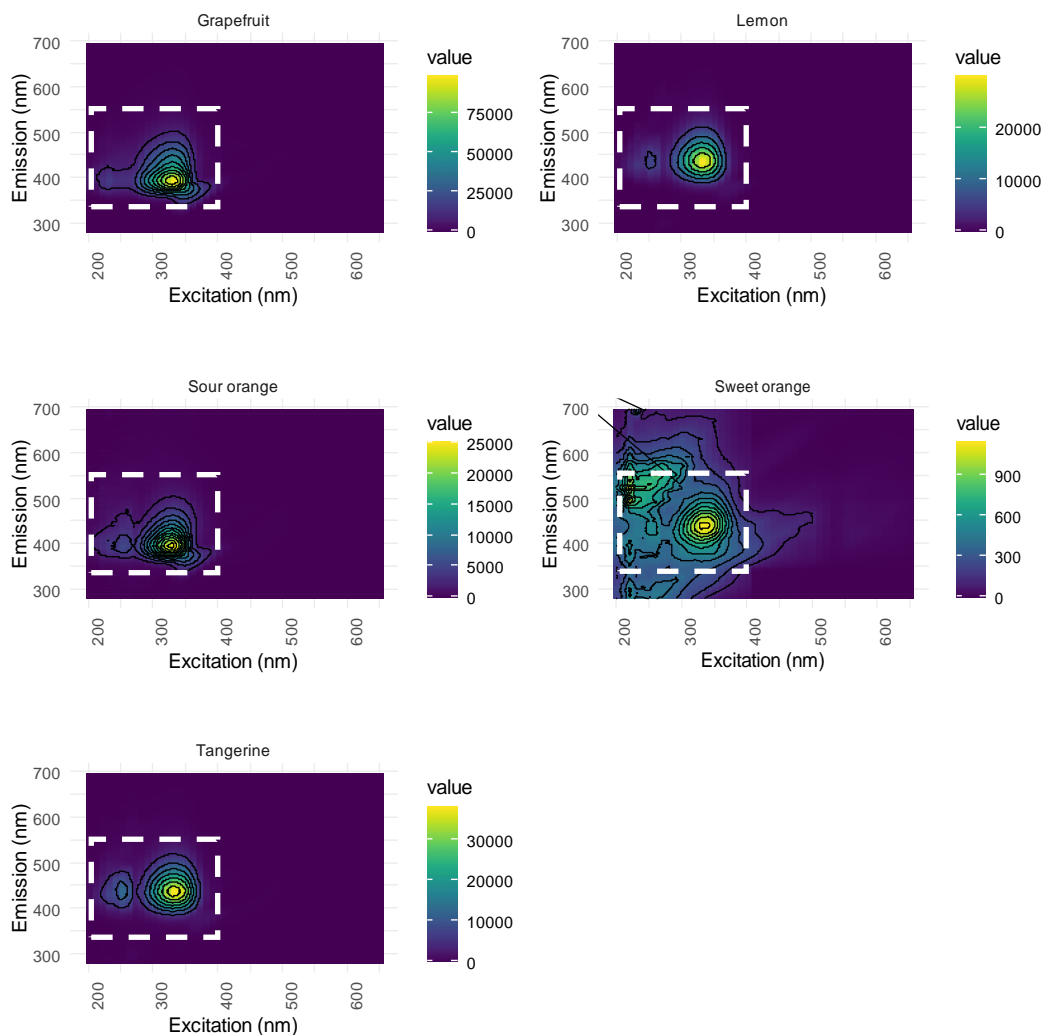


**Figure 5.5.** EEM contour obtained for CEOs in SFME media with scattering removing and blank subtraction. Intensity fluorescence in arbitrary units (a.u.) after optical filter correction. Dilution factor was not considered. Dashed white line represents the restricts wavelength range selected for chemometrics.

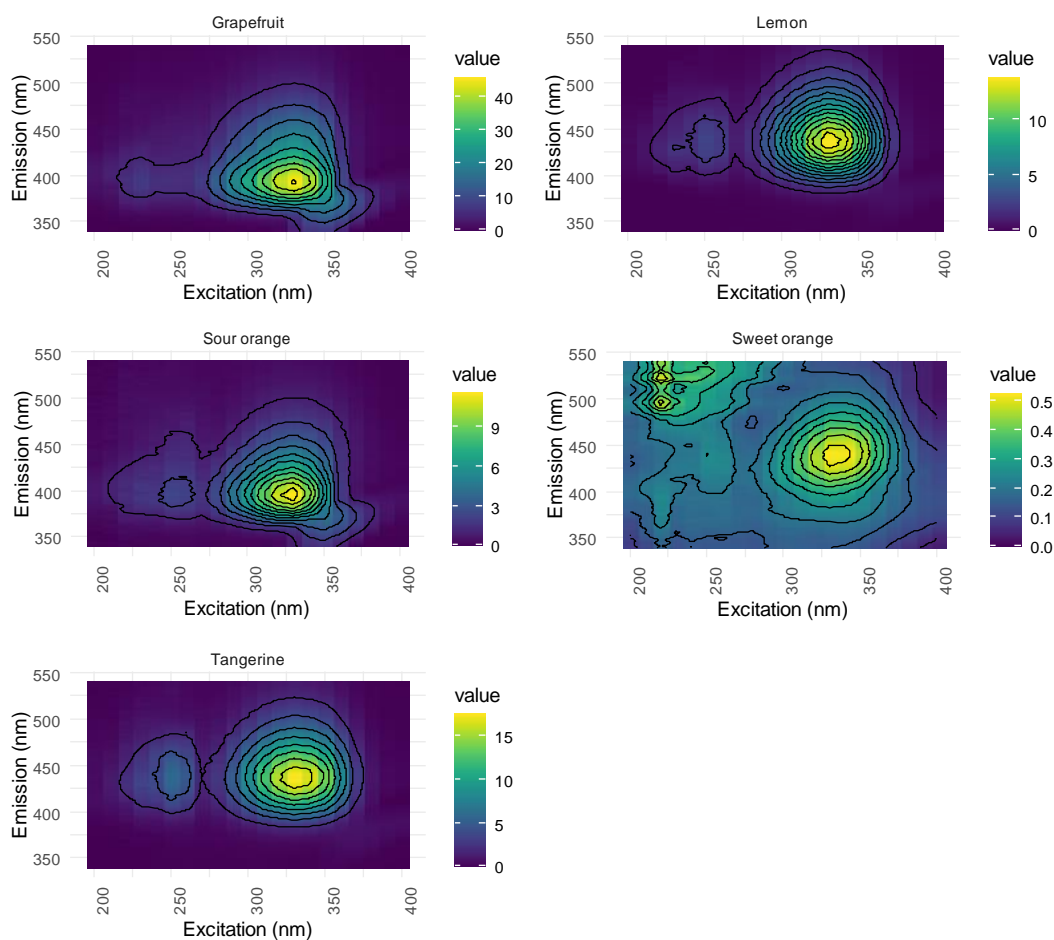


**Figure 5.6.** EEM contour obtained for CEOs in SFME media in a restricted wavelength range after scattering removing and blank subtraction. Intensity fluorescence in Raman units (R.u.). Dilution factor was not considered.

### 5.2.3

#### Chemometrics

Despite the similarity of the obtained spectra, in terms of the maximum excitation and emission wavelengths, it was possible to notice that they present differences in the pattern of the fluorescence intensities observed for each oil after 3D fluorescence spectroscopy analysis. In order to prove the potential of application of these systems to obtain fingerprint patterns useful for the differentiation of CEOs,

UPCA was applied as chemometric approach. As a result, the three first principal components (PCs) were sufficient to explain 99.5% of the variances (73.3%, 20.2% and 6.0% for PC1, PC2 and PC3 respectively). Two-dimensional score plots with data distribution for each replicate are shown in Figure 5.7A-C.

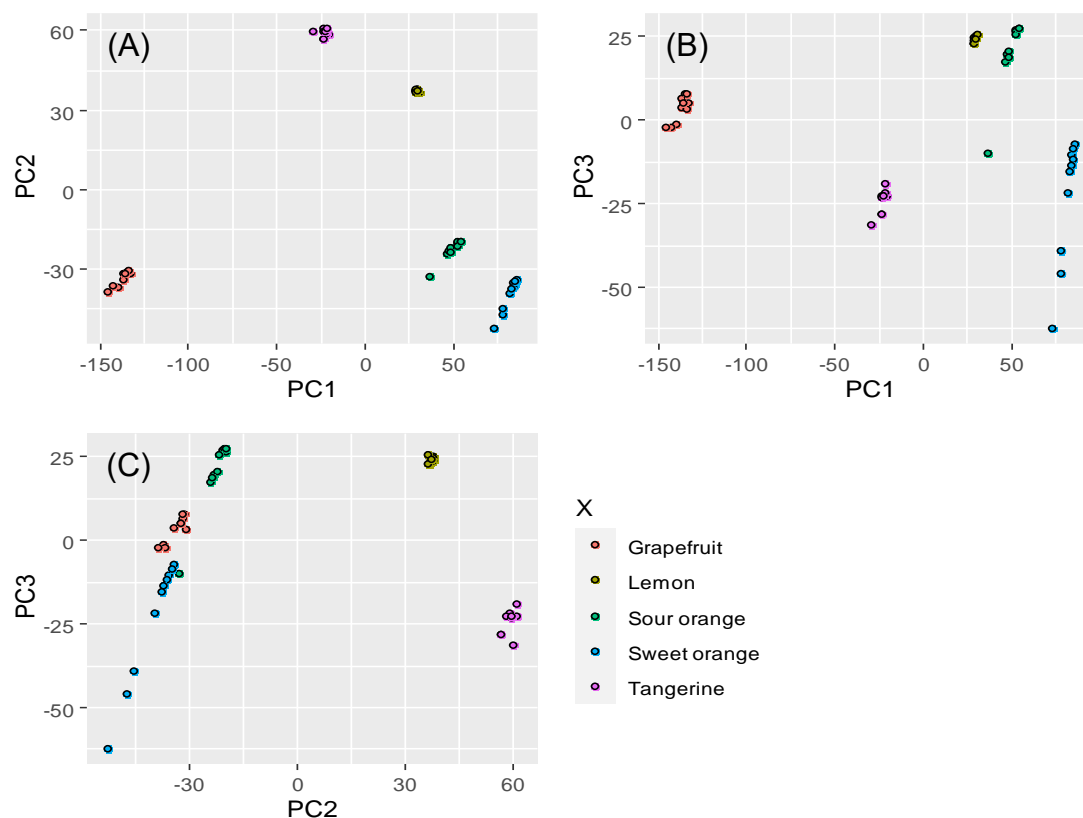


**Figure 5.7.** Two-three-dimensional scores plots for the citrus essential oils evaluated by 3D fluorescence spectroscopy in SFME media after UPCA treatment: (A) PC1  $\times$  PC2 (cumulative variance: 93.3%), (B) PC1  $\times$  PC3 (cumulative variance: 79,5%), (C) PC2  $\times$  PC3 (cumulative variance: 26,2%).

For UPCA clustering analysis, CEOs were grouped based on their species. In the first plot (Figure 5.7A), each type of oil occupies a different quadrant, except for sweet and sour orange EOs. In sequence, the eigenvectors were decomposed to

examine which pairs of excitation and emission wavelengths ( $\lambda_{\text{ex}}/\lambda_{\text{em}}$ ) exerts influence on each principal component (considering PC1, PC2, and PC3). Results are shown in Figure 5.8. It was found that 336 nm and 436 nm ( $\lambda_{\text{ex}}/\lambda_{\text{em}}$ ) proved to be relevant for the effective differentiation of various CEOs. Considering the excitation wavelength, the region below 250 nm is important for the third principal component. However, this region exhibits a significant spectral variation in the analyses conducted with sweet orange EO (Figure 5.9), which may explain the high variability observed among their replicates, especially when PC3 is taken into consideration (Figures 5.7B-C).

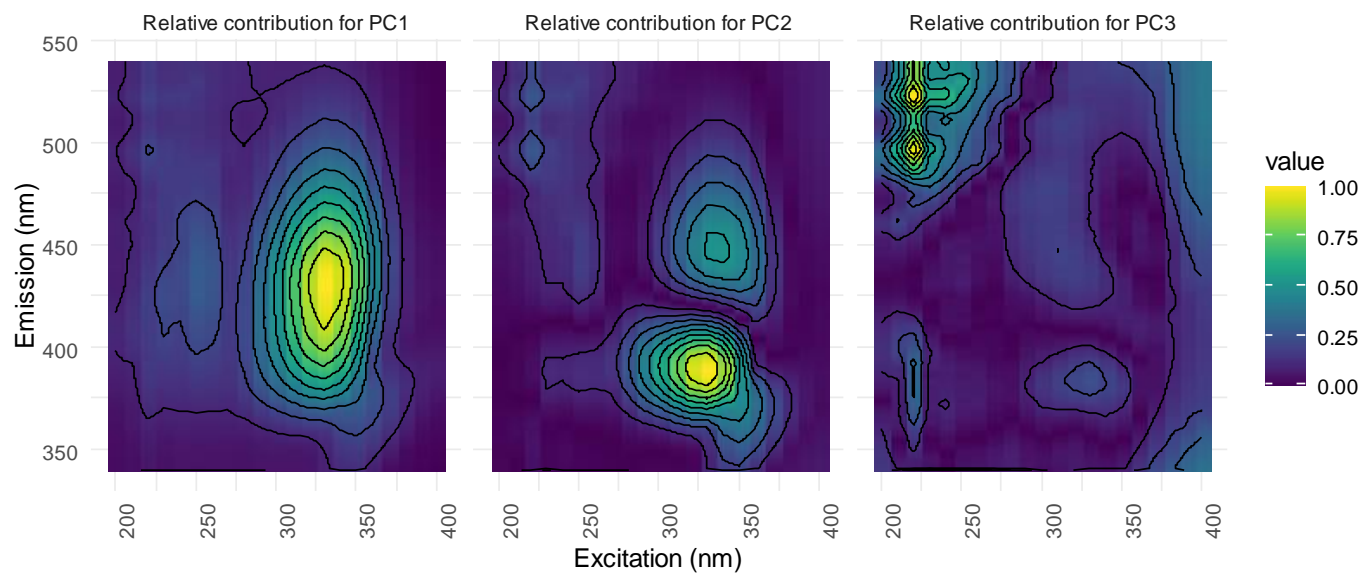


**Figure 5.8.** Contour surface with the relative contribution of each excitation and emission wavelength for the three principal components (PC1, PC2 and PC3) plotted as contour surfaces.

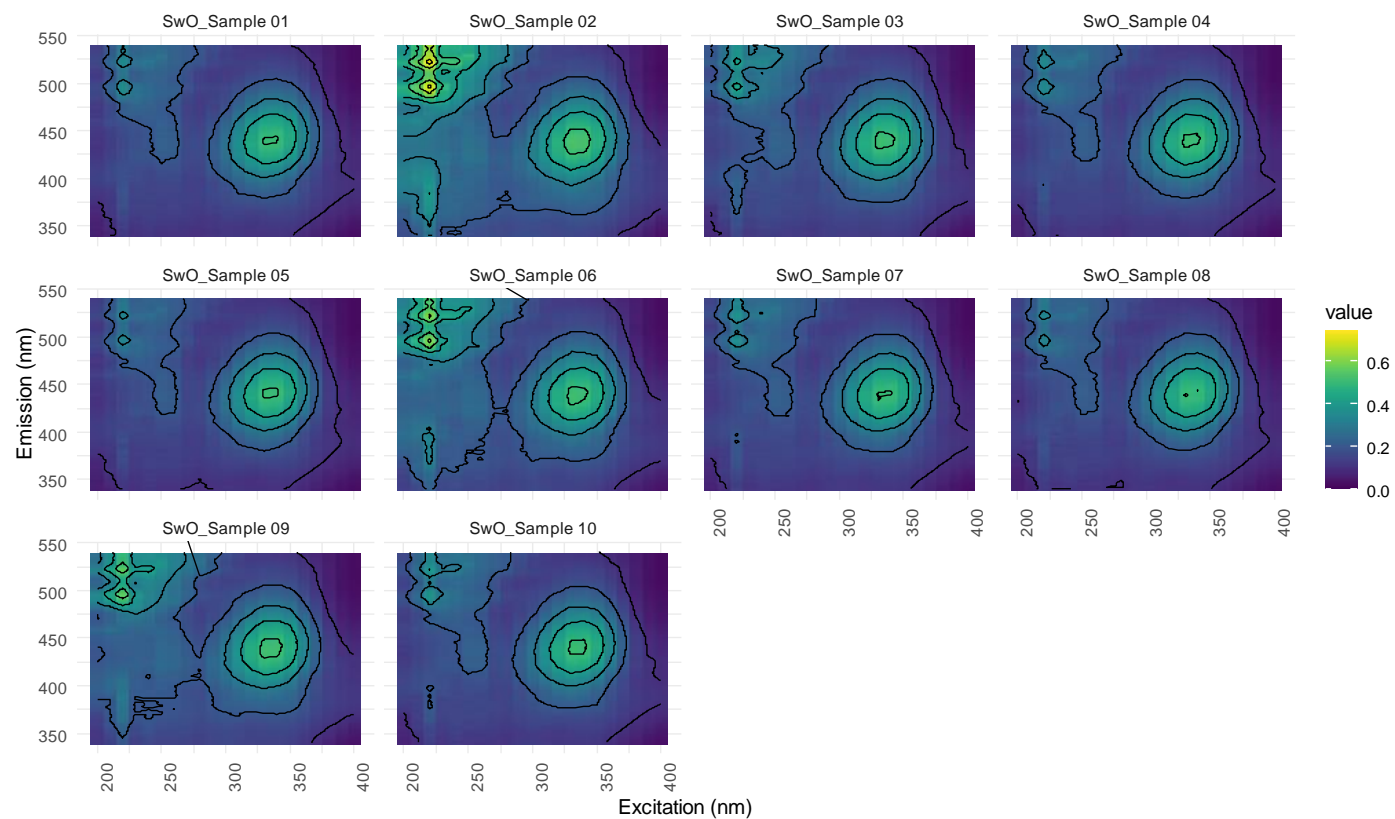


**Figure 5.9.** EEM contour for sweet orange EOs in SFME media, considering all replicates (individual samples, 1 to 10) used for UPCA treatment. EEM contour with scattering removing and blank subtraction. Intensity fluorescence in Raman units (R.u.) and with optical filter correction. Dilution factor was not considered.

#### 5.2.4

#### Chromatographic analysis

Commercial CEOs are usually obtained by fruit peels cold pressing. Consequently, they have a particular characteristic, that is the presence of a fraction containing non-volatile compounds. Primordially composed of coumarins, psoralens, and polymethoxyflavones (PMFs), this fraction can be considered important for the authenticity of CEOs due to its less complex composition [5]. In 2000, Fernández Izquierdo et al. [107] demonstrated the effectiveness of applying spectrofluorimetry in determining coumarins (umbelliferone, scopoletin, and 4-methylumbelliferone) in distilled beverages in a hydro-alcoholic medium. In this study, the group used similar wavelength values (340 and 425 nm). In 2013, Hroboňová et al. [108], determined herniarin in propolis (using ethanol as diluent) by HPLC (with fluorescence detector) operating at 320/450 nm ( $\lambda_{ex}/\lambda_{em}$ ) with limits of quantification 20,000 times smaller than the obtained using UV detection (at 280 nm).

To evaluate if the fluorophores observed on 3D spectra are non-volatile compounds, analyses were performed by HPLC using fluorescence detection at 336/436 nm ( $\lambda_{ex}/\lambda_{em}$ ). In this study, conditions used were adapted from other works [19,109], using hydro-alcoholic media as approach for sample preparation. Chromatograms were monitored by photometric absorption in a diode array detector (DAD) and by means of a fluorescence detector (FD). In order to identify the presence of the fluorophores responsible for the intense signal observed at 336/436 nm ( $\lambda_{ex}/\lambda_{em}$ ) in 3D spectroscopy analysis, these wavelengths were adopted for monitoring the chromatographic signal through fluorescence detection. Chromatograms obtained after HPLC-FD analysis (Figure 5.10A-E) indicated the

presence of numerous fluorophores capable of producing fluorescence in the region of interest. Monitoring using the DAD was also carried out since compounds typically present in this fraction (coumarins, psoralens, and polymethoxyflavones, Figure 2.1, subsection 2.1) have characteristic absorption spectra [5]. The absorption spectra corresponding to the peaks of the same retention time of the peaks with the highest intensity in the chromatograms (Figure 5.10B-E) were evaluated (Figure 5.11). Characteristic spectra of coumarins were observed for all compounds marked in Figure 5.10B-E.

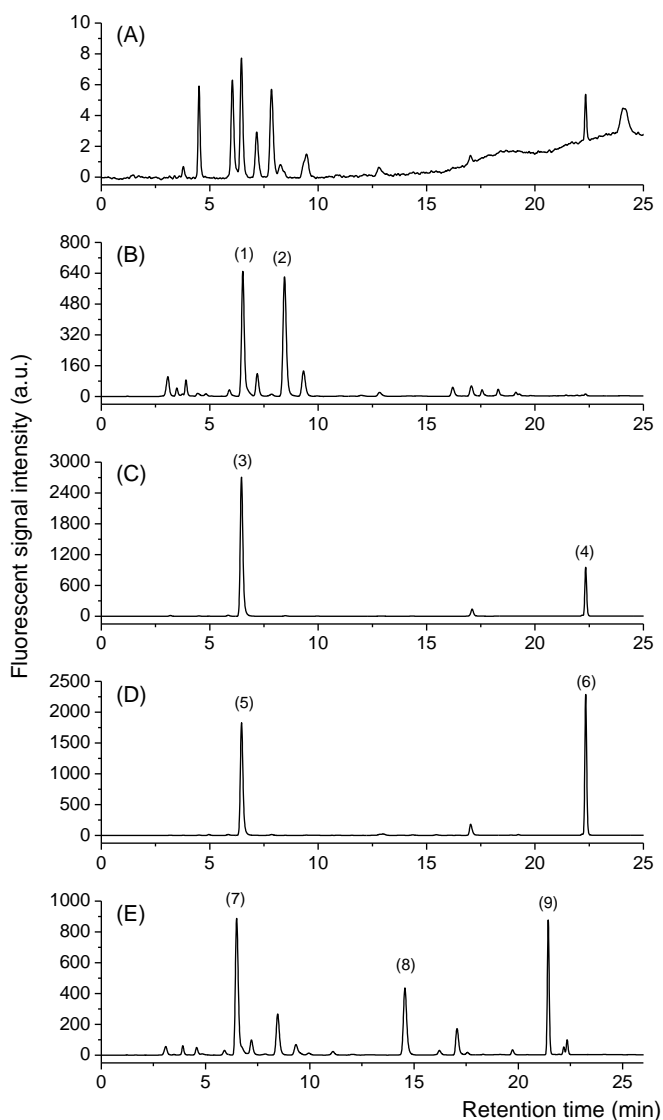


**Figure 5.10** Chromatograms obtained for (A) sweet orange, (B) sour orange, (C) lemon, (D) tangerine, and (E) grapefruit essential oils in hydro-alcoholic system (60  $\mu\text{L}$  of a mixture containing EO and octan-1-ol, 1:2 volume proportion, 2 mL of ultrapure water, and propan-1-ol up to 5 mL). Injection volume of 5.0  $\mu\text{L}$ , and mobile phase consisting of ultrapure water (A) and acetonitrile (B) with a linear gradient (0–7 min, 50% B; 7–13 min, 50–60% B; 13–15 min, 60–80% B; 15–17 min, 80% B; 17–20 min, 80–100% B; 20–25 min, 0% B; 25–27 min, 100–50% B; 27–30 min, 50% B) were used. Chromatograms were acquired using fluorescence detector (336/436 nm). Peaks with the highest intensity were marked (1 to 9).

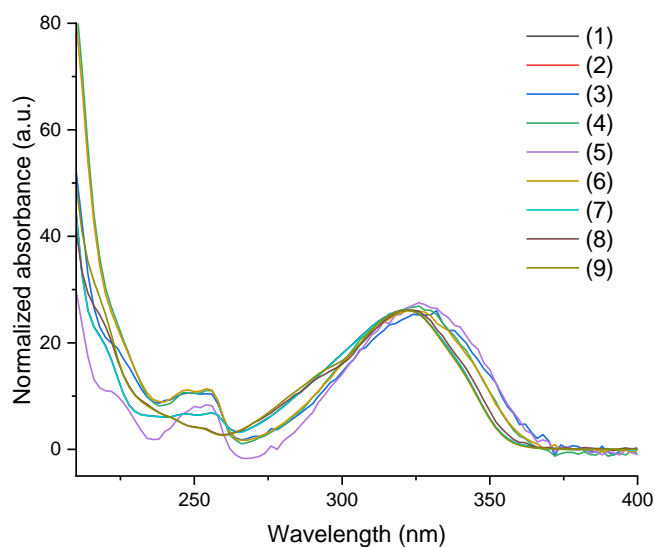


**Figure 5.11.** UV absorption spectra obtained at the same retention times of the highlighted peaks (1 to 9) in the chromatograms presented in Figure 5.10B-E. UV spectra were normalized for comparison purposes.

For sweet orange CEOs, low signal intensities were obtained, which did not permit the comparison of absorption spectra. Compared to other CEOs, sweet orange EO has a less complex non-volatile fraction, primarily composed of polymethoxyflavones [5]. In order to investigate if these substances were responsible for the observed fluorescence, a mixture containing five polymethoxyflavones (heptamethoxyflavone, nobiletin, sinensetin, scutellarein, and tangeretin) and chromen-2-one as internal standard was also used for chromatographic comparison (Figure 5.12). As a result, all PMFs exhibited signals in the monitored region (336/436 nm), corroborating the influence of the non-volatile fraction on the results found for sweet orange oil after 3D spectrofluorimetry analysis.

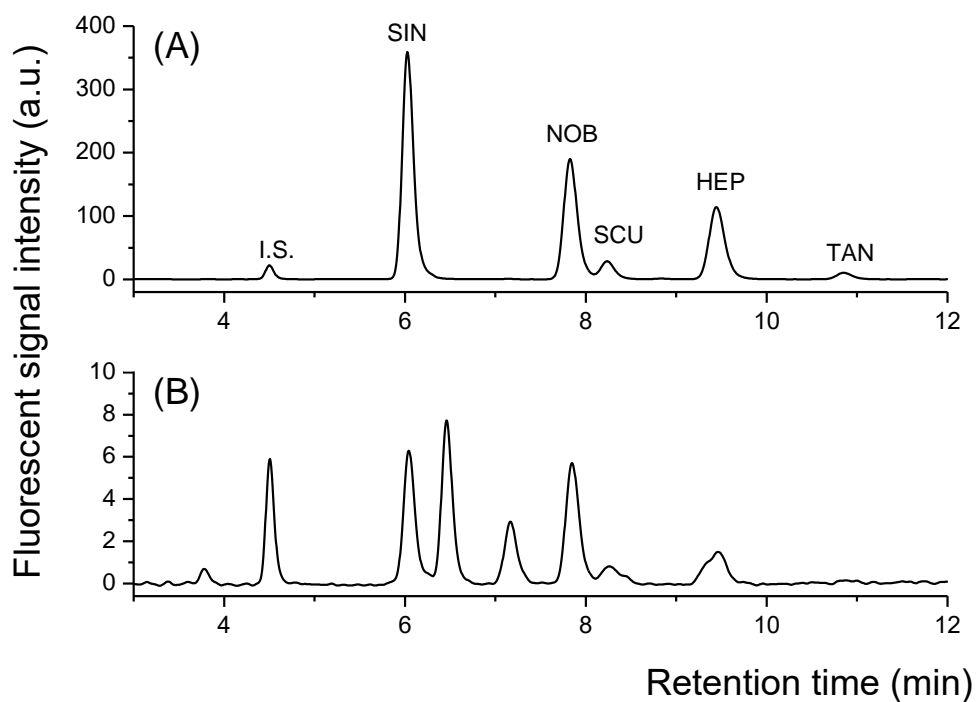


**Figure 5.12.** (A) Chromatograms of a mixture containing chromen-2-one as internal standard (I.S.) and five polymethoxyflavones: (1) sinensetin, (2) nobiletin, (3) scutellarein, (4) heptamethoxyflavone, and (5) tangeretin, at  $100 \text{ mg L}^{-1}$ . (B) Chromatograms of orange EO and chromen-2-one as I.S. in hydro-alcoholic system (60  $\mu\text{L}$  of a mixture containing EO and octan-1-ol, 1:2 volume proportion, 2 mL of ultrapure water, and propan-1-ol up to 5 mL). Injection volume of 5.0  $\mu\text{L}$ , and mobile phase consisting of ultrapure water (A) and acetonitrile (B) with a linear gradient (0–7 min, 50% B; 7–13 min, 50–60% B; 13–15 min, 60–80% B; 15–17 min, 80% B; 17–20 min, 80–100% B; 20–25 min, 0% B; 25–27 min, 100–50% B; 27–30 min, 50% B) were used. Chromatograms were acquired using fluorescence detector (336/436 nm).

### 5.3

#### Partial conclusion

3D fluorescence spectroscopy analysis was conducted for CEOs in hydro-alcoholic media. Following univariate optimization, a condition was adopted, utilizing 15  $\mu\text{L}$  of an oily phase (CEO and octan-1-ol, 1:2, v/v), 19 mL of ultrapure water and propan-1-ol up to 25 mL. This proportion was carefully chosen to encompass all evaluated CEOs in the study (sweet and sour orange, grapefruit, lemon, and tangerine) without compromising the reproducibility of the measurements, and with the lowest possible proportion of sample and organic solvents. Results allowed the application of these systems for CEOs differentiation through discriminant analysis by UPCA. Cumulative variance of 99.5% for the first PCs (73.3%, 20.2%, and 6.0% for PC1, PC2, and PC3, respectively) was achieved, and eigenvectors decomposition revealed a significant influence at 336/436 nm ( $\lambda_{\text{ex}}/\lambda_{\text{em}}$ ). Complementary analyses by HPLC support the hypothesis that this signal, common to all CEOs, corresponds to fluorophores present in the non-volatile fraction. Low sample consumption and high-water content make the application of these systems advantageous for EO monitoring. Transparency and low viscosity are also considered as positive aspects.

## 6

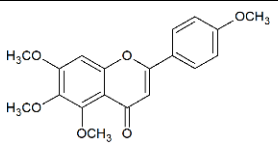
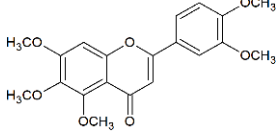
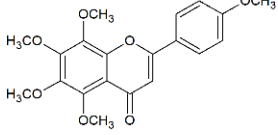
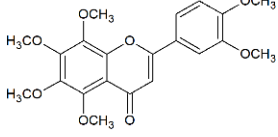
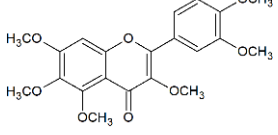
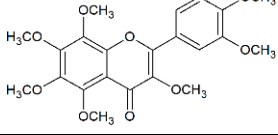
# Effect of sampling medium on the analysis of polymethoxyflavones in sweet orange essential oil by reversed-phase high-performance liquid chromatography

## 6.1

### Introduction

Sweet orange essential oil (EO) is a valuable byproduct of the juice industry, standing out as one of the most commercially produced EO. Its high production rates reflects in affordable market prices, and its diverse biological properties it is reputed as the most popular EO [16,110]. Traditionally obtained by cold pressing of the citrus peels, citrus EOs, including sweet orange, exhibit a very distinctive characteristic attributed to the presence of non-volatile compounds in their composition. In sweet orange EOs, this fraction constitutes approximately 1% of its composition [4]. Studies concerning the citrus EOs non-volatile fraction demonstrated that its composition is very similar despite the EO source. For sweet orange EOs (*Citrus sinensis*), this fraction consists primarily of polymethoxyflavones (PMFs), including heptamethoxyflavone, tangeretin, nobiletin, tetra-*O*-methyl scutellarein, hexamethoxyflavone, and sinensetin [5]. The chemical structures of these compounds are presented in Table 6.1.

**Table 6.1.** Polymethoxyflavones reported for non-volatile fraction of sweet orange essential oils.

Code	Compound (CAS number)	Formula	Structure
1	Tetra- <i>O</i> -methyl-scutellarein (1168-42-9)	C <sub>19</sub> H <sub>18</sub> O <sub>6</sub>	
2	Sinensetin (2306-27-6)	C <sub>20</sub> H <sub>20</sub> O <sub>7</sub>	
3	Tangeretin (481-53-8)	C <sub>20</sub> H <sub>20</sub> O <sub>7</sub>	
4	Nobiletin (478-01-3)	C <sub>21</sub> H <sub>22</sub> O <sub>8</sub>	
5	Hexamethoxyflavone (34170-18-8)	C <sub>21</sub> H <sub>22</sub> O <sub>8</sub>	
6	Heptamethoxyflavone (1178-24-1)	C <sub>22</sub> H <sub>24</sub> O <sub>9</sub>	

The non-volatile fraction, which is less complex than its volatile counterpart, has emerged as an interesting alternative for monitoring the authenticity of these products. Due to their minor contribution to the odor of EOs, adulterators do not invest much time in studying ways to mask the non-volatile fraction, making it valuable as markers. These facts, combined with the various properties already reported for these compounds, has increased the importance of studying this still relatively unexplored fraction [4,16,19]. The PMFs are recognized for their numerous activities, including anti-inflammatory, anti-

carcinogenic, anti-atherosclerotic, antioxidant, hypolipidemic, and/or antidiabetic effects [111–114].

Currently, high-performance liquid chromatography with absorciometric detection on diode array detector (HPLC-DAD) is the most commonly used technique for the non-volatile fraction analysis, not only for sweet orange EO, but for Citrus in general. Methods reported in the literature initially involved the use of normal-phase chromatographic columns. The application of reverse-phase (RP) columns, which also yielded satisfactory results, has become the choice for most studies reported for this purpose in recent years [5]. A concern regarding the analysis of these products by liquid chromatography involves the sample pre-treatment process. Currently, in the literature, it is possible to find analytical methods for the analysis of citrus EOs by reverse-phase liquid chromatography without sample pre-treatment, as summarized in Table 6.2. Some of these studies assess the use of different mobile phases, however, to date, no studies were found specifically focusing on evaluating the effect of the sampling composition in chromatographic analysis.

**Table 6.2.** Methods reported in the literature for the analysis of oxygen heterocyclic compounds in citrus essential oils using reverse-phase high (and ultra-high) performance liquid chromatography (RP-HPLC and RP-UHPLC) without sample pre-treatment, with a highlight for the evaluated polymethoxyflavones (tetra-*O*-methyl-scutellarein, **1**; sinensetin, **2**; tangeretin, **3**; nobiletin, **4**; hexamethoxyflavone, **5**; and heptamethoxyflavone, **6**).

Reference	Essential oil	Analytical technique*	Sample dilution	Mobile phase solvents**	PMFs identified
[115]	Bergamot, bitter orange, and lemon	HPLC/PDA	1:50, v/v in EtOH	H <sub>2</sub> O:MeOH:THF (85:10:5), and MeOH:THF (95:5)	<b>1, 2, 3, 4</b>
[116]	Bergamot, bigarade, grapefruit, lemon, lime, mandarin, and orange	UHPLC/TOF-MS	1:100, w/v in ACN:MeOH, 50:50	H <sub>2</sub> O:MeOH:THF (85:10:5), and MeOH:ACN:THF (65:30:5) (0.1% of formic acid and 5 mM ammonium formate)	<b>1, 5, 6</b>
[4]	Lemon arg, mandarin green, orange valencia, and tangerine florida	HPLC-UV	1:10, w/v in EtOH	H <sub>2</sub> O, and MeOH	<b>2, 3, 4</b>
[117]	Bergamot, bitter orange, grapefruit, key lime, mandarin, and sweet orange	HPLC/PDA	1:60, w/v (for quantitative analyses), and 1:120, w/v (for qualitative ultra-fast analyses) in EtOH	H <sub>2</sub> O:MeOH:THF (85:10:5), and MeOH:THF (95:5)	<b>1, 2, 3, 4, 5, 6</b>
[118]	Bergamot	HPLC/PDA and HPLC-MS-IT-ToF	1:60, w/v in EtOH	H <sub>2</sub> O:MeOH:THF (85:10:5), and MeOH:THF (95:5)	<b>1, 2, 3, 4</b>
[119]	Bergamot, bitter orange, grapefruit, key lime, lemon, mandarin, and sweet orange	HPLC/PDA	1:60, w/v (for lemon lime and bergamot EOs), and 1:50, w/v (for grapefruit, bitter orange, sweet orange, and mandarin EOs) in EtOH	H <sub>2</sub> O:MeOH:THF (85:10:5), and MeOH:THF (95:5)	<b>1, 2, 3, 4, 5, 6</b>

**Table 6.2:** cont.

Reference	Essential oil	Analytical technique*	Sample dilution	Mobile phase solvents**	PMFs identified
[120]	Bergamot	HPLC/PDA and HPLC-MS-IT-TOF	Not reported	H <sub>2</sub> O:MeOH:THF (85:10:5), and MeOH:THF (95:5)	<b>1, 2</b>
[121]	Bitter orange	HPLC-PDA	1:50, w/v in EtOH	H <sub>2</sub> O:MeOH:THF (85:10:5), and MeOH:THF (95:5)	<b>3, 4, 6</b>
[122]	Mandarin	HPLC-PDA and LSMS-IT-TOF	1:50, w/v in EtOH	H <sub>2</sub> O:MeOH:THF (85:10:5), and MeOH:THF (95:5)	<b>1, 2, 3, 4, 6</b>
[123]	Mandarin	HPLC/PDA	1:20, w/v in ACN	H <sub>2</sub> O, and ACN	<b>1, 2, 3, 5, 6</b>
[124]	Bergamot, bitter orange, grapefruit, lemon, lime, and mandarin	HPLC-UV	1:50, w/v in EtOH	H <sub>2</sub> O:ACN:THF (85:10:5), and ACN:MeOH:THF (65:30:5)	<b>3, 4, 6</b>
[125]	Grapefruit, lime	HPLC-DAD	2–5 mg in ACN:H <sub>2</sub> O, 1:1 (proportions not reported)	H <sub>2</sub> O, and ACN	<b>1, 4</b>
[126]	Bergamot, mandarin, and sweet orange	HPLC-UV	1:10 in ACN	THF, ACN, MeOH, and H <sub>2</sub> O	<b>1, 2, 3, 4, 6</b>
[127]	Bergamot, bitter orange, grapefruit, mandarin, and sweet orange	HPLC-UV and HPLC/API/MS	1:10, v/v in ACN	THF:ACN:MeOH:H <sub>2</sub> O (15:5:22:58), and ACN	<b>1, 3, 4, 5, 6</b>
[19]	Bergamot, bitter orange, lemon, red mandarin, and sweet blond orange	HPLC/PDA	1:100 in ACN	H <sub>2</sub> O, and ACN	<b>1, 2, 3, 4, 5, 6</b>

\* Abbreviations are reported in the table as cited in the reference. (U)HPLC: (ultra-)high-performance liquid chromatography; API: atmospheric pressure ionization; DAD: diode array detection; IT: ion trap; LSMS: Liquid chromatograph mass spectrometer; MS: mass spectrometry; PDA: photodiode array detector; TOF (or ToF): time-of-flight; UV: ultraviolet; \*\* ACN: acetonitrile; EtOH: ethanol; MeOH: methanol; THF: tetrahydrofuran; H<sub>2</sub>O: water.

Russo et al. (2012) [119] compared the use of methanol instead of acetonitrile as mobile phase for the analysis of different citrus EOs (bergamot, bitter orange, grapefruit, key lime, lemon, mandarin, and sweet orange) by RP-HPLC coupled with absorciometric PDA detector aiming 36 oxygen heterocyclic compounds (coumarins, psoralens and polymethoxyflavones). The use of methanol, tetrahydrofuran and water resulted in a satisfactory baseline separation of nearly all the evaluated compounds, along with improvement in the resolution for critical pairs of psoralens (byakangelicol/oxypeucedanin, isopimpinellin/bergapten, and isomeranzin/bergapten). No assessment was conducted regarding the medium (ethanol) used to introduce samples. Considering the use of complex mobile phases, the influence of the media for sampling, different from those used as eluent should be taken into account, as it can significantly affect the solubility, and the quality of the analytical response, affecting intensity and causing distortions in the chromatographic peak [55].

The present study aims to develop a method for sweet orange EOs analysis by RP-HPLC with focus on the main PMFs (tetra-*O*-methyl-scutellarein, **1**; sinensetin, **2**; tangeretin, **3**; nobiletin, **4**; and heptamethoxyflavone, **6**) with a careful evaluation of the medium used for sampling into the HPLC system. Hexamethoxyflavone (**5**) was not included due to the unavailability of analytical standards. The use of two mobile phases with less complexity in terms of composition was also evaluated (acetonitrile and methanol/water) employing absorciometric and fluorimetric detection.

## 6.2

### Results and discussion

#### 6.2.1

##### HPLC analysis with absorciometric photodiode array detection (HPLC-DAD)

Preliminary analyses by HPLC-DAD, monitoring absorbance within the 190 – 400 nm range, were performed using individual analytical standards of the five PMFs at 100 mg L<sup>-1</sup> in ethanol, to identify the chromatographic peaks corresponding to the PMFs using two mobile phases (methods A and B) and to evaluate the optimal wavelength to be used for absorciometric detection. Ethanol was chosen for the sample preparation of initial studies as it is the most commonly selected solvent according to methods reported in the literature (Table 6.2). During the standard solutions preparation, there was difficulty in solubilize, especially for tetra-*O*-methyl-scutellarein, sinensetin, and nobiletin, requiring sonication for complete dissolution. Similar problem was also reported by Arigò et al. (2019) [115]. Absorption spectrum for each evaluated PMF is presented in Figure 6.1 and very similar spectra were obtained for both mobile phases. Considering working with a single wavelength finding a compromise condition in term of analytical sensitivity, it was decided to continue the analyses with HPLC-DAD using the 336 nm wavelength to avoid degrading quantification of **6**. Chromatograms obtained by HPLC at 336 nm using both mobile phases are presented in Figure 6.2A-B.

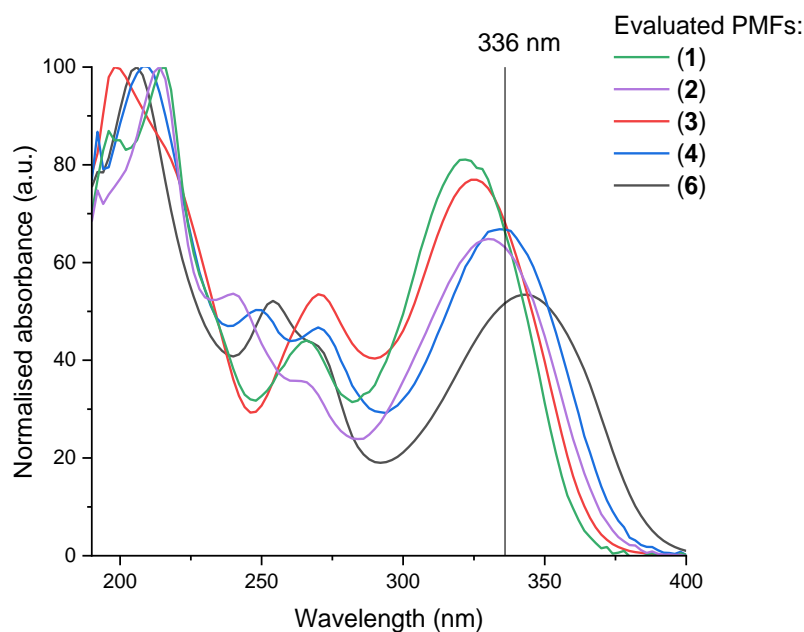


**Figure 6.1.** UV absorption spectra obtained during HPLC-DAD analysis for the evaluated polymethoxyflavones (PMFs): tetra-*O*-methyl-scutellarein, **1**; sinensetin, **2**; tangeretin, **3**; nobiletin, **4**; heptamethoxyflavone, **6**. Chromatograms were obtained using acetonitrile/water (50:50% v/v) as mobile phase. Introduced volume of 10  $\mu\text{L}$  (standard solution of PMFs at 100  $\text{mg L}^{-1}$  in ethanol), flow rate at 1.0  $\text{mL min}^{-1}$ , and 30°C. Absorbance values were normalized for comparison.

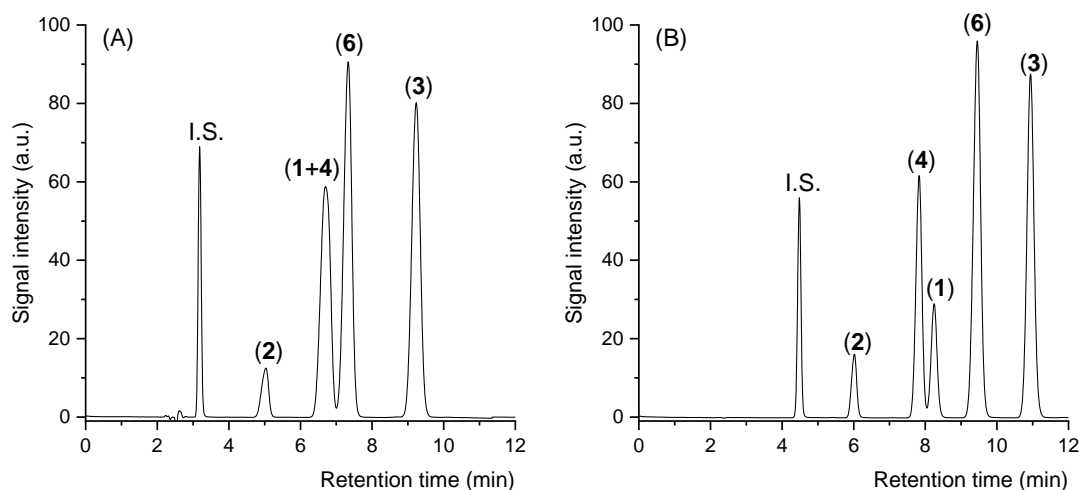


**Figure 6.2.** Chromatograms of a mixture containing chromen-2-one as internal standard (I.S.) and five polymethoxyflavones (tetra-*O*-methyl-scutellarein, **1**; sinensetin, **2**; tangeretin, **3**; nobiletin, **4**; heptamethoxyflavone, **6**) at  $100 \text{ mg L}^{-1}$  in ethanol. Chromatograms were obtained by HPLC-DAD at 336 nm using (A) methanol/water (73:27%, v/v), and (B) acetonitrile/water (50:50%, v/v) as mobile phases. Introduced volume of  $10 \mu\text{L}$ , flow rate at  $1.0 \text{ mL min}^{-1}$ , and  $30^\circ\text{C}$ .

The mobile phases used for methods A and B were chosen considering the use of solvents commonly employed for the development of methods in reverse-phase HPLC. However, it is shown in Table 6.2 that many methods developed for this purpose involved more complex mobile phases, including the use of mixtures containing tetrahydrofuran (THF). Although the option for more complex mobile phases may be reasonable when analyzing citrus EOs, which is characterized by more complex compositions, it may not be necessary for the present study, which focused on the analysis of PMFs in sweet orange EO. The non-volatile fraction of this variety of EO exhibits a less intricate composition. Therefore, using simpler mobile phases in an isocratic mode could be a viable and simple alternative for this

work. Additionally, it is essential to consider all the practical implications and hazards associated with the use of THF as a mobile phase in HPLC systems [54].

Preliminary tests were conducted using methanol and water as mobile phase. Despite experimenting with different proportions and gradient elution, satisfactory results were not attained besides using a mixture of methanol and water in a ratio of 73:27% (v/v) that produced good peak separation except for two peaks that co-eluted under these conditions (compounds **1** and **4**, as shown in Figure 6.2A). In addition to methanol, mixtures of acetonitrile with water were also tested.

In order to find proper acetonitrile-to-water proportion, Equation 6.1 was first applied to ascertain which condition would maintain a polarity similar to that of the mobile phase set with methanol [53]. This step was carried out taking into account the efficiency in sample solubilization. Subsequently, HPLC experiments were conducted to fine-tuning the experimental condition. As a result, a mobile phase consisting of a 50:50% (v/v) mixture of acetonitrile and water was chosen. The chromatogram obtained for the second mobile phase is depicted in Figure 6.2B.

$$\Phi_B = \frac{\Phi_A \times S_A}{S_B} = \frac{0,73 \times 2,6}{3,2} = 0,59 \text{ (or 59\%)} \quad (\text{Eq. 6.1})$$

$\Phi_A$  and  $\Phi_B$  correspond to the volume fractions of methanol and acetonitrile, respectively (in this case,  $\Phi_A = 73\% = 0,73$ ).  $S_A$  and  $S_B$  are the weight force factor of methanol (2,6) and acetonitrile (3,2), respectively.

Upon comparing the two selected mobile phases through the chromatograms obtained and presented in Figure 6.2A-B, it is evident that for method B, all PMFs could be analyzed. Gradient elution was also tested to enhance the resolution of peaks corresponding to PMFs (**1**) and (**4**) but the broadening of

peaks did not justify a change in the chosen solvent ratio as the mobile phase and a change from isocratic conditions.

### 6.2.2

#### **Effect of sampling medium for HPLC introduction**

Although the use of acetonitrile and water as the mobile phase is more advantageous due to the absence of co-eluted peaks, the composition of the sampling medium was also evaluated in separations using two mobile phases (methods A and B). Sweet orange EO samples were prepared in different solvents (100  $\mu$ L of EO in 5.0 mL). During these preliminary assessments, the PMF content in EO samples were monitored saving the high cost PMF standards for the final adjustments and validation step. Initially, the study aimed to investigate the influence of acetonitrile, ethanol, and methanol, which, as already mentioned, are commonly used solvents according to the literature (Table 6.2). Chromatograms are presented in Figure 6.3A-B where sharpening in chromatographic peaks, without affecting the peak area, is obtained when methanol was used in sampling medium. This aspect is particularly relevant when considering the complexity of samples and analytical sensitivity of the method if quantification of compounds at low concentration levels requires peak height measurements.

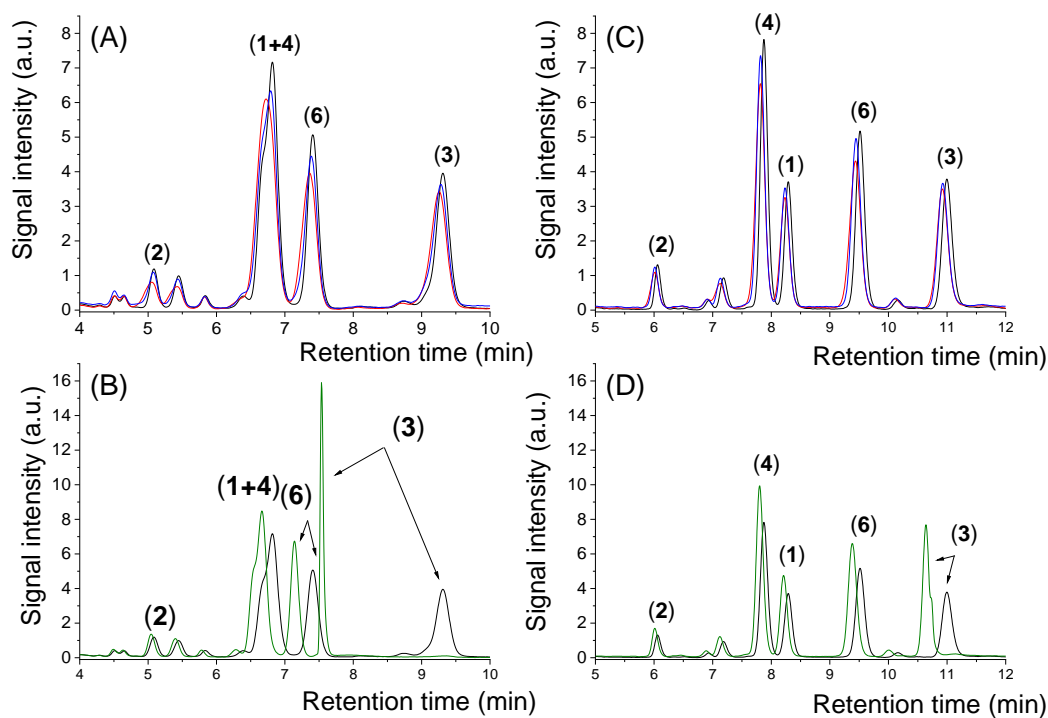


**Figure 6.3:** Chromatograms obtained for sweet orange EO analysis (100  $\mu$ L EO in 5 mL) with peaks corresponding to the evaluated PMFs highlighted (tetra-*O*-methyl-scutellarein, **1**; sinensetin, **2**; tangeretin, **3**; nobiletin, **4**; heptamethoxyflavone, **6**). (A) and (B) methanol/water (73:27%, v/v); (C) and (D) acetonitrile/water (50:50%, v/v) were used as mobile phase. Line colors representing solvents used in sampling (sample introduction medium): methanol (black), ethanol (red), acetonitrile (blue), and methanol:octan-1-ol (10:3 w/w) (green). HPLC-DAD at 336 nm.

A recent study by Macedo et al. (2023) [104] using spectrofluorimetry reported that the addition of octan-1-ol significantly influences the solubilization of sweet orange EO in hydroalcoholic systems through the formation of micelle-like aggregations. Improvements in the fluorescence measured from EOs were also observed in these systems. Since water is used as a component in the mobile phase during chromatographic separation, it was also decided to include mixtures of

methanol (which was the one producing better results in the initial assessment) with octan-1-ol (10:3 w/w) to evaluate if octan-1-ol addition could influence the elution of analytes during the chromatographic separation process. Results obtained for this evaluation are presented in Figure 6.3C-D. The octan-1-ol addition resulted in a significant decreasing in PMF retention times and sharpening in peak widths, without affecting the peak areas, highlighting a substantial advantage in the use of octan-1-ol. This advantage is particularly noteworthy for tangeretin, where a 300% increase in peak intensity was obtained when using methanol/water as the mobile phase while 103% increase was observed when acetonitrile and water were used as the mobile phase. These results indicate that the addition of octan-1-ol not only enhances the method's sensitivity but also decreasing total chromatographic running time (reducing reagent consumption in long term).

Initially, combination with octan-1-ol in at 10:3 w/w were used, similar the condition used by Macedo et al. (2023) [104]. Subsequently, other octan-1-ol weight proportions were also tested, including 10:1 w/w and 2:1 (or 10:5) w/w. Comparative chromatograms are presented in Figure 6.4A-B reinforcing the influence of the presence of octan-1-ol on the retention times of PMFs, especially for heptamethoxyflavone (**6**) and tangeretin (**3**), which among the evaluated PMFs, are the ones that exhibited the greatest interaction with the chromatographic column. For these two compounds, in particular, the use of methanol/water as the mobile phase can be extremely advantageous, making it a viable alternative for applications involving the analysis of these compounds. In analyses with acetonitrile/water as the mobile phase, this effect was not as pronounced. However, despite this, it remains the best alternative for the analysis of the PMFs in question due to the absence of co-elution.

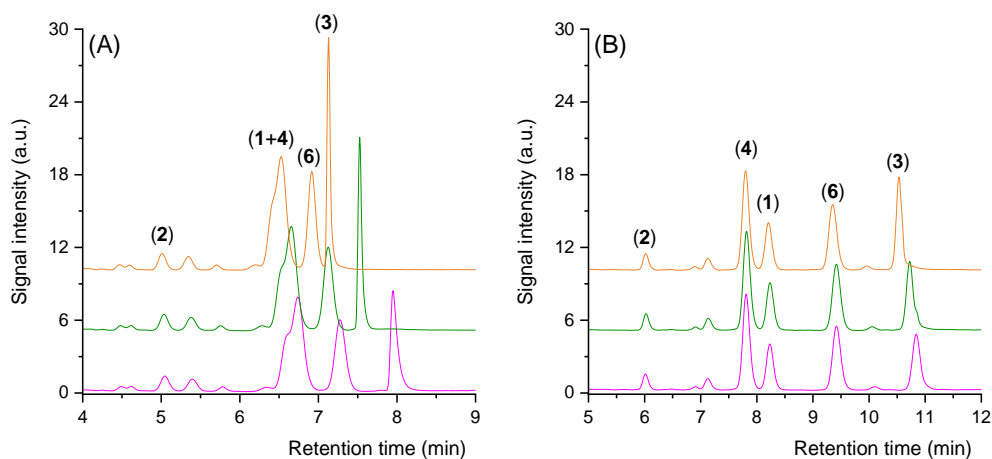


**Figure 6.4.** Chromatograms obtained for sweet orange essential oil analysis (100  $\mu$ L EO in 5 mL) with the peaks corresponded to the evaluated PMFs (tetra-*O*-methyl-scutellarein, **1**; sinensetin, **2**; tangeretin, **3**; nobiletin, **4**; heptamethoxyflavone, **6**). (A) Methanol/water (73:27%, v/v), and (B) acetonitrile/water (50:50%, v/v) were used as mobile phase. Line colors represent sample medium: methanol/octan-1-ol 10:1 w/w (magenta), 10:3, w/w (green) and 2:1 w/w (orange) HPLC-DAD at 336 nm.

As reported by Macedo et al. (2023) [104], the octan-1-ol addition can facilitate the solubilization of EOs through the formation of SFME which are homogeneous systems formed by two phases (aqueous and oily) through the addition of short-chain alcohols [37]. Since the mobile phase, consisting of methanol and water, sustains the hydroalcoholic medium during chromatographic runs, this effect is believed to be more pronounced in this system due to this specific reason.

### 6.2.3

#### **Spectrofluorimetric and HPLC analysis with fluorimetric detection (HPLC-FD)**

Fluorescence detection usually provides greater selectivity and analytical sensitivity when compared to absorciometric detection in HPLC. In order to utilize HPLC-FD for the analysis of sweet orange EOs, a previous study was conducted using spectrofluorimetry to find the compromise pair of wavelengths ( $\lambda_{\text{ex}}/\lambda_{\text{em}}$ ) to be utilized. For this preliminary investigation, the standard solutions prepared in ethanol were employed. Results indicated possibilities for excitation and emission wavelength pairs ( $\lambda_{\text{ex}}/\lambda_{\text{em}}$ ): 361/502 nm for tetra-*O*-methyl-scutellarein (**1**), 366/430 nm for sinensetin (**2**), 377/423 nm for tangeretin (**3**), 377/432 nm for nobiletin (**4**), and 388/433 nm for heptamethoxyflavone (**6**). The fluorescence excitation and emission spectra obtained for each compound are shown in Figure 6.5A-E.

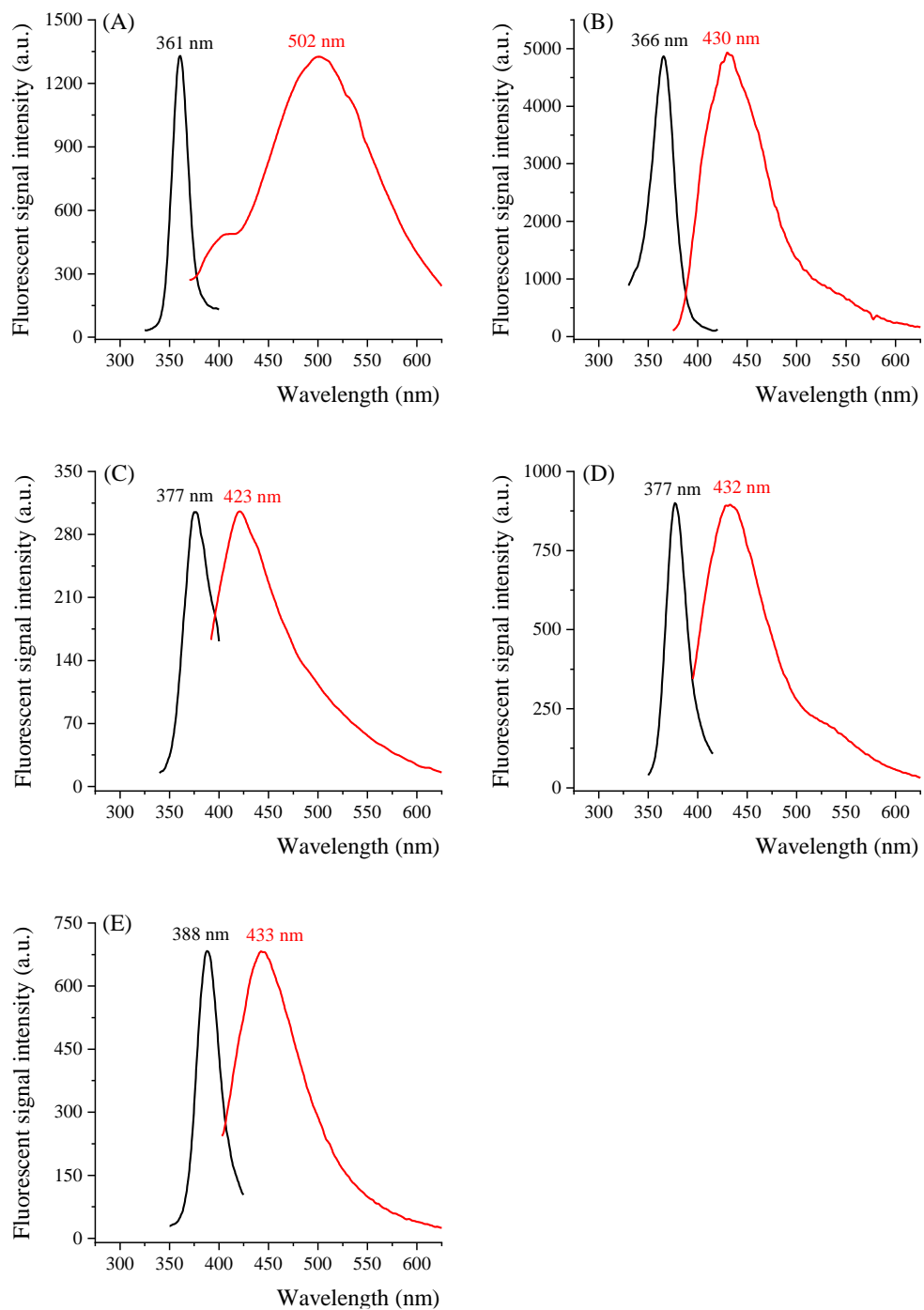


**Figure 6.5.** Fluorescence excitation (black lines) and emission (red lines) spectra for the polymethoxyflavones (at 100 mg L<sup>-1</sup> in ethanol): (A) tetra-*O*-methylscutellarein, **1**; (B) sinensetin, **2**; (C) tangeretin, **3**; (D) nobiletin, **4**; and (E) heptamethoxyflavone, **6**.

The study presented in the previous chapter of this thesis concluded that compounds from the non-volatile fraction of citrus EOs emitted stronger fluorescence (at 336/436 nm) in hydro-alcoholic media. Due to the use of methanol and water as components of mobile phase, it was decided to test not only the ( $\lambda_{\text{ex}}/\lambda_{\text{em}}$ ) pair, observed after spectrofluorimetric analysis, but also included the 336/436 nm pair. Chromatographic introduction (in HPLC-FD) was then conducted using a system containing the evaluated PMFs prepared using methanol and octan-1-ol in at 2:1 weight proportion. During the preparation of standard solutions in the chosen system, it was not necessary to subject the samples to ultrasound, unlike what was observed during preparation in ethanol, as there was a prompt solubilization of the target analytes. Chromatograms obtained using either of mobile phases (A and B) by HPLC-FD analysis are presented in Figure 6.6A-D. Results indicated that the chosen wavelength was an appropriate option in terms of analytical sensitivity for all PMFs, especially for sinensetin (**2**), highlighting the significant influence of the media in the analysis of PMFs by spectrofluorimetry.

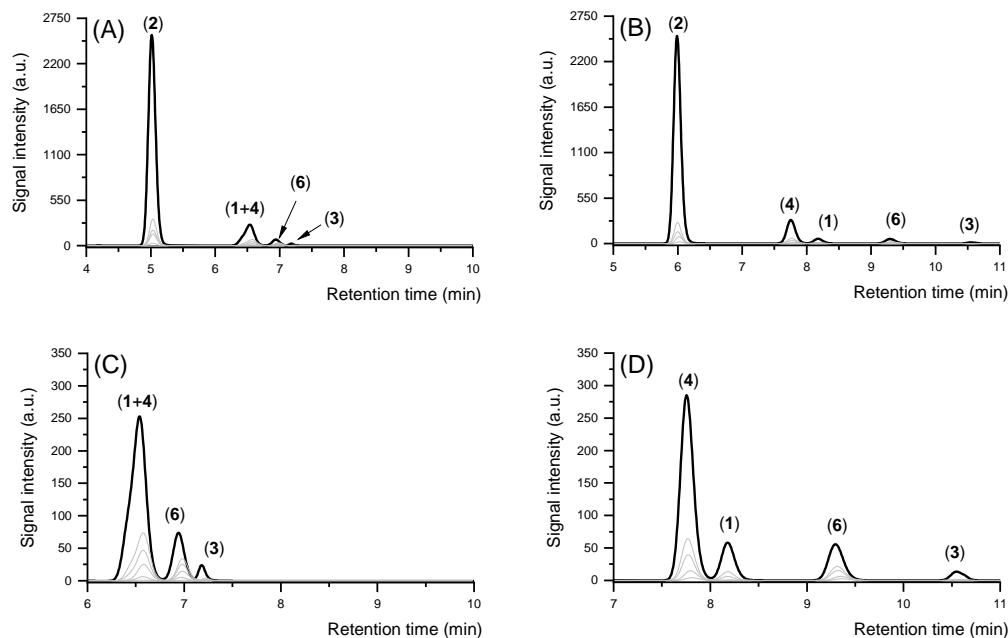


**Figure 6.6.** Chromatograms of a mixture containing five polymethoxyflavones (tetra-*O*-methyl-scutellarein, **1**; sinensetin, **2**; tangeretin, **3**; nobiletin, **4**; heptamethoxyflavone, **6**) at 100 mg L<sup>-1</sup> in methanol/octan-1-ol 2:1 w/w. Chromatograms were obtained by HPLC-FD using (A) methanol/water (73:27% v/v) and (B) acetonitrile/water (50:50% v/v) as mobile phase. (C) and (D) correspond to chromatograms (A) and (B), respectively, with a zoom for better observation of peaks for substances with lower intensity. Black lines represent chromatograms obtained at 336/436 nm, and the gray lines correspond to chromatograms obtained at 361/502 nm, 366/430 nm, 377/423 nm, 377/432 nm, and 388/433 nm.

#### 6.2.4

##### Method validation

Before proceeding with method validation, the standard solution containing the PMFs dissolved in methanol/octan-1-ol (2:1 w/w) was analyzed by HPLC using both mobile phases (A and B) (Figure 6.7A-F). Despite the observed co-elution between tetra-*O*-methyl-scutellarein and nobiletin, mobile phase A was efficient separation for the remaining compounds, with a shorter total analysis time (under 8 min), making it a viable alternative for general applications. However, despite requiring a longer total analysis time for EOs analysis, mobile phase B (under 11 min) was found to be more suitable, as it efficiently separates all compounds of interest. Based on this, the conditions established for the method using mobile phase B were selected for the next stage of the study, which includes the validation of the analytical method and its application to a commercial sample of sweet orange EO.

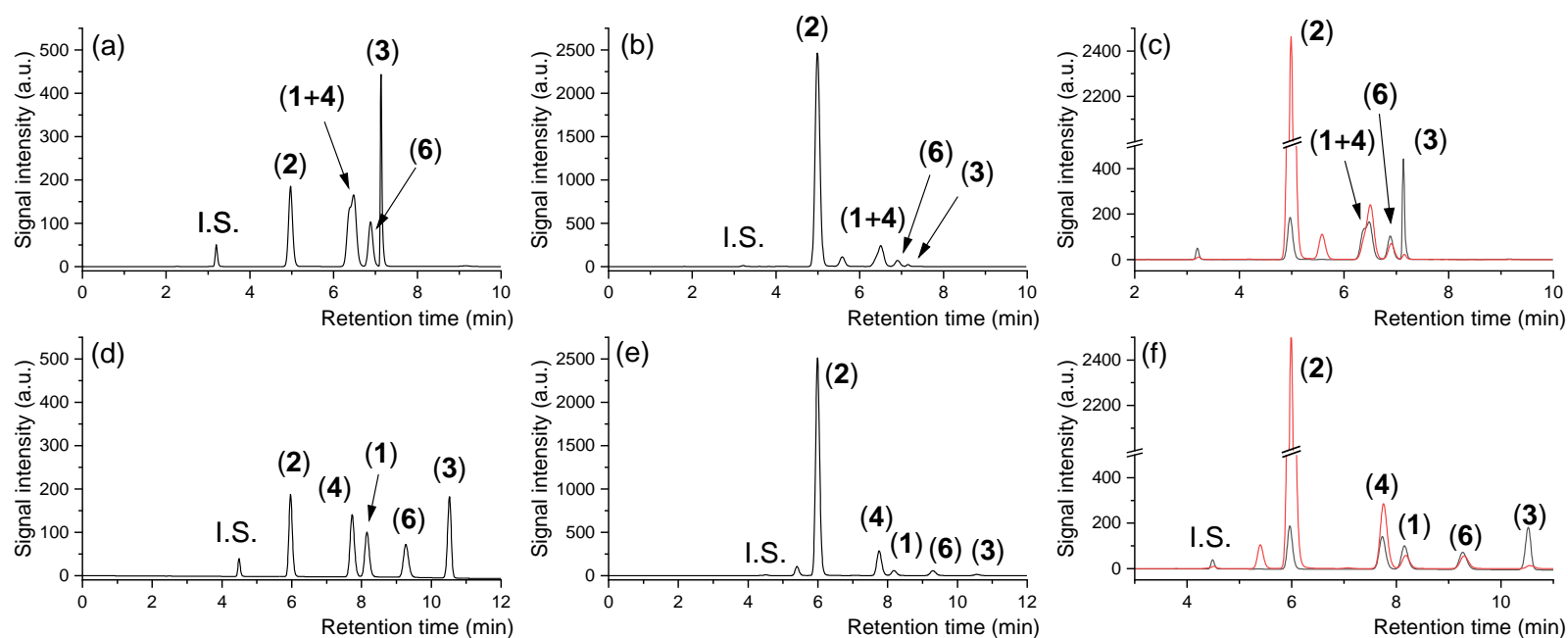


**Figure 6.7.** Chromatograms of a mixture containing five polymethoxyflavones (tetra-*O*-methyl-scutellarein, **1**; sinensetin, **2**; tangeretin, **3**; nobiletin, **4**; heptamethoxyflavone, **6**) at  $100 \text{ mg L}^{-1}$ , and chromen-2-one (internal standard, I.S.) at  $100 \text{ mg L}^{-1}$  solubilized in methanol: octan-1-ol 2:1 weight proportion. (a) Mobile phase A by HPLC-DAD, (b) Mobile phase A by HPLC-FD, and (c) overlapped chromatograms (a) and (b). (d) Mobile phase B by HPLC-DAD, (e) Mobile phase B by HPLC-FD, and (f) overlay of chromatograms (d) and (e) with zoom.

Comparing Figures 2B and 7D, which represent chromatograms obtained for analytical standards introduced from systems containing ethanol and methanol-octan-1-ol (2:1, w/w), respectively, it is evident that peaks of higher intensities were observed in the latter. This phenomenon can be attributed to the significant improvement in solubilizing analytical standards due to the presence of octan-1-ol. In the analysis of the five PMFs, the method using mobile phase B produced the most favorable outcome, achieving satisfactory separation of all evaluated compounds. When comparing the two detection systems (Figure 6.7D-F), the use of fluorimetric detection proves highly advantageous, especially for sinensetin, which is particularly beneficial when considering markers for potential adulteration by lower-grade oils. Furthermore, the precise quantification capability of this substance holds relevance across various matrices, suggesting that this method can be effectively applied in different situations.

With the analytical conditions carefully evaluated, analytical figures on merit were obtained (Table 6.3) highlighting the results obtained through the two detection systems (DAD and FD). Linearity of response was evaluated as determination coefficient ( $R^2$ ) ranging from 0.9962 to 1.0000 indicating a highly satisfactory correlation within the linear working range. Coefficient of variation values below 3.0 % indicates that the method exhibits adequate precision. Inter-day repeatability was calculated in terms of peaks areas for all the evaluated PMFs at 0.05 mg L<sup>-1</sup> in ten replicates. From the applied *Student-t*-test (95% level of significance), it was possible to confirm that there was no significant difference between the results obtained in two consecutive days, indicating satisfactory inter-day precision. Additionally, the LOD and LOD obtained in this work were comparable with the values reported in the literature, considering two similar

studies [119,128] as seen in Table 6.4, but it is worth noting that in these reported studies employed chromatographic columns with a particle size of 2.7  $\mu\text{m}$  and mobile phases, characterized by complex compositions and elution gradients (Table 6.2).

**Table 6.3.** Validation parameters for the calibration curves obtained by HPLC analysis (method with mobile phase B, indicated in Table 3.3). In this case, methanol: octan-1-ol was used as solvent injection and chromen-2-one as internal standard (at 100 mg L<sup>-1</sup>). PMFs: tetra-*O*-methylscutellarein (1), sinensetin (2), tangeretin (3), nobiletin (4), and heptamethoxyflavone (6).

PMF	Range (mg L <sup>-1</sup> )	Analytical curve	R <sup>2</sup>	LOD (mg L <sup>-1</sup> )	LOQ (mg L <sup>-1</sup> )	CV (%)	
HPLC-DAD	(1)	1 – 100	$y = 0.0371x + 0.0066$	1.0000	0.029	0.097	0.4
	(2)	1 – 100	$y = 0.0528x + 0.0156$	0.9990	0.031	0.104	0.4
	(3)	1 – 100	$y = 0.0551x + 0.0105$	1.0000	0.053	0.177	0.4
	(4)	1 – 100	$y = 0.0505x + 0.0743$	0.9972	0.094	0.312	0.7
	(6)	1 – 100	$y = 0.0314x + 0.0083$	1.0000	0.063	0.211	0.7
HPLC-FD	(1)	1 – 100	$y = 0.0876X + 0.0328$	0.9999	0.245	0.818	2.4
	(2)	0.05 – 100	$y = 2.590x + 0.8691$	0.9998	0.001	0.003	1.0
	(3)	5 – 100	$y = 0.0183X + 0.0701$	0.9992	0.831	2.771	3.0
	(4)	1 – 100	$y = 0.3538X + 0.4140$	0.9975	0.013	0.044	1.3
	(6)	1 – 100	$y = 0.0818X + 0.0364$	1.0000	0.096	0.319	1.6

**Table 6.4.** Comparison of the figures of merit of similar methods reported in the literature for the quantification of polymethoxyflavones (PMFs) in citrus essential oils using reverse-phase high (and ultra-high) performance liquid chromatography (RP-HPLC and RP-UHPLC) without sample pre-treatment. Only the evaluated PMFs were presented: tetra-*O*-methyl-scutellarein (**1**), sinensetin (**2**), tangeretin (**3**), nobiletin (**4**), and heptamethoxyflavone (**6**). Linearity range, LOD, and LOQ are expressed in mg L<sup>-1</sup>.

Reference	Linearity range	PMFs included in the study											
		(1)		(2)		(3)		(4)		(6)			
		LOD	LOQ	LOD	LOQ	LOD	LOQ	LOD	LOQ	LOD	LOQ		
Present work	HPLC-DAD	1 – 100		0.029	0.097	0.031	0.104	0.053	0.177	0.094	0.312	0.063	0.211
	HPLC-FD	1 – 100 ( <b>1, 4, 6</b> ); 0.05 – 100 ( <b>2</b> ); 5 – 100 ( <b>3</b> )		0.245	0.818	0.001	0.003	0.831	2.771	0.013	0.044	0.096	0.319
[117]	0.1–100	0.042	0.068	0.042	0.068	0.042	0.068	0.063	0.087	0.076	0.106		
[119]	0.1–100	0.021	0.029	0.021	0.029	0.021	0.029	0.029	0.041	0.031	0.043		

n.a.: not applicable. \*Conditions employed in HPLC analysis (method B) are described on Table 3.3.

The proposed method was applied to a commercial sample of sweet orange EO, using six authentic replicates. The chromatograms obtained after analysis by HPLC-DAD and HPLC-FD using the conditions of the method using mobile phase B are shown in Figure 6.8 from where it is evident that HPLC-FD reveals additional compounds, at a shortest retention times, not apparent when using HPLC-DAD analysis. In addition, for compounds (1), (6), and (3) there is a probable co-elution, which hindered their quantification using this detection system. Despite this, for these three compounds, HPLC-DAD analysis is more advantageous in terms of sensitivity. On the other hand, compounds (2) and (4), besides appearing as peaks with adequate resolution, HPLC-FD detection is more favorable. Results with the concentrations obtained for each evaluated PMF are presented in Table 6.5.

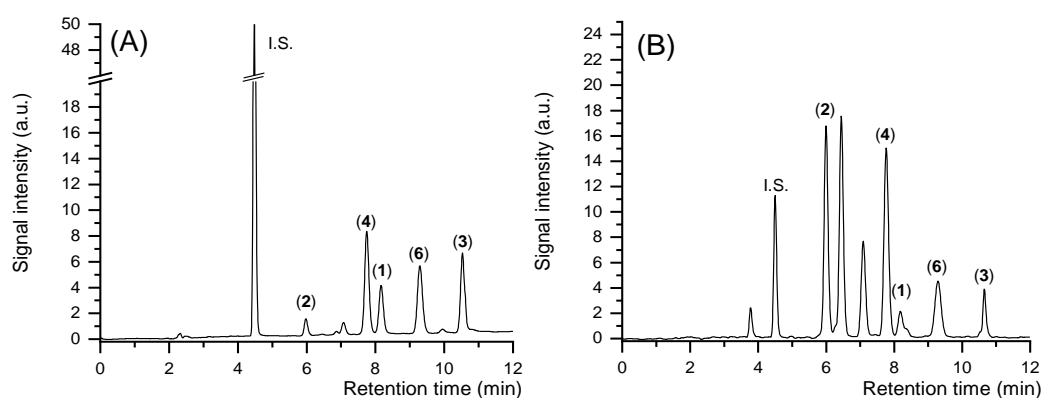


**Figure 6.8.** Chromatograms obtained for sweet orange essential oil analysis (100  $\mu\text{L}$  of EO in 5 mL) with the peaks corresponded to the evaluated PMFs highlighted (tetra-*O*-methyl-scutellarein, **1**; sinensetin, **2**; tangeretin, **3**; nobiletin, **4**; heptamethoxyflavone, **6**). Chromatograms were obtained after HPLC analysis (mobile phase B) with two detectors: (A) DAD at 336 nm and (B) FLD at 336/436 nm ( $\lambda_{\text{ex}}/\lambda_{\text{em}}$ ). Methanol: octan-1-ol 2:1 w/w were used as solvent of injection.

**Table 6.5.** Concentration in mg L<sup>-1</sup> of the evaluated PMFs (tetra-*O*-methylscutellarein, **1**; sinensetin, **2**; tangeretin, **3**; nobiletin, **4**; heptamethoxyflavone, **6**) in the analyzed sweet orange essential oil sample. Method with mobile phase B (Table 3.3) was used for HPLC analysis.

PMF	Concentration (mg L <sup>-1</sup> ), n = 6	
	HPLC-DAD	HPLC-FD
(1)	180.53 ± 2.81 (CV = 1.6%)	n.a.
(2)	21.21 ± 0.79 (CV = 3.7%)	21.56 ± 0.63 (CV = 2.9%)
(3)	194.72 ± 9.56 (CV = 4.9%)	n.a.
(4)	214.24 ± 4.00 (CV = 1.9%)	220.80 ± 2.03 (CV = 0.92%)
(6)	345.53 ± 3.51 (CV = 1.0%)	n.a.

n.a: non-applied due to appearance of a myriad of peaks from unidentified compounds.

### 6.3

#### Partial conclusion

In this study, the effect of the sampling medium used to introduce sweet orange EOs into the chromatographic system was systematically evaluated. Two methods (A and B) were employed for this purpose, using two mobile phases (methanol/water, 73:27% and acetonitrile/water, 50:50%) and isocratic elution. Different sampling media were tested, including methanol, ethanol, acetonitrile, and mixtures of methanol and octan-1-ol, which significantly influences chromatographic elution, affecting band width and retention time. Methanol and octan-1-ol (2:1, w/w) produced better results, reducing analysis time, and intensifying peak responses, particularly for tangeretin. Using both mobile phases, satisfactory LOD and LOQ values, with fluorescence detection proved to be advantageous for sinensetin and nobiletin analysis. Despite challenges in co-elution using mobile phase A, efficient separation for the remaining compounds, notably

tangeretin, along with a shorter total analysis time, positioned it as a better alternative for diverse applications. Conversely, method using mobile phase B, despite a longer analysis time, proved to be efficient in separating all compounds, being applied to commercial sweet orange EO samples yielding consistent results for all evaluated PMFs. Emphasizing the significance of these compounds as markers for sweet orange EO adulteration, this research significantly contributes to advancing analytical techniques for these compounds.

## 7

### General conclusion

In this study, analytical methods for CEO analysis were developed, utilizing SFMEs for sample treatment. Initially, the SFME formation region was explored for sweet orange essential oils (EOs) in five different weight proportions with water (1:4, 1:2, 1:1, 2:1, 4:1), using propan-1-ol and octan-1-ol (10:3 w/w) to stabilize both phases in a macroscopically homogeneous system. 3D fluorescence spectroscopy analysis results demonstrated that SFMEs greatly increased the fluorescence signals and spectral details. Nine Brazilian sweet orange EO brands were evaluated, and clustering analysis by UPCA was performed. A cumulative variance of 96.7% was obtained for the first three principal components, confirming the effectiveness of these systems in obtaining fingerprint patterns. Storage conditions, considering the effect of light exposure, and adulteration through addition of canola and mineral oil, were also evaluated, with these systems proving to be efficient for this purpose.

In a subsequent stage, new SFME systems were optimized and replicated for different CEOs, including sweet orange and sour orange, tangerine, lemon, and grapefruit. These systems allowed for precise and efficient analysis with low sample (5 $\mu$ L) consumption and high reproducibility. The presence of water in a high proportion (19 mL in a final volume of 25 mL) facilitated the cleaning of materials and reduced the risk of cross-contamination. Furthermore, the proposed dilution led to a reduction in the effect of the internal filter, eliminating the need for spectral correction, without compromising the observed signal intensities. Taking

into account the obtained results, these systems can be an interesting resource for the use of 3D fluorescence spectroscopy as a complementary and effective method to ensure better monitoring of these products. Currently, few studies are reported with this approach due to the intrinsic complexity of these samples. Additionally, complementary analyses by HPLC confirm the relationship between fluorophores and the non-volatile fraction.

In the final stage, the impact of the sampling medium on the analysis of PMFs in sweet orange EO by RP-HPLC was assessed, leveraging insights from earlier stages on SFME system formation. The focus was on analyzing PMFs in the non-volatile fraction of sweet orange EO, including tetra-*O*-methyl-scutellarein, sinensetin, tangeretin, nobiletin, and heptamethoxyflavone. Two isocratic elution were used, and the effect of different sampling solvents was evaluated using absorciometric and fluorimetric detection. The choice of sampling medium significantly impacted chromatographic elution, potentially influencing peak width and retention time, particularly notable for tangeretin. Fluorescence detection demonstrated lower LOQ for sinensetin and nobiletin ( $3 \mu\text{g mL}^{-1}$ , and  $44 \mu\text{g mL}^{-1}$ ) compared to literature values. The method was successfully applied to commercial sweet orange EO samples, providing consistent results for all targeted compounds. This highlights the method's importance in enabling accurate and efficient analysis of polymethoxyflavones in essential oils, offering potential applications in quality control and adulteration detection within the industry.

## 8

## References

- [1] B. Singh, J.P. Singh, A. Kaur, M.P. Yadav, Insights into the chemical composition and bioactivities of citrus peel essential oils, *Food Research International*, 143 (2021) 110231. <https://doi.org/10.1016/j.foodres.2021.110231>.
- [2] A. Arce, A. Soto, Citrus essential oils: Extraction and deterpenation, *Tree and Forestry Science and Biotechnology*, 2 (2008) 1–9. [http://www.globalsciencebooks.info/Online/GSBOnline/images/0812/TFSB\\_2\(SI1\)/TFSB\\_2\(SI1\)1-9o.pdf](http://www.globalsciencebooks.info/Online/GSBOnline/images/0812/TFSB_2(SI1)/TFSB_2(SI1)1-9o.pdf) (accessed February 24, 2024).
- [3] W.P. Silvestre, N.F. Livinalli, C. Baldasso, I.C. Tessaro, Pervaporation in the separation of essential oil components: A review, *Trends in Food Science and Technology*, 93 (2019) 42–52. <https://doi.org/10.1016/j.tifs.2019.09.003>.
- [4] H. Fan, Q. Wu, J.E. Simon, S.N. Lou, C.T. Ho, Authenticity analysis of citrus essential oils by HPLC-UV-MS on oxygenated heterocyclic components, *Journal of Food and Drug Analysis*, 23 (2015) 30–39. <https://doi.org/10.1016/j.jfda.2014.05.008>.
- [5] M. Russo, F. Rigano, A. Arigò, P. Dugo, L. Mondello, Coumarins, psoralens and polymethoxyflavones in cold-pressed citrus essential oils: A review, *Journal of Essential Oil Research*, 33 (2021) 221–239. <https://doi.org/10.1080/10412905.2020.1857855>.
- [6] G. Dugo, A. Giacomo, *Citrus: The genus Citrus*, 1st ed., Taylor & Francis, London, 2004. [https://doi.org/https://doi.org/10.1201/9780203216613](https://doi.org/10.1201/9780203216613).
- [7] Z. Mushtaq, M. Aslam, M. Imran, M.A. Abdelgawad, F. Saeed, T. Khursheed, M. Umar, W. Al Abdulmonem, A.H.A. Ghorab, S.A. Alsagaby, T. Tufail, M.A. Raza, M. Hussain, E. Al JBawi, Polymethoxyflavones: An

- updated review on pharmacological properties and underlying molecular mechanisms, *International Journal of Food Properties*, 26 (2023) 866–893. <https://doi.org/10.1080/10942912.2023.2189568>.
- [8] S.C. Shim, Y.H. Jeon, D.W. Kim, G.S. Han, D.J. Yoo, Photochemistry and photobiology of psoralens, *Journal of Photoscience*, 2 (1995) 37–45. <https://koreascience.kr/article/JAKO199511919745955.pdf> (accessed February 24, 2024).
- [9] H.R. Bizzo, C.M. Rezende, The market of essential oils in Brazil and in the world in the last decade, *Química Nova*, 45 (2022) 949–958. <https://doi.org/10.21577/0100-4042.20170889>.
- [10] H.R. Bizzo, A.M.C. Hovell, C.M. Rezende, Brazilian essential oils: General view, developments and perspectives, *Química Nova*, 32 (2009) 588–594. <https://doi.org/10.1590/S0100-40422009000300005>.
- [11] A.C. de Groot, E. Schmidt, Essential oils, part III: Chemical composition, *Dermatitis*, 27 (2016) 161–169. <https://doi.org/10.1097/DER.0000000000000193>.
- [12] A.C. Figueiredo, J.G. Barroso, L.G. Pedro, J.J.C. Scheffer, Factors affecting secondary metabolite production in plants: Volatile components and essential oils, *Flavour and Fragrance Journal*, 23 (2008) 213–226. <https://doi.org/10.1002/ffj.1875>.
- [13] C. Turek, F.C. Stintzing, Impact of different storage conditions on the quality of selected essential oils, *Food Research International*, 46 (2012) 341–353. <https://doi.org/10.1016/j.foodres.2011.12.028>.
- [14] C. Turek, F.C. Stintzing, Stability of essential oils: A review, *Comprehensive Reviews in Food Science and Food Safety*, 12 (2013) 40–53. <https://doi.org/10.1111/1541-4337.12006>.
- [15] P.V. Jentzsch, L.R. Guerrero, V. Ciobota, Detection of essential oils adulteration: A quick overview and current challenges, *American Journal of Biomedical Science & Research*, 4 (2019) 10–11. <https://doi.org/10.34297/ajbsr.2019.04.000746>.

- [16] T.K.T. Do, F. Hadji-Minaglou, S. Antoniotti, X. Fernandez, Authenticity of essential oils, *TrAC - Trends in Analytical Chemistry*, 66 (2015) 146–157. <https://doi.org/10.1016/j.trac.2014.10.007>.
- [17] A. Smelcerovic, A. Djordjevic, J. Lazarevic, G. Stojanovic, Recent advances in analysis of essential oils, *Current Analytical Chemistry*, 9 (2013) 61–70. <https://doi.org/10.2174/1573411011309010061>.
- [18] C. Turek, F.C. Stintzing, Application of high-performance liquid chromatography diode array detection and mass spectrometry to the analysis of characteristic compounds in various essential oils, *Analytical and Bioanalytical Chemistry*, 400 (2011) 3109–3123. <https://doi.org/10.1007/s00216-011-4976-5>.
- [19] I.L. Bonaccorsi, H.M. McNair, L.A. Brunner, P. Dugo, G. Dugo, Fast HPLC for the analysis of oxygen heterocyclic compounds of citrus essential oils, *Journal of Agricultural and Food Chemistry*, 47 (1999) 4237–4239. <https://doi.org/10.1021/jf990417s>.
- [20] W. Gerbacia, H.L. Rosano, Microemulsions: Formation and stabilization, *Journal of Colloid and Interface Science*, 44 (1973) 242–248. [https://doi.org/10.1016/0021-9797\(73\)90216-6](https://doi.org/10.1016/0021-9797(73)90216-6).
- [21] T.P. Hoar, J.H. Schulman, Transparent water-in-oil dispersions: The oleopathic hydro-micelle, *Nature*, 152 (1943) 102–103. <https://doi.org/10.1038/152102a0>.
- [22] B.P.A. Winsor, von Hahn, Hydrotrophy, Solubilisation and related emulsification processes. Part I, *Transactions of the Faraday Society*, 44 (1948) 376–398. <https://doi.org/https://doi.org/10.1039/TF9484400376>.
- [23] J.H. Schulman, W. Stoeckenius, L.M. Prince, Mechanism of formation and structure of micro emulsions by electron microscopy, *The Journal of Physical Chemistry*, 63 (1959) 1677–1680. <https://doi.org/10.1021/j150580a027>.

- [24] M.J. Lawrence, G.D. Rees, Microemulsion-based media as novel drug delivery systems, *Advanced Drug Delivery Reviews*, 45 (2000) 89–121. [https://doi.org/10.1016/s0169-409x\(00\)00103-4](https://doi.org/10.1016/s0169-409x(00)00103-4).
- [25] R.C. Santana, F.A. Perrechil, R.L. Cunha, High- and low-energy emulsifications for food applications: A focus on process parameters, *Food Engineering Reviews*, 5 (2013) 107–122. <https://doi.org/10.1007/s12393-013-9065-4>.
- [26] J. Sjöblom, R. Lindberg, S.E. Friberg, Microemulsions - Phase equilibria characterization, structures, applications and chemical reactions, *Advances in Colloid and Interface Science*, 65 (1996) 125–287. [https://doi.org/10.1016/0001-8686\(96\)00293-X](https://doi.org/10.1016/0001-8686(96)00293-X).
- [27] G.D. Smith, C.E. Donelan, R.E. Barden, Oil-continuous microemulsions composed of hexane, water, and 2-propanol, *Journal of Colloid and Interface Science*, 60 (1977) 488–496. [https://doi.org/10.1016/0021-9797\(77\)90313-7](https://doi.org/10.1016/0021-9797(77)90313-7)
- [28] D. Rak, M. Sedlák, On the mesoscale solubility in liquid solutions and mixtures, *Journal of Physical Chemistry B*, 123 (2019) 1365–1374. <https://doi.org/10.1021/acs.jpcc.8b10638>.
- [29] S. Schöttl, J. Marcus, O. Diat, D. Touraud, W. Kunz, T. Zemb, D. Horinek, Emergence of surfactant-free micelles from ternary solutions, *Chemical Science*, 5 (2014) 2949–2954. <https://doi.org/10.1039/c4sc00153b>.
- [30] S. Prévost, S. Krickl, S. Marčelja, W. Kunz, T. Zemb, I. Grillo, Spontaneous Ouzo emulsions coexist with pre-Ouzo ultraflexible microemulsions, *Langmuir*, 37 (2021) 3817–3827. <https://doi.org/10.1021/acs.langmuir.0c02935>.
- [31] B. Lagourette, J. Peyrelasse, C. et al. Boned, Percolative conduction in microemulsion type systems, *Nature*, 281 (1979) 60–62. <https://doi.org/https://doi.org/10.1038/281060b0>.

- [32] M. Clause, J. Peyrelasse, J. Heil, C. Boned, B. Lagourette, Bicontinuous structure zones in microemulsions, *Nature*, 293 (1981) 636–638. <https://doi.org/https://doi.org/10.1038/293636a0>.
- [33] M. Clause, L. Nicolas-Morgantini, A. Zradba, D. Touraud, Microemulsion systems, in: *Surfactant Science Series, Volume 24*, 1st ed., Marcel Dekker Inc., New York and Basel (1987).
- [34] J. Xu, A. Yin, J. Zhao, D. Li, W. Hou, Surfactant-free microemulsion composed of oleic acid, n-propanol, and H<sub>2</sub>O, *Journal of Physical Chemistry B*, 117 (2013) 450–456. <https://doi.org/10.1021/jp310282a>.
- [35] Y. Gao, S. Wang, L. Zheng, S. Han, X. Zhang, D. Lu, L. Yu, Y. Ji, G. Zhang, Microregion detection of ionic liquid microemulsions, *Journal of Colloid and Interface Science*, 301 (2006) 612–616. <https://doi.org/10.1016/j.jcis.2006.05.010>.
- [36] Y. Gao, N. Li, S. Zhang, L. Zheng, X. Li, B. Dong, L. Yu, Organic solvents induce the formation of oil-in-ionic liquid microemulsion aggregations, *Journal of Physical Chemistry B*, 113 (2009) 1389–1395. <https://doi.org/10.1021/jp808522b>.
- [37] W. Hou, J. Xu, Surfactant-free microemulsions, *Current Opinion Colloid & Interface Science*, 25 (2016) 67–74. <https://doi.org/10.1016/j.cocis.2016.06.013>.
- [38] K.A. Singh, Fluorescence spectroscopy as a basic tool of analytical chemists: A review, *IOSR Journal of Applied Chemistry*, 9 (2016) 37–39. <https://www.iosrjournals.org/iosr-jac/papers/vol9-issue4/Version-1/G0904013739.pdf> (accessed February 24, 2024).
- [39] Joseph R. Lakowicz, *Principles of fluorescence spectroscopy*, 3rd Edition, *Analytical and Bioanalytical Chemistry*, 390 (2008) 1223–1224. <https://doi.org/10.1007/s00216-007-1822-x>.
- [40] P.T.C. So, C.Y. Dong, Fluorescence spectrophotometry, *Encyclopedia of Life Sciences* (2001). <https://doi.org/10.1038/npg.els.0002978>.

- [41] J. Chen, E.J. Leboeuf, S. Dai, B. Gu, Fluorescence spectroscopic studies of natural organic matter fractions, *Chemosphere*, 50 (2003) 639–647. [https://doi.org/10.1016/S0045-6535\(02\)00616-1](https://doi.org/10.1016/S0045-6535(02)00616-1).
- [42] Á. Andrade-Eiroa, G. de-Armas, J.M. Estela, V. Cerdà, Critical approach to synchronous spectrofluorimetry. II, *TrAC - Trends in Analytical Chemistry*, 29 (2010) 902–927. <https://doi.org/10.1016/j.trac.2010.05.002>.
- [43] Á.U. Andrade-Eiroa, M. Canle, V. Cerdá, Environmental applications of excitation-emission spectrofluorimetry: An in-depth review I, *Applied Spectroscopy Reviews*, 48 (2013) 1–49. <https://doi.org/10.1080/05704928.2012.692104>.
- [44] Y.S. Polyakov, L.A. Shiffers, Some new fluorescence-analysis methods for multicomponent mixtures (review), *Zhurnal Prikladnoi Spektroskopii* 41 (1983) 181–190. <https://doi.org/10.1007/BF00659829>
- [45] L. Li, Y. Wang, W. Zhang, S. Yu, X. Wang, N. Gao, New advances in fluorescence excitation-emission matrix spectroscopy for the characterization of dissolved organic matter in drinking water treatment: A review, *Chemical Engineering Journal*, 381 (2020) 122676. <https://doi.org/10.1016/j.cej.2019.122676>.
- [46] I. Sciscenko, A. Arques, P. Micó, M. Mora, S. García-Ballesteros, Emerging applications of EEM-PARAFAC for water treatment: A concise review, *Chemical Engineering Journal Advances*, 10 (2022) 100286. <https://doi.org/10.1016/j.cej.2022.100286>.
- [47] A.J. Lawaetz, C.A. Stedmon, Fluorescence intensity calibration using the Raman scatter peak of water, *Applied Spectroscopy*, 63 (2009) 936–940. <https://doi.org/10.1366/000370209788964548>.
- [48] S. Kumar Panigrahi, A. Kumar Mishra, Inner filter effect in fluorescence spectroscopy: As a problem and as a solution, *Journal of Photochemistry and Photobiology C: Photochemistry Reviews*, 41 (2019) 100318. <https://doi.org/10.1016/j.jphotochemrev.2019.100318>.

- [49] M. Pucher, U. Wunsch, G. Weigelhofer, K. Murphy, T. Hein, D. Graeber, StaRdom: Versatile software for analyzing spectroscopic data of dissolved organic matter in R, *Water*, 11 (2019) 2366. <https://doi.org/10.3390/w11112366>.
- [50] M. Pucher, PARAFAC analysis of EEM data to separate DOM components in R - staRdom: Spectroscopic analysis of dissolved organic matter in R (2023). [https://cran.r-project.org/web/packages/staRdom/vignettes/PARAFAC\\_analysis\\_of\\_EEM.html](https://cran.r-project.org/web/packages/staRdom/vignettes/PARAFAC_analysis_of_EEM.html) (accessed February 24, 2024).
- [51] S. Karamizadeh, S.M. Abdullah, A.A. Manaf, M. Zamani, A. Hooman, An overview of principal component analysis, *Journal of Signal and Information Processing*, 04 (2013) 173–175. <https://doi.org/10.4236/jsip.2013.43b031>.
- [52] R. Bro, A.K. Smilde, Principal component analysis, *Analytical Methods*, 6 (2014) 2812–2831. <https://doi.org/10.1039/c3ay41907j>.
- [53] C.H. Collins, G.L. Braga, P.S. Bonato, *Fundamentos de cromatografia*, 1st ed., Editora da UNICAMP, Campinas (2006).
- [54] D.V. Mccalley, Effect of organic solvent modifier and nature of solute on the performance of bonded silica reversed-phase columns for the analysis of strongly basic compounds by high-performance liquid chromatography, *Journal of Chromatography A*, 738 (1996) 169–179. [https://doi.org/https://doi.org/10.1016/0021-9673\(96\)00136-7](https://doi.org/https://doi.org/10.1016/0021-9673(96)00136-7).
- [55] B.J. VanMiddlesworth, J.G. Dorsey, Quantifying injection solvent effects in reversed-phase liquid chromatography, *Journal of Chromatography A*, 1236 (2012) 77–89. <https://doi.org/10.1016/j.chroma.2012.02.075>.
- [56] N.E. Hamilton, M. Ferry, Ggtern: Ternary diagrams using ggplot2, *Journal of Statistical Software*, 87 (2018). <https://doi.org/10.18637/jss.v087.c03>.
- [57] P. Schauburger, A. Walker, L. Braglia, J. Sturm, J.M. Garbuszus, J.M. Barbone, Package “openxlsx”: Read, write and edit xlsx files (2021).

- <https://cran.r-project.org/web/packages/openxlsx/openxlsx.pdf> (accessed February 24, 2024).
- [58] P. Massicotte, Package “eemR”: Tools for pre-processing emission-excitation-matrix (EEM) fluorescence data (2022). <https://cran.r-project.org/web/packages/eemR/eemR.pdf> (accessed February 24, 2024)..
- [59] H. Wickham, D. Vaughan, M. Girlich, K. Ushey, P.S. PBC, Package “tidyr”: Tidy messy data (2024). <https://cran.r-project.org/web/packages/tidyr/tidyr.pdf> (accessed February 24, 2024).
- [60] H. Wickham, R. François, L. Henry, K. Müller, D. Vaughan, P.S. PBC, Package “dplyr”: A grammar of data manipulation (2023). <https://cran.r-project.org/web/packages/dplyr/dplyr.pdf> (accessed February 24, 2024).
- [61] J. Reichling, Plant-microbe interactions and secondary metabolites with antibacterial, antifungal and antiviral properties, in: Annual plant reviews: Functions and biotechnology of plant secondary metabolites, Volume 39, 2nd ed., Michael Wink, Wiley-Blackwell, Oxford (2010). <https://doi.org/10.1002/9781444318876.ch4>.
- [62] F. Bakkali, S. Averbeck, D. Averbeck, M. Idaomar, Biological effects of essential oils - A review, *Food and Chemical Toxicology*, 46 (2008) 446–475. <https://doi.org/10.1016/j.fct.2007.09.106>.
- [63] S. Tariq, S. Wani, W. Rasool, K. Shafi, M.A. Bhat, A. Prabhakar, A.H. Shalla, M.A. Rather, A comprehensive review of the antibacterial, antifungal and antiviral potential of essential oils and their chemical constituents against drug-resistant microbial pathogens, *Microbial Pathogenesis*, 134 (2019) 103580. <https://doi.org/10.1016/j.micpath.2019.103580>.
- [64] M. del C. Razola-Díaz, E.J. Guerra-Hernández, B. García-Villanova, V. Verardo, Recent developments in extraction and encapsulation techniques of orange essential oil, *Food Chemistry*, 354 (2021) 129575. <https://doi.org/10.1016/j.foodchem.2021.129575>.

- [65] N.S. Dosoky, W.N. Setzer, Biological activities and safety of *Citrus spp.* essential oils, *International Journal of Molecular Sciences*, 19 (2018) 1–25. <https://doi.org/10.3390/ijms19071966>.
- [66] M.L. Magalhães, M. Ionta, G.Á. Ferreira, M.L.L. Campidelli, D.L. Nelson, V.R.F. Ferreira, D.A. de C.S. Rezende, M. das G. Cardoso, Biological activities of the essential oil from the Moro orange peel (*Citrus sinensis* (L.) *Osbeck*), *Flavour and Fragrance Journal*, 35 (2020) 294–301. <https://doi.org/10.1002/ffj.3561>.
- [67] M. Baranska, H. Schulz, A. Walter, P. Rösch, R. Quilitzsch, G. Lösing, J. Popp, Investigation of eucalyptus essential oil by using vibrational spectroscopy methods, *Vibrational Spectroscopy*, 42 (2006) 341–345. <https://doi.org/10.1016/j.vibspec.2006.08.004>.
- [68] H.R. Juliani, J. Kapteyn, D. Jones, A.R. Koroch, M. Wang, D. Charles, J.E. Simon, Application of near-infrared spectroscopy in quality control and determination of adulteration of african essential oils, *Phytochemical Analysis*, 17 (2006) 121–128. <https://doi.org/10.1002/pca.895>.
- [69] H. Schulz, M. Baranska, R. Quilitzsch, W. Schütze, G. Lösing, Characterization of peppercorn, pepper oil, and pepper oleoresin by vibrational spectroscopy methods, *Journal of Agricultural and Food Chemistry*, 53 (2005) 3358–3363. <https://doi.org/10.1021/jf048137m>.
- [70] Y.W. Wu, S.Q. Sun, Q. Zhou, H.W. Leung, Fourier transform mid-infrared (MIR) and near-infrared (NIR) spectroscopy for rapid quality assessment of Chinese medicine preparation Honghua Oil, *Journal of Pharmaceutical and Biomedical Analysis*, 46 (2008) 498–504. <https://doi.org/10.1016/j.jpba.2007.11.021>.
- [71] H. Schulz, M. Baranska, H.H. Belz, P. Rösch, M.A. Strehle, Jürgen Popp, Chemotaxonomic characterisation of essential oil plants by vibrational spectroscopy measurements, *Vibrational Spectroscopy*, 35 (2004) 81–86. <https://doi.org/10.1016/j.vibspec.2003.12.014>.

- [72] K. Bounaas, N. Bouzidi, Y. Daghbouche, S. Garrigues, M. de la Guardia, M. el Hattab, Essential oil counterfeit identification through middle infrared spectroscopy, *Microchemical Journal*, 139 (2018) 347–356. <https://doi.org/10.1016/j.microc.2018.03.008>.
- [73] G. Gudi, A. Krähmer, H. Krüger, H. Schulz, Attenuated total reflectance-Fourier transform infrared spectroscopy on intact dried leaves of sage (*Salvia officinalis* L.): Accelerated chemotaxonomic discrimination and analysis of essential oil composition, *Journal of Agricultural and Food Chemistry*, 63 (2015) 8743–8750. <https://doi.org/10.1021/acs.jafc.5b03852>.
- [74] S. Kuriakose, H. Joe, Qualitative and quantitative analysis in sandalwood oils using near infrared spectroscopy combined with chemometric techniques, *Food Chemistry*, 135 (2012) 213–218. <https://doi.org/10.1016/j.foodchem.2012.04.073>.
- [75] N. Cebi, M. Arici, O. Sagdic, The famous Turkish rose essential oil: Characterization and authenticity monitoring by FTIR, Raman and GC–MS techniques combined with chemometrics, *Food Chemistry*, 354 (2021) 129495. <https://doi.org/10.1016/j.foodchem.2021.129495>.
- [76] M. Minteguiaga, E. Dellacassa, M.A. Iramain, C.A.N. Catalán, S.A. Brandán, FT-IR, FT-Raman, UV–Vis, NMR and structural studies of carquejyl acetate, a distinctive component of the essential oil from *Baccharis trimera* (less.) DC. (*Asteraceae*), *Journal of Molecular Structure*, 1177 (2019) 499–510. <https://doi.org/10.1016/j.molstruc.2018.10.010>.
- [77] T.C.M. Pastore, L.R. Braga, D.C.G. da C. Kunze, L.F. Soares, F. Pastore, A.C. de O. Moreira, P.V. dos Anjos, C.S. Lara, V.T.R. Coradin, J.W.B. Braga, A green and direct method for authentication of rosewood essential oil by handheld near infrared spectrometer and one-class classification modeling, *Microchemical Journal*, 182 (2022) 107916. <https://doi.org/https://doi.org/10.1016/j.microc.2022.107916>.
- [78] P. Vargas Jentsch, C. Sandoval Pauker, P. Zárate Pozo, M. Sinche Serra, G. Jácome Camacho, V. Rueda-Ayala, P. Garrido, L. Ramos Guerrero, V. Ciobotă, Raman spectroscopy in the detection of adulterated essential oils:

- The case of nonvolatile adulterants, *Journal of Raman Spectroscopy*, 52 (2021) 1055–1063. <https://doi.org/10.1002/jrs.6089>.
- [79] K. Seidler-Lozykowska, M. Baranska, R. Baranski, D. Krol, Raman analysis of caraway (*Carum carvi L.*) single fruits. evaluation of essential oil content and its composition, *J Agric Food Chemistry*, 58 (2010) 5271–5275. <https://doi.org/10.1021/jf100298z>.
- [80] M.R. Almeida, C.H.V. Fidelis, L.E.S. Barata, R.J. Poppi, Classification of Amazonian rosewood essential oil by Raman spectroscopy and PLS-DA with reliability estimation, *Talanta*, 117 (2013) 305–311. <https://doi.org/10.1016/j.talanta.2013.09.025>.
- [81] S. Lafhal, P. Vanloot, I. Bombarda, R. Valls, J. Kister, N. Dupuy, Raman spectroscopy for identification and quantification analysis of essential oil varieties: A multivariate approach applied to lavender and lavandin essential oils, *Journal of Raman Spectroscopy*, 46 (2015) 577–585. <https://doi.org/10.1002/jrs.4697>.
- [82] N.G. Siatis, A.C. Kimbaris, C.S. Pappas, P.A. Tarantilis, D.J. Daferera, M.G. Polissiou, Rapid method for simultaneous quantitative determination of four major essential oil components from oregano (*Oreganum sp.*) and thyme (*Thymus sp.*) using FT-Raman spectroscopy, *Journal of Agricultural and Food Chemistry*, 53 (2005) 202–206. <https://doi.org/10.1021/jf048930f>.
- [83] P. Vargas Jentsch, F. Gualpa, L.A. Ramos, V. Ciobotă, Adulteration of clove essential oil: Detection using a handheld Raman spectrometer, *Flavour and Fragrance Journal*, 33 (2018) 184–190. <https://doi.org/10.1002/ffj.3438>.
- [84] M. Strzemski, M. Wójciak-Kosior, I. Sowa, M. Agacka-Mołdoch, P. Drączkowski, D. Matosiuk, Ł. Kurach, R. Kocjan, S. Dresler, Application of Raman spectroscopy for direct analysis of *Carlina acanthifolia* subsp. *utzka* root essential oil, *Talanta*, 174 (2017) 633–637. <https://doi.org/10.1016/j.talanta.2017.06.070>.

- [85] W.M. Feudjio, H. Ghalila, M. Nsangou, Y.G.M. Kongbonga, Y. Majdi, Excitation-emission matrix fluorescence coupled to chemometrics for the exploration of essential oils, *Talanta*, 130 (2014) 148–154. <https://doi.org/10.1016/j.talanta.2014.06.048>.
- [86] W. Mbogning Feudjio, H. Ghalila, M. Nsangou, Y. Majdi, Y. Mbesse Kongbonga, N. Jaïdane, Fluorescence spectroscopy combined with chemometrics for the investigation of the adulteration of essential oils, *Food Analytical Methods* 10 (2017) 2539–2548. <https://doi.org/10.1007/s12161-017-0823-4>.
- [87] D.F. Al Riza, S. Widodo, Y.A. Purwanto, N. Kondo, Authentication of the geographical origin of patchouli oil using front-face fluorescence spectroscopy and chemometric analysis, *Flavour and Fragrance Journal* 34 (2019) 15–20. <https://doi.org/10.1002/ffj.3473>.
- [88] L. Wang, Y. Zhang, G. Fan, J.N. Ren, L.L. Zhang, S.Y. Pan, Effects of orange essential oil on intestinal microflora in mice, *Journal of the Science of Food and Agriculture*, 99 (2019) 4019–4028. <https://doi.org/10.1002/jsfa.9629>.
- [89] L. Chauhan, P. Thakur, S. Sharma, Microemulsions: New vista in novel drug delivery system, *Innovations in Pharmaceuticals and Pharmacotherapy*, 7 (2019) 37–44. [http://www.innpharmacotherapy.com/VolumeArticles/FullTextPDF/10190\\_03\\_IPP-07-JM-2019-17\\_REV.pdf](http://www.innpharmacotherapy.com/VolumeArticles/FullTextPDF/10190_03_IPP-07-JM-2019-17_REV.pdf) (accessed February 24, 2024).
- [90] S.N. Kale, S.L. Deore, Emulsion micro emulsion and nano emulsion: A review, *Systematic Reviews in Pharmacy*, 8 (2016) 39–47. <https://doi.org/10.5530/srp.2017.1.8>.
- [91] G. Dugo, A. Verzera, I.S. d’Alcontres, A. Cotroneo, A. Trozzi, L. Mondello, On the genuineness of citrus essential oils. Part XLIII. The composition of the volatile fraction of italian sweet orange oils (*Citrus sinensis* (L.) *Osbeck*), *Journal of Essential Oil Research*, 6 (1994) 101–137. <https://doi.org/10.1080/10412905.1994.9698342>.

- [92] A. Verzera, A. Trozzi, G. Dugo, G. Di Bella, A. Cotroneo, Biological lemon and sweet orange essential oil composition, *Flavour and Fragrance Journal*, 19 (2004) 544–548. <https://doi.org/10.1002/ffj.1348>.
- [93] S.M. Njoroge, N.T.L. Phi, M. Sawamura, Chemical composition of peel essential oils of sweet oranges (*Citrus sinensis*) from Uganda and Rwanda, *Journal of Essential Oil Bearing Plants*, 12 (2009) 26–33. <https://doi.org/10.1080/0972060X.2009.10643687>.
- [94] P. Bošković, V. Sokol, T. Zemb, D. Touraud, W. Kunz, Weak micelle-like aggregation in ternary liquid mixtures as revealed by conductivity, surface tension, and light scattering, *Journal of Physical Chemistry B*, 119 (2015) 9933–9939. <https://doi.org/10.1021/acs.jpcc.5b06228>.
- [95] European Commission, CosIng (2009), European Commission database for information on cosmetic substances and ingredients. Retrieved from [https://ec.europa.eu/growth/tools-databases/cosing/index.cfm?fuseaction=search.details\\_v2&id=82156](https://ec.europa.eu/growth/tools-databases/cosing/index.cfm?fuseaction=search.details_v2&id=82156) (accessed March 22, 2023).
- [96] E. Palazzolo, V.A. Laudicina, M.A. Germanà, Current and potential use of citrus essential oils, *Current Organic Chemistry*, 17 (2013) 3042–3049. <https://iris.unipa.it/retrieve/handle/10447/99440/127970/011-Vito%20Armando%20Laudicina%202013.pdf> (accessed February 24, 2024).
- [97] P.Q. Tranchida, I. Bonaccorsi, P. Dugo, L. Mondello, G. Dugo, Analysis of citrus essential oils: State of the art and future perspectives. A review, *Flavour and Fragrance Journal*, 27 (2012) 98–123. <https://doi.org/10.1002/ffj.2089>.
- [98] M. Baranska, K. Chruszcz-Lipska, Raman optical activity: A powerful technique to investigate essential oil components, *Natural Product Communications*, 5 (2010) 1417–1420. <https://doi.org/10.1177/1934578X1000500914>.

- [99] I. Ahmad, A.E. Arifianti, J.A. Nur Fikri, S. Abdullah, A. Munim, The combination of ATR-FTIR and chemometrics for rapid analysis of essential oil from *Myrtaceae* plants – A review, *Journal of Applied Pharmaceutical Science*, 12 (2022) 30–42. <https://doi.org/10.7324/japs.2022.120604>.
- [100] D.W. Johnson, J.B. Callis, G.D. Christian, Rapid Scanning Fluorescence Spectroscopy, *Analytical Chemistry*, 49 (1977) 747–757. <https://doi.org/10.1021/ac50016a008>.
- [101] T. Geng, Y. Wang, X.-L. Yin, W. Chen, H.-W. Gu, A comprehensive review on the excitation-emission matrix fluorescence spectroscopic characterization of petroleum-containing substances: Principles, methods, and applications, *Critical Reviews in Analytical Chemistry* (2023). <https://doi.org/10.1080/10408347.2023.2205500>.
- [102] J. Lozano-Castellón, A. López-Yerena, I. Domínguez-López, A. Siscart-Serra, N. Fraga, S. Sámano, C. López-Sabater, R.M. Lamuela-Raventós, A. Vallverdú-Queralt, M. Pérez, Extra virgin olive oil: A comprehensive review of efforts to ensure its authenticity, traceability, and safety, *Comprehensive Reviews in Food Science and Food Safety*, 21 (2022) 2639–2664. <https://doi.org/10.1111/1541-4337.12949>.
- [103] E.J. Rifna, R. Pandiselvam, A. Kothakota, K. V. Subba Rao, M. Dwivedi, M. Kumar, R. Thirumdas, S. V. Ramesh, Advanced process analytical tools for identification of adulterants in edible oils – A review, *Food Chemistry*, 369 (2022) 130898. <https://doi.org/10.1016/j.foodchem.2021.130898>.
- [104] R.C. Macedo, M.J. Pedrozo-Peñafiel, A.L.M.C. da Cunha, R.Q. Aucelio, Fingerprinting pattern of orange essential oils in surfactant-free microemulsion by 3D fluorescence spectroscopy, *Food Chemistry Advances*, 3 (2023) 100482. <https://doi.org/10.1016/j.focha.2023.100482>.
- [105] S. Schöttl, D. Horinek, Aggregation in detergent-free ternary mixtures with microemulsion-like properties, *Current Opinion in Colloid & Interface Science*, 22 (2016) 8–13. <https://doi.org/10.1016/j.cocis.2016.02.003>.

- [106] B. Sadat Mirhoseini, A. Salabat, A novel surfactant-free microemulsion system for the synthesis of poly(methyl methacrylate)/Ag nanocomposite, *Journal of Molecular Liquids*, 342 (2021) 117555. <https://doi.org/10.1016/j.molliq.2021.117555>.
- [107] M.E. Fernández Izquierdo, J. Quesada Granados, M. Villalón Mir, M.C. López Martínez, Comparison of methods for determining coumarins in distilled beverages, *Food Chemistry*, 70 (2000) 251–258. [https://doi.org/10.1016/S0308-8146\(00\)00071-6](https://doi.org/10.1016/S0308-8146(00)00071-6).
- [108] K. Hroboňová, J. Lehotay, J. Čižmárik, J. Sádecká, Comparison HPLC and fluorescence spectrometry methods for determination of coumarin derivatives in propolis, *Journal of Liquid Chromatography & Related Technologies*, 36 (2013) 486–503. <https://doi.org/10.1080/10826076.2012.660724>.
- [109] W. Feger, H. Brandauer, P. Gabris, H. Ziegler, Nonvolatiles of commercial lime and grapefruit oils separated by high-speed countercurrent chromatography, *J Agric Food Chemistry*, 54 (2006) 2242–2252. <https://doi.org/10.1021/jf052267t>.
- [110] A.S. Brah, F.A. Armah, C. Obuah, S.A. Akwetey, C.K. Adokoh, Toxicity and therapeutic applications of citrus essential oils (CEOs): A review, *International Journal of Food Properties*, 26 (2023) 301–326. <https://doi.org/10.1080/10942912.2022.2158864>.
- [111] A. Gossiau, K.Y. Chen, C.T. Ho, S. Li, Anti-inflammatory effects of characterized orange peel extracts enriched with bioactive polymethoxyflavones, *Food Science and Human Wellness*, 3 (2014) 26–35. <https://doi.org/10.1016/j.fshw.2014.02.002>.
- [112] K. Matsuzaki, Y. Ohizumi, Beneficial effects of citrus-derived polymethoxylated flavones for central nervous system disorders, *Nutrients*, 13 (2021) 1–22. <https://doi.org/10.3390/nu13010145>.
- [113] L.A. Nichols, D.E. Jackson, J.A. Manthey, S.D. Shukla, L.J. Holland, Citrus flavonoids repress the mRNA for stearoyl-CoA desaturase, a key enzyme in

- lipid synthesis and obesity control, in rat primary hepatocytes, *Lipids in Health and Disease*, 10 (2011). <https://doi.org/10.1186/1476-511X-10-36>.
- [114] S. Li, M.-H. Pan, • Zhenyu Wang, T. Lambros, C.-T. Ho, Biological activity, metabolism and separation of polymethoxyflavonoids from citrus peels, *Tree and Forestry Science and Biotechnology*, 2 (2008) 36–51. [http://www.globalsciencebooks.info/Online/GSBOnline/images/0812/TFSB\\_2\(SI1\)/TFSB\\_2\(SI1\)36-51o.pdf](http://www.globalsciencebooks.info/Online/GSBOnline/images/0812/TFSB_2(SI1)/TFSB_2(SI1)36-51o.pdf) (accessed February 24, 2024).
- [115] A. Arigò, F. Rigano, G. Micalizzi, P. Dugo, L. Mondello, Oxygen heterocyclic compound screening in citrus essential oils by linear retention index approach applied to liquid chromatography coupled to photodiode array detector, *Flavour and Fragrance Journal*, 34 (2019) 349–364. <https://doi.org/10.1002/ffj.3515>.
- [116] J. Masson, E. Liberto, J.C. Beolor, H. Brevard, C. Bicchi, P. Rubiolo, Oxygenated heterocyclic compounds to differentiate *Citrus spp.* essential oils through metabolomic strategies, *Food Chemistry*, 206 (2016) 223–233. <https://doi.org/10.1016/j.foodchem.2016.03.057>.
- [117] M. Russo, I. Bonaccorsi, R. Costa, A. Trozzi, P. Dugo, L. Mondello, Reduced time HPLC analyses for fast quality control of citrus essential oils, *Journal of Essential Oil Research*, 27 (2015) 307–315. <https://doi.org/10.1080/10412905.2015.1027419>.
- [118] P. Donato, I. Bonaccorsi, M. Russo, P. Dugo, Determination of new bioflavonoids in bergamot (*Citrus bergamia*) peel oil by liquid chromatography coupled to tandem ion trap-time-of-flight mass spectrometry, *Flavour and Fragrance Journal*, 29 (2014) 131–136. <https://doi.org/10.1002/ffj.3188>.
- [119] M. Russo, G. Torre, C. Carnovale, I. Bonaccorsi, L. Mondello, P. Dugo, A new HPLC method developed for the analysis of oxygen heterocyclic compounds in citrus essential oils, *Journal of Essential Oil Research*, 24 (2012) 119–129. <https://doi.org/10.1080/10412905.2012.659523>.

- [120] G. Dugo, I. Bonaccorsi, D. Sciarrone, L. Schipilliti, M. Russo, A. Cotroneo, P. Dugo, L. Mondello, V. Raymo, Characterization of cold-pressed and processed bergamot oils by using GC-FID, GC-MS, GC-C-IRMS, enantio-GC, MDGC, HPLC and HPLC-MS-IT-TOF, *Journal of Essential Oil Research*, 24 (2012) 93–117. <https://doi.org/10.1080/10412905.2012.659526>.
- [121] G. Dugo, I. Bonaccorsi, D. Sciarrone, R. Costa, P. Dugo, L. Mondello, L. Santi, H.A. Fakhry, Characterization of oils from the fruits, leaves and flowers of the bitter orange tree, *Journal of Essential Oil Research*, 23 (2011) 45–59. <https://doi.org/10.1080/10412905.2011.9700446>.
- [122] P. Dugo, I. Bonaccorsi, C. Ragonese, M. Russo, P. Donato, L. Santi, L. Mondello, Analytical characterization of mandarin (*Citrus deliciosa Ten.*) essential oil, *Flavour and Fragrance Journal*, 26 (2011) 34–46. <https://doi.org/10.1002/ffj.2014>.
- [123] I. Bonaccorsi, P. Dugo, A. Trozzi, A. Cotroneo, G. Dugo, Characterization of mandarin (*Citrus deliciosa Ten.*) essential oil. Determination of volatiles, non-volatiles, physico-chemical indices and enantiomeric ratios, *Natural Products Communication*, 4 (2009) 1595–1600. <https://pubmed.ncbi.nlm.nih.gov/19967998/> (accessed February 24, 2024).
- [124] P. Dugo, A. Piperno, R. Romeo, M. Cambria, M. Russo, C. Carnovale, L. Mondello, Determination of oxygen heterocyclic components in citrus products by HPLC with UV detection, *Journal of Agricultural and Food Chemistry*, 57 (2009) 6543–6551. <https://doi.org/10.1021/jf901209r>.
- [125] W. Feger, H. Brandauer, P. Gabris, H. Ziegler, Nonvolatiles of commercial lime and grapefruit oils separated by high-speed countercurrent chromatography, *Journal of Agricultural and Food Chemistry*, 54 (2006) 2242–2252. <https://doi.org/10.1021/jf052267t>.
- [126] A. Cavazza, K.D. Bartle, P. Dugo, L. Mondello, Analysis of oxygen heterocyclic compounds in citrus essential oils by capillary electrochromatography and comparison with HPLC, *Chromatographia*, 53 (2001) 57–62. <https://doi.org/10.1007/BF02492428>.

- [127] P. Dugo, L. Mondello, L. Dugo, R. Stancanelli, G. Dugo, LC-MS for the identification of oxygen heterocyclic compounds in citrus essential oils, *Journal of Pharmaceutical and Biomedical Analysis*, 24 (2000) 147–154. [https://doi.org/10.1016/S0731-7085\(00\)00400-3](https://doi.org/10.1016/S0731-7085(00)00400-3).
- [128] M. Russo, I. Bonaccorsi, R. Costa, A. Trozzi, P. Dugo, L. Mondello, Reduced time HPLC analyses for fast quality control of citrus essential oils, *Journal of Essential Oil Research*, 27 (2015) 307–315. <https://doi.org/10.1080/10412905.2015.1027419>.

## 9

## Attachment

## A

## Published papers in the scope of this thesis

Food Chemistry Advances 3 (2023) 100482

Contents lists available at ScienceDirect

**Food Chemistry Advances**

journal homepage: [www.elsevier.com/locate/focha](http://www.elsevier.com/locate/focha)

**FOOD CHEMISTRY ADVANCES**

Check for updates

### Fingerprinting pattern of orange essential oils in surfactant-free microemulsion by 3D fluorescence spectroscopy

Rosana Candida Macedo<sup>a,b</sup>, Marlin Jeannette Pedrozo-Peñafiel<sup>a</sup>, Alessandra Licursi Maia Cerqueira da Cunha<sup>b</sup>, Ricardo Queiroz Aucelio<sup>a,\*</sup>

<sup>a</sup> Chemistry Department, Pontifical Catholic University of Rio de Janeiro (PUC-Rio), Rio de Janeiro, RJ 22451-900, Brazil  
<sup>b</sup> Chemistry Department, Education, Science and Technology Federal Institute of Rio de Janeiro (IFRJ), Rio de Janeiro, RJ 20270-021, Brazil

---

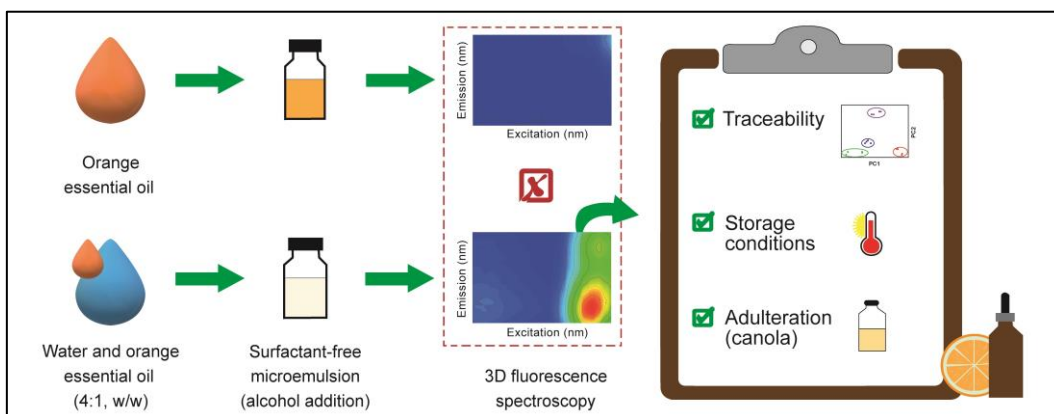
**ARTICLE INFO**

**Keywords:**  
 Orange essential oil  
 Surfactant-free microemulsion  
 3D fluorescence spectroscopy  
 Discriminant analysis  
 Oil adulteration

**ABSTRACT**

The effect caused by surfactant-free microemulsion (SFME) systems in orange essential oil analysis was evaluated by 3D fluorescence spectroscopy. The SFME formation region was studied at different water:EO proportions (1:4, 1:2, 1:1, 2:1, 4:1 w/w) in the presence of propanol and octanol (10:3 w/w). Conductometric titrations indicated micellar aggregates containing EO (oil-in-water microemulsion) for the 4:1 proportion (droplets of hydrodynamic radius of  $95.7 \pm 5.3$  nm). In such conditions, fluorescence increased allowing the use of 3D fluorescence spectroscopy to obtain spectroscopic fingerprint pattern that was used aiming discriminant analysis, considering nine EO Brazilian brands, along with unfold principal component analysis (UPCA). Cumulative variance of 96.7 % was obtained for the first three principal components and score plots showed distinct location for each group. Preliminary study showed the capability of these systems in evaluating storage conditions, and adulteration. The impact of storage conditions was made over 21 days exposed to light with results showing large spectral differences compared to a sample stored in amber flask at 22 °C. Adulteration of EOs by canola and mineral oil fortification was detected at different levels (1, 5, 10 and 20 %, in mass proportion) and, in addition to the spectral differences, a change in microemulsion stability was observed.

## Graphical Abstract:



## B

## Articles published as co-author

Determination of vitamins K1 and K3 in green tea and in pharmaceutical supplements by capillary micellar electrokinetic chromatography

Published in *Food Chemistry Advances*, 2024 (4) 100594.

DOI: 10.1016/j.focha.2023.100594

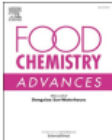
Author Contributions: Software, data curation, green metric application, writing – original draft, writing – review & editing, and visualization.

Food Chemistry Advances 4 (2024) 100594

Contents lists available at ScienceDirect

**Food Chemistry Advances**

journal homepage: [www.elsevier.com/locate/focha](http://www.elsevier.com/locate/focha)

**Determination of vitamins K1 and K3 in green tea and in pharmaceutical supplements by capillary micellar electrokinetic chromatography**

Tatiane V.D. Gomes<sup>a</sup>, Rosana C. Macedo<sup>b,c</sup>, Anastácia S. Canto<sup>b</sup>, Elisabeth C. Monteiro<sup>a</sup>,  
Alessandra Licursi M.C. da Cunha<sup>b,\*</sup>, Ricardo Q. Aucélio<sup>a,c</sup>

<sup>a</sup> Postgraduate Programme in Metrology (PósMQ), Pontifical Catholic University of Rio de Janeiro (PUC-Rio), RJ, Rio de Janeiro 22451-900, Brazil  
<sup>b</sup> Chemistry Department, Education, Science and Technology Federal Institute of Rio de Janeiro (IFRJ), RJ, Rio de Janeiro 20270-021, Brazil  
<sup>c</sup> Chemistry Department, Pontifical Catholic University of Rio de Janeiro (PUC-Rio), RJ, Rio de Janeiro 22451-900, Brazil

---

**ARTICLE INFO**

**Keywords:**  
Vitamins K1 and K3  
Green tea  
Vitamin supplement  
Capillary micellar electrokinetic chromatography  
Measurement uncertainty

**ABSTRACT**

A method based on capillary micellar electrokinetic chromatography (MEKC) was developed for vitamin K1 and K3 determination. Experimental and instrumental parameters optimized for electrophoretic separation with better peak efficiency were: borate buffer at 0.05 mol L<sup>-1</sup>, pH 8.5, cetyltrimethylammonium bromide (CTAB) at 0.05 mol L<sup>-1</sup>, acetonitrile 20 % v/v, 25 °C and a negative potential difference of 30 kV. Sample introduction was made by hydrodynamic at 50 mbar for 15 s. Migration times for vitamins K1 and K3 were (5.2 ± 0.1) and (3.4 ± 0.1) min respectively. Limits of detection and quantification were on the order of 10<sup>-5</sup> g L<sup>-1</sup> and 10<sup>-4</sup> g L<sup>-1</sup>. For vitamin K1, the precision was between 2 and 7 % for the peak area. Recoveries were 101 ± 2 % and 103 ± 2 % for green tea and vitamin supplement samples, respectively. For vitamin K3, recoveries were 99 ± 3 % for vitamin supplement. Comparative tests were performed with the reference method based on liquid chromatography with agreement of results. The uncertainty and the contribution of the relevant sources was carefully evaluated. The method was found adequate to enable reliable and sensitive measurements of different forms of vitamin K with low consumption of solvents and less generation of waste.

# Determination of trifloxystrobin in soy grape juice and natural water by photo-induced fluorescence and high-performance liquid chromatography

Published in *Journal of the Brazilian Chemical Society*, 2023 (34) 12.

DOI: 10.21577/0103-5053.20230080

Author Contributions: Investigation, methodology, formal analysis (sample pre-treatment, dispersive liquid-liquid microextraction), writing – original draft, writing – review & editing, and visualization.

Article

<https://dx.doi.org/10.21577/0103-5053.20230080>  
*J. Braz. Chem. Soc.*, Vol. 34, No. 12, 1877-1886, 2023  
 ©2023 Sociedade Brasileira de Química

A

### Determination of Trifloxystrobin in Soy Grape Juice and Natural Water by Photo-Induced Fluorescence and High-Performance Liquid Chromatography

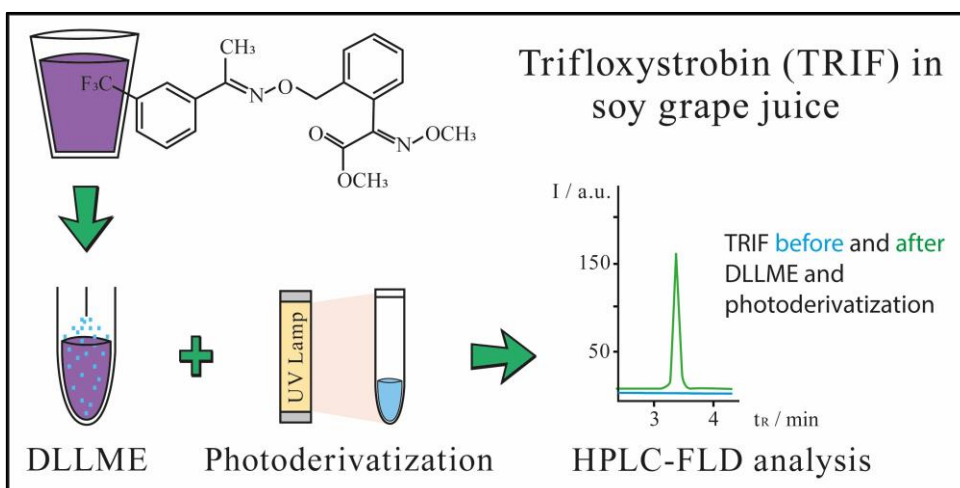
**Joseany M. S. Almeida,<sup>a</sup> Rosana C. Macedo,<sup>a,b</sup> Alessandra L. M. C. da Cunha,<sup>b</sup> Carlos A. T. Toloza<sup>a,c</sup> and Ricardo Q. Aucélio<sup>a</sup>**

<sup>a</sup>Laboratório de Espectroanalítica e Eletroanalítica Aplicada (LEEA), Departamento de Química, Pontifícia Universidade Católica do Rio de Janeiro (PUC-Rio), 22451-900 Rio de Janeiro-RJ, Brazil  
<sup>b</sup>Instituto Federal de Educação, Ciência e Tecnologia do Rio de Janeiro (IFRJ), Campus Realengo, 21710-240 Rio de Janeiro-RJ, Brazil  
<sup>c</sup>Department of Natural and Exact Sciences, Universidad de la Costa, 080002, Barranquilla, Colombia

A fluorescent (340/380 nm) photochemical product, identified at  $m/z$  206 by mass spectrometry was obtained by photo-derivatization (15 s ultraviolet exposure) in water/acetonitrile 10/90 v/v. The photoproduct was used for indirect determination of trifloxystrobin in water and soy grape juice by high-performance liquid chromatography and fluorescence detection. Separation was made under isocratic conditions (acetonitrile/water 70/30% v/v, at 1.0 mL min<sup>-1</sup> and 35 °C) with trifloxystrobin photo-derivative eluting at 3.2 min. The influence of ultraviolet exposure was evaluated in short and long terms with photoproduct showing stability up to 120 min after 15 s of ultraviolet exposure. The limit of detection was 57 µg L<sup>-1</sup> in water (87-109% recoveries). For soy grape juice, dispersive liquid-liquid micro-extraction was used to clean up and for pre-concentration (limit of detection of 9.5 µg kg<sup>-1</sup> and 93-101% recoveries) attending to the maximum residue limits for citrus juices established by regulatory agencies. Potential interference by triazoles was evaluated.

**Keywords:** fungicide, trifloxystrobin, high-performance liquid chromatography, photochemically-induced fluorescence, dispersive liquid-liquid microextraction

Graphical Abstract:



**C****Participation in events**

1- Oral presentation: Monitoramento e avaliação da autenticidade de óleo essencial de laranja doce por espectrofluorimetria 3D e em microemulsão sem surfactante.

**VII Jornada de Pós-Graduação em Química - PUC/Rio, 2023.**

First place in the category of best oral presentation.

2- Oral presentation: Análise de óleos essenciais de laranja doce por HPLC-DAD utilizando microemulsão sem detergente: Um estudo comparativo do efeito do solvente.

**VI Jornada de Pós-Graduação em Química - PUC/Rio, 2022.**

3- Oral presentation: Impressão digital de óleos essenciais cítricos por espectrofluorimetria e tratamento quimiométrico, utilizando microemulsões sem detergente.

**V Jornada de Pós-Graduação em Química - PUC/Rio, 2021.**

4- Oral presentation: Desenvolvimento de microemulsões sem detergente para posterior aplicação no controle da autenticidade de óleos essenciais cítricos por HPLC.

**IV Jornada de Pós-Graduação em Química - PUC/Rio, 2020.**

## 10

### Supplementary material

#### A

##### R Script used for Ternary Diagram Generation [56,57]

# Previously, data was organized in an Excel spreadsheet. For this case the file name was “Ternarydiagram”:

# sheet 1: weight values obtained during titration process for Essential Oil (Col A), Alcohol Mix (Col B), Water (Col C). System (Col D) classification as “Biphasic solution”, “Pre-ouzo effect”, “Single-phase solution”. Total weight (Col F)

# sheet 2: data converted in weight proportion (%): Essential Oil (Col A), Alcohol Mix (Col B), Water (Col C). System classification (Col D) as “Biphasic solution”, “Pre-ouzo effect”, “Single-phase solution”.

# R Script:

# Import or load required packages:

```
library("openxlsx")
```

```
library("ggtern")
```

# Create a data.frame named "Results" with the data from the Excel spreadsheet. Within the parentheses, the correct filename should be specified. The number 2 after the comma indicates that the program should retrieve only Sheet 2.

```
Results<-read.xlsx("Ternarydiagram.xlsx",2)
```

data=Results indicates that the data for plotting the points should be obtained from the data.frame named in the previous command.

# mapping=aes(Essential Oil, Alcohol Mix, Water) indicates which columns represent the X, Y, and Z axes, respectively.

```
ggtern ()
```

```
ggtern(data=Results, mapping=aes(Essential Oil,Alcohol Mix,Water))+
```

```
# This command renames the titles of each axis (X, Y, and Z, respectively). To
avoid issues with data conversion, the columns in the Excel spreadsheet do not
contain characters such as %. Therefore, the modification was necessary here to
include the unit of measurement.
```

```
xlab(' Essential Oil, %')+ ylab(' Alcohol Mix, %')+zlab(' Water, %')+
```

```
# 'Geom_point', Indicates that the points should be geometric shapes (in this case,
it will automatically generate as circles).
```

```
# aes(colour=Sistema) indicates that the color of each point should be based on the
response presented in the column 'System'.
```

```
Geom_point(aes(colour=System))+
```

```
# In the next command, colors are chosen for each point based on what is written
in the "Systems" column.
```

```
# The program understands some basic colors by name; however, in this case, as a
gradient color evolution was desired, HTML formatting codes were used for a more
elaborate selection.
```

```
Scale_colour_manual('System',values=c('Biphasic solution'='#FF9999','Single-
phase solution'='#CC3333','Pre-ouzo effect '='#FF6666'), breaks=c('Biphasic
solution','Pre-ouzo effect','Single-phase solution'))+
```

```
# In this part of the code, you should write the desired title for the diagram.
```

```
labs(title="Pseudoternary Diagram: Sweet orange EO")+
```

```
# The "theme_" command is useful for changing the layout of the diagram. In this
case, two themes were overlaid.
```

```
theme_bvbw()+theme_hidetitles()+
```

```
# In this command, the legend formatting was performed:
```

```
theme(legend.position = "right",  
  
      legend.background = element_rect(fill = "NA"),  
  
      legend.key = element_rect(fill = "NA", color = "NA"),  
  
      legend.key.size = unit(0.5, "cm"),  
  
      legend.key.width = unit(0.5, "cm"),  
  
      legend.title = element_text(face='bold'),  
  
    )
```

**B****R Script used for 3D Fluorescence Spectra obtention [49,50,58–60]**

```
# Previously, data from the 3D fluorescence spectra were organized into CSV  
# spreadsheets (excitation and emission wavelengths as columns and rows,  
# respectively).
```

```
# R Script:
```

```
# Import or load required packages:
```

```
library(dplyr)
```

```
library(tidyr)
```

```
library(staRdom)
```

```
library(eemR)
```

```
# Create a data frame with the spectra csv files contained in the folder (in this case  
# named 'foldername' for demonstration).
```

```
cores <- detectCores(logical = FALSE)
```

```
eem_list <- eem_read("foldername", recursive = TRUE, import_function =  
eem_csv)
```

```
# Provide an image with the raw spectra contained in the folder. Use 'spp=1' for one  
# spectrum. For nine spectra, for example, use 'spp=c(3,3)' to arrange the spectra  
# image in three rows and three columns.
```

```
# At any time, for spectra visualization, use this comand:
```

```
eem_overview_plot(eem_list, spp=1, contour = TRUE)
```

```
#blank subtraction (the blank matrix should be taken in the same excitation and  
# emission wavelength range as the samples).
```

```
eem_list <- eem_extend2largest(eem_list2, interpolation = 1, extend = FALSE,  
cores = cores)
```

```
eem_list <- eem_remove_blank(eem_list)
```

```
# Raman normalization (when applicable).

eem_list <- eem_raman_normalisation2(eem_list, blank = "blank")

#blank file removal.

eem_list <- eem_extract(eem_list, c("blank"),ignore_case = TRUE)

#Scattering vectors removal.

remove_scatter <- c(FALSE, FALSE, TRUE, FALSE)

remove_scatter_width <- c(18,18,18,18)

eem_list <- eem_rem_scatter(eem_list, remove_scatter = remove_scatter,
remove_scatter_width = remove_scatter_width)

#Adjust the image after scattering vectors removal:

eem_list <- eem_interp(eem_list, cores = cores, type = 1, extend = FALSE)

#For smooth:

eem4peaks <- eem_smooth(eem_list, n = 1, cores = cores)

#For spectra visualization. Remember to adjust the command spp for the number
of spectra in the figure.

eem_overview_plot(eem4peaks, spp=1, contour = TRUE)

# summary for data verification.

summary(eem_list)

# Save normalized files as CSV separated by column (if you want to generate the
images in another program, for example, Origin). Vary from [1] to the total number
of spectra. Choose a file name.

write.csv(eem_list[[1]], file="Filename", sep="\t", row.names=TRUE)
```